Engineering Characterisation and Implementation of pH Control in Microscale *Saccharopolyspora erythraea* Fermentations

A thesis submitted to the University College London for the degree of ENGINEERING DOCTORATE

By

Iman Elmahdi

The Advanced Centre for Biochemical Engineering
Department of Biochemical Engineering
University College London
Torrington Place
London

ProQuest LLC
789 East Eisenhower Parkway
P.O. Box 1346
Ann Arbor, MI 48106-1346

Abstract

Microscale operations are rapidly emerging as a useful tool for reducing the time and cost involved in fermentation process development. For both microbial and mammalian fermentations pH is a vital process parameter since it has a marked affect on cell growth rate, viability and product synthesis. It is the objective of this thesis to investigate the influence of pH on growth and erythromycin synthesis by *Saccharopolyspora erythraea* CA340 and implement an automated pH control system at the microscale.

The engineering properties of mixing and gas-liquid mass transfer in a 24-well microtitre plate system were characterised. k_La values up to 0.014 s^{-1} could be obtained for a soluble complex medium (SCM) and generally increased with increasing shaking frequencies and decreasing fill volumes. Similar trends were identified for measured liquid phase mixing times which were around 5-2284 s under operational conditions. The influence of different fermentation media types; oil based medium (OBM), starch based medium (SBM), and SCM and various pH control strategies on growth and erythromycin synthesis by *S. erythraea* at the 7 L and 5 L scales were next investigated. Faster rates of growth were achieved during fermentations carried out with the SCM and SBM, with the maximum specific growth rate (μ_{max}) reaching 0.12 h^{-1}. Growth rates were slower in the more viscous OBM, but erythromycin A titres were double those obtained with the SCM and SBM, however, the long mixing times and high viscosities associated with growth on OBM made this medium unsuitable for microwell fermentations of *S. erythraea* CA340.

At the 7 L scale the implementation of base only or full pH control (NaOH and H_3PO_4 additions) increased both the maximum growth rate and erythromycin

concentrations attained compared to fermentations without pH control. The effects were accurately reproduced in manually pH-controlled microwell fermentations (1000-fold scale translation).

The outcome of these studies led to the specification of an automated pH control system at the microscale using a LabView-based software controller integrated with a robotic liquid handling system to monitor and control the pH during microwell fermentations. A specially designed microwell plate was built that allowed the insertion of a micro-pH probe into each well (total well volume 7 mL) and was used during automated pH controlled microwell fermentations. The implementation of base pH control at the microwell scale led to almost one and a half fold increase in both biomass yield and erythromycin A production. It also enabled the operation of a fed-batch process at the microwell scale which further increased erythromycin A production by 60 %. The prototype system thus has the potential to support fermentation process development at the microwell scale.

to the memory of
Mohammad Elmahdi

Acknowledgments

It is not easy to thank all the people who have helped me through this and give them the acknowledgment they deserve. By all means this thesis could not have been completed without the help and support from my family, friends, and colleagues.

Special thanks goes to my supervisor Gary Lye for all his help and guidance. Frank Baganz for his input and advice. I am grateful for all the support I received from Kieth Dixon, David Sugden, Tony Harrop, Michelle O'Hara and Peter Schiener at Pfizer.

I would also like to thank Billy Doyle and Ian Buchanan for all their help with the fermentations. A special thanks to Martin Town and all the UCL workshop staff, Martyn Vale and team for all their technical support.

I am grateful to the Engineering and Physical Science Research Council (EPSRC) for financial support.

Finally, my husband, George, who has kept me a clear and critical thinker, his love and encouragement will always be my forward drive in life.

Table of Contents

List of Figures

List of Tables

List of Abbreviations

a	interfacial mass transfer area (m^2)
BL	branch length (μm)
C	concentration of oxygen in the liquid phase ($molesL^{-1}$
C^*	concentration of oxygen in the gas phase (moles L^{-1})
C_{base}	base concentration (M)
CER	carbon dioxide evolution rate ($mmmolL^{-1}h^{-1}$)
C_L	normalised concentration of oxygen
D	impeller diameter (m)
DOT	dissolved oxygen tension
eryA	gene responsible for erythromycin A synthesis.
EA	erythromycin A
EB	erythromycin B
ED	erythromycin D
HPLC	high performance liquid chromatography
J	controller output signal
J_0	controller output when error is zero
K_C	constant
K_I	constant
K_D	constant
k_La	combined mass transfer coefficient (s^{-1})
L_{O2}	oxygen solubility (mol/ Pa)
ML	main length (μm)
N	impeller speed (rps)
OBM	oil based medium

OTR	oxygen transfer rate
OUR	oxygen uptake rate ($mmolL^{-1}h^{-1}$)
ΔpH	net change in pH
$p_{O2,gas}$	oxygen partial pressure in the gas phase (Pa)
$p_{O2,liquid}$	oxygen partial pressure in the liquid phase (Pa)
Re	Rynolds number (dimensionless)
RQ	respiratory quotient
SCM	soluble complex medium
t	time (s)
t_m	liquid phase mixing time (s)
vvm	volume of air per volume of medium per minute
V_L	liquid fill volume (L)
X	maximum biomass concentration (gL^{-1})
$Y_{x/s}$	yield of biomass on substrate ($mg\ mg^{-1}$)

Greek symbols

ε	error
μ_{max}	maximum specific growth rate (h^{-1})
μ.	apparent viscosity (Pa.s)
τ_p	sensor response time (s)
ρ	density ($kg\ m^{-3}$)
σ	liquid vapour surface tension (mNm^{-1})

1.0 Introduction

1.1 Fermentation Process Development

Fermentation, in the broad sense in which the term is now generally used, may be defined as a metabolic process in which changes are brought about in an organic substrate through the activities of enzymes secreted by micoorganisms. Development of microbial cell cultivation can be divided into three main stages (Doig *et al.*, 2004):

- Strain selection: set in the principal that certain microorganisms are better suited for particular tasks and environments than others. The selectivity approaches are designed around the main biochemistry of the biosynthesis of the antibiotic and metabolism of the microorganism.

- Strain enhancement: achieved by random mutagenesis and screening following genetic changes or more recently, by using metabolic engineering.

- Process optimisation and scale-up: once the right microorganism is available, the aim is to reduce the production costs by further increasing productivity or bioactivity in an iterative process. Bioprocess optimisation can be achieved at the level of process optimisation and at the level of strain improvement.

Success of a fermentation process on an industrial scale depends on a number of factors including, the ability of the selected organism to give a consistently high yield of the desired product in a reasonable time from a cheap, available substrate,

the easy recovery of the product in pure form and the manufacture of a unique product which is in demand, but difficult to obtain by other methods.

1.1.1 Media

The prime requirement of a biotechnological process is a high-yielding organism, but optimum culture conditions must be developed for all stages of the process if the maximum yields are to be obtained. Pirt, (1964) has listed five criteria for optimal growth of microorganisms: an energy source, nutrients to provide essential materials for growth, absence of inhibitors, a viable inoculum and suitable physiochemical conditions.

In order to obtain rapid growth and production, the medium must contain sources of energy, carbon, nitrogen, phosphate, trace elements and any specific growth factors which the organism itself cannot manufacture. A single carbohydrate material may act as both carbon and energy source although a second material, usually a lipid, may be required and the carbon skeletons of nitrogenous organic compounds may contribute to both requirements (Lee *et al.*, 1997). As much as 15% of the biomass dry weight may be composed of nitrogen, therefore the medium must provide at least this amount of suitable ingredients. The requirement for phosphate is usually supplied as either the sodium or potassium salt of orthophosphoric acid. As a consequence of using crude technical grade materials, the required trace elements may be supplied automatically. It is common practice to add growth factors, such as yeast extract as part of a complex mixture, as a result the nature is imperfectly understood (Goodfellow, 1983).

It is easier to design media for good initial growth than for the subsequent steps of maximum product accretion. This is particularly the case where a secondary

metabolite is required; here a final-stage medium which becomes deficient in one or more nutrients after an initial rapid growth phase is necessary (Bu'Lock, 1974).

1.1.2 Sterilisation and Aseptic Operation

The preliminary step in all fermentation processes is the sterilisation of the medium to remove unwanted organisms which could have a detrimental effect on productivity if they were allowed to flourish. Rapid growth of contaminating organisms can reduce the level of nutrients available for the producer organism. This would usually be the carbohydrate and nitrogenous sources but even expensive secondary metabolite precursors *e.g.* phenyl acetic acid for penicillin production can be very rapidly utilised by a contaminating organism. The unwanted organism may produce such a mass of growth that it increases the viscosity of the medium to such an extent that agitation is impaired or efficiency of the harvest equipment is reduced. This is particularly the case if the contaminating organism has a filamentous growth form. Heating complex chemical mixtures to temperatures above 120 °C for periods exceeding 20 min can cause destruction of medium constituents may be either by direct thermal degradation or by unwanted chemical reactions. The best known case is the destruction of glucose by the Millard or browning reaction when heating in the presence of amines. Not only is glucose destroyed by the reaction but toxic products are formed which interfere with the subsequent fermentation (Bechtle, 1974). In such cases it is usual to sterilise the glucose solution separately and add it to the remainder of the medium after it has also been sterilised.

1.1.3 Mixing and oxygen transfer

Agitation serves two primary purposes in fermentation processes (1) to provide uniform environment for the organisms and (2) to transfer oxygen from air to the liquid phase for microbial uptake. The first purpose represents a blending operation and generally requires significantly less power input than the second purpose of gas dispersion and mass transfer. In *Streptomycetes* fermentations, like many other aerobic fermentations, oxygen is required for growth and secondary metabolite production. The economics of the fermentation process are such that it is desirable to achieve high cell densities and hence high productivity rates during the fermentation (Drew and Demain, 1977). The maximum cell yield achievable during the fermentation is closely linked to the capability of the agitation and aeration system to transfer the required oxygen. For this reason agitation and oxygen transfer became critical factors in the development and scale up of most fermentation processes (Heydarian, 1998a).

At the laboratory scale typical shake flask fermentations are conducted on rotary shakers which run at 200-300 rpm. Mixing in the shake flask is rotary in motion and maximum shear rates are relatively low. Aeration is primarily through surface gas diffusion to the liquid. The rate of oxygen transfer to the liquid is highly dependant upon the shaker speed, the type of sterile closure used on the flask, the size and design of the flask, the quantity of medium added to the flask and the viscosity of the broth (Buchs, 2001; Maier and Buchs 2001; Tibor and Buchs 2001). Dissolved oxygen tension (DOT) is known to influence the microbial synthesis of many antibiotics. Early reports by Bartholomew *et al*, (1950) described the effect of aeration and agitation on product formation; this was later verified by correlating product formation directly with measured DOT (Hilton,

1999). The rate of oxygen transfer to the cells can be one of the main limiting factors in product formation. It is known that increasing the rate of oxygen transfer can enhance the rate of product formation in many fermentations (Heydarian *et al.*, 1996). Gas hold up and the liquid volumetric mass transfer coefficient are commonly used to characterize oxygen transfer (Kumar *et al.*, 2004).

1.2 Bioprocess Monitoring and Control

1.2.1 Advances in fermentation process monitoring and control

Because of the complex nature of microorganism growth and product formation in batch and fed-batch cultures, which are often used in preference to continuous cultures, the control of bioprocesses continues to present a challenge to biochemical engineers (Karl, 2001). Extensive developments in the area of process control have recently begun to impact in bioprocess development (Stoeckli *et al.*, 1999), but much work remains to be done to couple model-based control methods to bioreactor technology.

At the heart of fermentation process control is the ability to monitor important process variables such as pH, temperature, DOT, oxygen uptake rate (OUR) and carbon dioxide evolution rate (CER), although additional measurements have become available recently (Harms *et al.*, 2002). However, the inability to measure certain variables need not keep the bioprocess engineer from extracting valuable information from a bioreactor. Advanced control systems typically employ mathematical models that describe the process being controlled (Morari and Zafiriou, 1997; Bastin and Dochain, 1990). The use of a mathematical technique in conjunction with the measurements can enable the estimation of parameters or process variables that cannot be directly measured. On-line estimation allows

performance refinement and the ability to query the metabolic state of the cell and reactor system. The degree to which one can estimate the state of the system is dependent on the availability of accurate measurements of process variables such as pH, DOT and off-gas composition. More informative measurements, such as measurements of metabolic products or intracellular metabolites, can provide a more comprehensive description of the system. However, these measurements often suffer from greater inaccuracy and incomplete information. Thus, the improved performance of the estimator is not guaranteed.

1.2.2 PID Control

A basic control system contains three types of primary elements: inputs from the process being controlled, control loops that utilises the inputs to produce outputs and outputs that change a variable in the process being controlled. In addition, control systems also perform other secondary duties such as data display, data logging, and may also provide means for configuring, modifying and controlling overall system behaviour (Pollard, 2001).

Most controllers use a negative feedback system in which a measured process output is subtracted from a desired value (set point) to generate an error signal.

Figure 1.1 shows a typical feedback control system which utilise proportional (P), integral (I) and derivative control (D) action. This type of controller is the most common in bioprocess monitoring and control. The output of a proportional (P) controller is proportional to the error signal. The greater the magnitude of the error the greater the corrective action, this will however lead to an offset. The output of integral element (I) of a PID controller is determined by the integral of the error over the time of the operation. As a consequence integral action is slow in the beginning of its response, therefore, allows a large deviation but does not have any

offset. The output of the derivative element (D) of a PID controller is proportional to the rate of change of the error; as a consequence, if the error is not changing no action will occur.

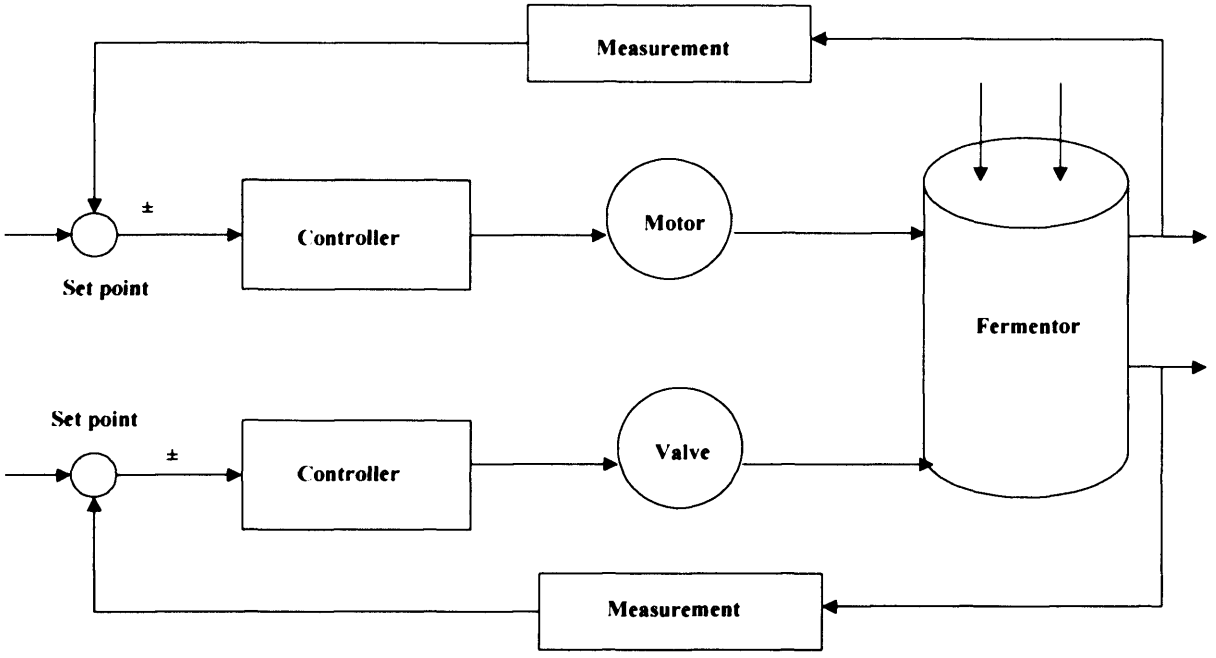

Figure 1.1 Typical feed-back control system

Combined proportional and integral (PI) control gives a higher maximum deviation, a longer response time and a longer period of oscillation but no offset. Proportional and derivative action will reduce the deviation, give faster stabilisation and reduce offset as compared with proportional alone. Combined PID control gives a best option with reduced deviations, minimal oscillation and no offset.

1.2.3 On-line Sensors

Development for reliable, high-performance systems for the control of fermentation processes able to handle intelligently various process situations has long been a challenge for bioprocess engineers (Karl, 2001).

Figure 1.2 shows an example of a typical On-line monitoring and control system for bioprocess operation. There are a number of parameters that are routinely measured and controlled during fermentation. These can generally be characterised into two types:

- On-line monitoring: for measuring those parameters for which an *in situ* measurement can be obtained. The sensing element can be non-invasive, direct or protected by a membrane but characterised by a short response time.
- Off-line monitoring: here measurements are obtained by the removal of a sample and determination of a value at a subsequent time.

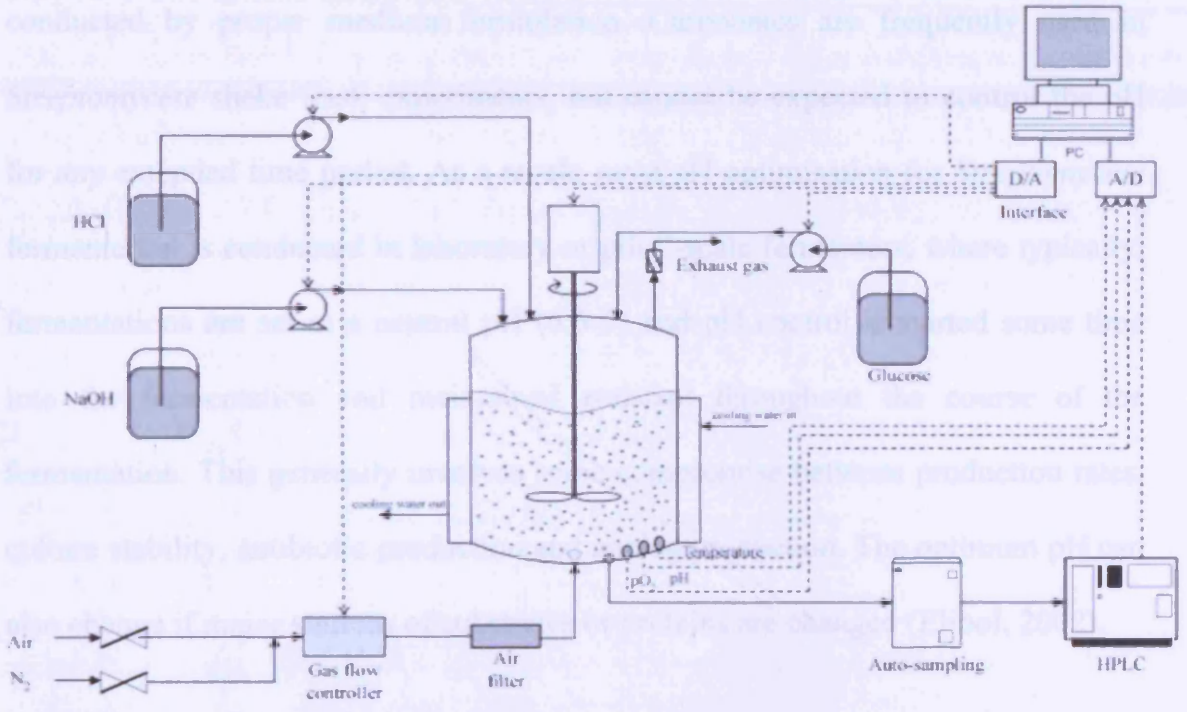

Figure 1.2 On-line monitoring and control system, showing auto sampling equipment, HPLC, and control components (Yen-Chun *et al.*, 2001).

There are wide range of physical sensors available for measuring process parameters during a fermentation, including temperature, pressure, power, liquid level detection, stirrer speed and gas and liquid flows (Karl, 2001). Dissolved oxygen, pH and exit gas analysis are carried out using chemical sensors, although other methods such as mass spectrometry, NIR and biosensors are increasingly being used (Wong *et al.*, 1979; Wong *et al.*, 1984; Kurz, 1996).

1.2.4 pH Monitoring

In fermenters, the pH is generally measured on-line with a steam sterilisable pH electrode. During the fermentation, the pH can be controlled at any desired set-point by the addition of acid or alkaline. It is not generally possible to actively control the pH in shake flasks. Typically, any control of pH in shake flasks is conducted by proper medium formulation. Carbonates are frequently used in *Streptomycete* shake flask experiments, but cannot be expected to control the pH for any extended time period. As a result, most pH optimisation for *Streptomycete* fermentation is conducted in laboratory or pilot -scale fermenters, where typically, fermentations are set at a neutral pH (6.5-7) and pH control is started some time into the fermentation and maintained constant throughout the course of the fermentation. This generally involves some compromise between production rates, culture stability, antibiotic production and analog production. The optimum pH can also change if major sources of substrates or proteins are changed (Elibol, 2002).

1.3 Scale-down methods

1.3.1 Microwell systems

Microwells or microtitre plates were initially introduced and used for analytical purposes in the early 1950's (Manns, 1999), since then their application widened to

include high throughput screening laboratory applications, namely medical diagnostics (Leach, 1997), combinatorial chemistry (Hart, 2001; Nakayama, 2001), cell and tissue culture (Girard *et al.*, 2001), and most recently small-scale fermentation and biocatalysis (Doig *et al.*, 2005; Reeves *et al.*, 2004; Weis *et al.*, 2004, Doig *et al.*, 2002; Duetz *et al.*, 2000). Microwell plates have the potential of offering a large number of parallel and miniaturised reactors with identical shape and fluid dynamic characteristics and hence, allow for parallel automated processing using robotics and modern pipetting and dispensing systems (Kumar *et al.*, 2004; Lye *et al.*, 2003).

As Leach (1997) reported, microwell plates are injection moulded rectangular plastic trays made of polypropylene or polystyrene, although some are silicone dioxide coated, with a rectangular shape containing columns and rows of wells. The typical standard dimensions of a well plate are 856 mm wide and 1276 mm in length (Leach, 1997). Figure 1.3 shows a picture of typical microwell plates. The well geometry may vary from either rectangular or circular deep or shallow, with round flat or square bottom. The number of wells in a single microwell plate can range from 4 to 9600, with a nominal fill volume range of 0.2 μL-5 mL (Burbaum, 1998; Wolcke and Ullmann, 2001; Kumar *et al.*, 2004). All of the microwell formats are accommodated within the standard foot print. The 96-well plate is the most widely used format in microbial cell cultivation as reported by Doig *et al.*, 2005; Weis *et al.*, 2004; Reeves *et al.*, 2004; Casey *et al.*, 2004 and Duetz *et al.*, 2000. Wolcke and Ullmann reported that for fill volumes below 1 μL, limitations existed regarding liquid handling, surface to volume ratio and liquid evaporation.

A major bottle-neck in the use of microwell plates during microbial and animal cell cultivation is the risk of cross–contamination caused by aerosol formation at high shaking rates (Duetz and Witholt, 2001). Evaporation of the process medium can also be a critical factor particularly for slow growing organisms (Deutz *et al.*, 2000), however, liquid evaporation and cross-contamination can be minimised by using a suitable closure at the top of the plate that allows gaseous exchange (Zimmermann *et al.*, 2003; Wittmann *et al.*, 2003; Burbaum, 1998). Dutez *et al.*, (2000) reported covering a 96-square deep well plate with a thin layer of cotton wool sandwiched between a spongy silicone plate and a rigid polypropylene plate containing perforated holes. This device prevented contamination and evaporation was limited to 10 µL per well per day. Reeves *et al.*, (2004) reported covering microwell plates with tissue paper lined lids to reduce evaporation and well-to-well splashing as the microwell plate was agitated.

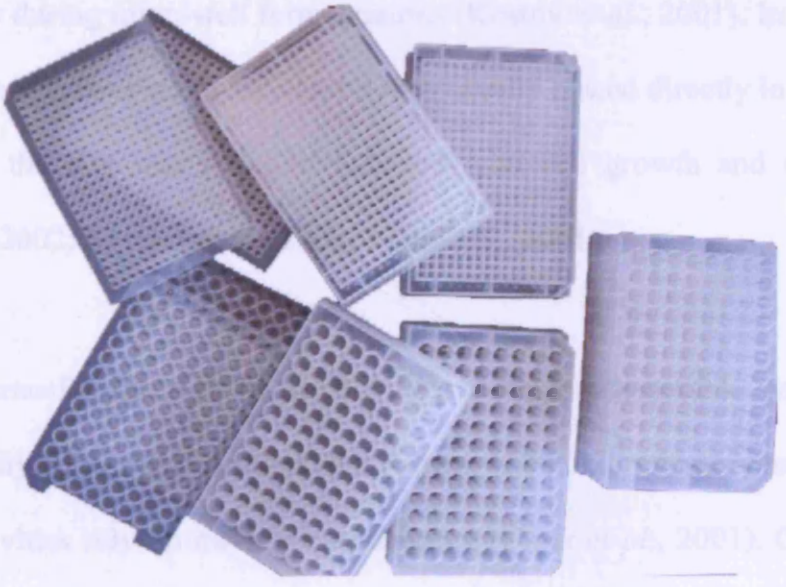

Figure 1.3 Microwell plates with different geometry, adapted from www.perkinelmer.com

1.3.2 Monitoring and control in microwell systems

Although monitoring and control of process parameters such as pH and dissolved oxygen concentration are totally automated processes in virtually all laboratory and large scale bioreactors (Amanullah *et al.*, 2001; Leib *et al.*, 2001), they are quite uncommon in small microwell systems. If microwell plates are to be used as tools for process development and optimisation, predictive data relating to the larger scale must be obtained from microwell studies. In order to achieve this, it is important to monitor and control important process parameters such as DOT, optical density (OD), temperature and pH.

Kostov *et al.*, (2001) reported the design of a micro-bioreactor (2 mL working volume) for the continuous measurement of pH, DOT and OD during *E. coli* fermentation using optical chemical sensors. These sensors rely on the variable fluorescence quenching of certain dyes immobilised on the end of a fibre optic cable and have proved reliable in the measurement of process parameters such as optical density during microwell fermentations (Kostov *et al.*, 2001). In the case of pH measurement, however, an indicator dye is usually placed directly in the growth medium with the risk that it might interfere with cell growth and metabolism (Harms *et al.*, 2002; Kermis *et al.*, 2002; John *et al.*, 2001).

The oxygen transfer rate (OTR) is the most suitable measurable parameter to quantify the physiological condition of a culture of aerobic microorganisms, since metabolic activities rely on oxygen consumption (Tibor *et al.*, 2001). Clark *et al.*, (1995) emphasised the importance of oxygen limitation on screening for secondary metabolites, stating that "industrial screening programmes for novel microbial metabolites are often designed so that each isolate under test is grown in a variety

of media designed to provide different growth limiting nutrient. The required range of growth rate limiting nutrients may not be possible if the design of the culture vessel results in oxygen limitation and this may reduce potential product diversity in screens". Although on-line measurement of OTR in stirred bioreactors is a state of the art, the sterile on-line determination of OTR in shaken microwell plates has not been possible until recently (Lamping *et al.*, 2003). One of the challenges facing researchers in this area is the lack of fundamental knowledge about the physical engineering environment and controlling parameters within the small scale shaken systems. Quantification of mixing, oxygen supply and removal of carbon dioxide is very difficult on this small scale (Hermann *et al.*, 2002). According to Maier and Buchs, (2001), the factors influencing gas-liquid mass transfer rate, the state of the art and systematic approach to the oxygen transfer, are the mass transfer coefficient (k_L), the specific transfer area (a), the oxygen solubility (L_{O2}), and the driving pressure difference across the gas-liquid interface ($p_{O2,\ gas} - p_{O2,\ liquid}$). Therefore, OTR can be described as follows (Maier and Buchs, 2001):

$$OTR = k_L a\ L_{O2}\ (p_{O2,\ gas} - p_{O2,\ liquid}) \qquad \textbf{(1.1)}$$

The mass transfer coefficient (k_L) depends on the electrolyte concentration and the viscosity of the liquid phase while the specific transfer area (a) is influenced only by the viscosity of the solution.

Some researchers have reported studies on gas-liquid mass transfer for small scale cultures systems used for screening purposes, such as shake flasks (Henzler and Schedel, 1991; Maier and Buchs, 2001; van Suijdam *et al.*, 1978; Veglio *et al.*, 1998) and test tubes (Danielson *et al.*, 2004). However, Duetz *et al.*, (2000), was

the first to estimate the OTR in a 96-deep well micotiter plate from the increase in cell mass during oxygen limited growth of *Pseudomonas putida,* followed by Doig *et al.*, (2005b) who determined oxygen mass transfer rates in 48-deep microwell plate using *Bacillus Subtillus.* Although this method is valid for application at any scale, it is often experimentally laborious and requires assumptions about the growth kinetics of the organism used. On the other hand, Doig *et al.*, (2005a) used dimensionless group numbers to predict the mass transfer coefficient (k_La) over a wide range of operating conditions and a comparison was made with experimental results obtained with a model of *Bacillus subtilis.* Kenny *et al.*, (2005) also reported a bio-oxidation method for the measurement of k_La based on the oxidation of the enzyme catechol-2,3-dioxygenase, but this method is only limited to small scale and depends on the availability of the enzyme.

An investigation of the liquid hydrodynamic flow in a shaken 96-well plate was reported by Duetz and Witholt, (2001), and Hermann *et al.*, (2002), both concluded that there is a critical shaking frequency at which an increase of the liquid height occurred and thus the maximum oxygen transfer rate is achieved. Buchs *et al.*, (2001), reported an influence of the surface properties of the shake flask material on the oxygen mass transfer and Maier and Buchs (2001), stated that the maximum oxygen transfer capacity in shaking flasks with hydrophilic walls is higher than in hydrophobic flasks. This was thought to be due to a liquid film formed on the hydrophilic walls, which acts as an additional mass transfer area.

1.3.3 Automated Liquid Handling

In order to increase the efficiency of screening processes, ways to increase sample throughput without adding labour are typically required. This result can be achieved via automation of the media, culture handling steps, sample transfer and

storage. In one such industrial system, sterile media are robotically dispensed into custom-designed sterilizable and disposable modules, each having over 100 tubes or bottles (Vinici and Byng 1998). Individual clones are detected by an optical system and plugged from agar-based medium into liquid seed medium. Robots also accomplish the inoculation of seed-stage culture into fermentation vials. Solvent extraction and HPLC analysis of the fermentation broth are also automated to match the throughput of the screening stage. The advantage of such automation is that it facilitates the capture and downloading of process data and allows statistical process control to be implemented where refinement of the process is required. The success of automated programs requires constant monitoring and evaluation of the screening system to ensure that all aspects of the automation are functioning efficiently without introducing variability. A significant disadvantage of robotic systems is the initial capital investment and continued maintenance of equipment and software (Nolan, 1986), however, the use of commercially available laboratory automation may ease this concern.

In general, the key challenge in the automation of fermentation process development operations is the ability to miniaturise culture conditions. The equipment needed for robotic handling will be determined by the smallest volumes in which fermentation conditions can be developed. These volumes should be statistically reliable to model the larger-scale production process (Lye *et al*, 2003). One solution is to build customised equipment for handling samples of several millititers (Vinici and Byng 1998). This approach can be very expensive and often cannot be upgraded with commercial equipment as new advances in technology arise. An alternative approach is to employ materials and equipment that were

developed for high-throughput discovery screening operations or immunological assays. These commercially available systems are focused on the use of microtiter plates generally in 96-, 24-, or 384-well format. The use of this technology would allow significant cost reductions to be made, as the quantities of reagents are minute compared to traditional pilot scale. Some key intermediates and reagents are prohibitively expensive and prevent a bioprocess from being fully developed at the pilot scale. The reduction in reagent costs must however be balanced against the initial capital cost of the liquid handling robot.

The possibility of integrating automated liquid handling robots with fast analytical devices, such as microwell plate readers (Nealon *et al.*, 2005) can widen the application of microscale technology. A number of commercial vendors design and market equipment for inoculation, liquid-liquid transfer, and assay of small volumes. Picking and/or transfer of colonies is carried out using robotic systems. It is expected that the growing advances in hardware and software will drive automation volumes and costs downward. It is conceivable that strain improvement and process development will be done with significantly fewer resources than are generally used today. The critical issue in the evaluation of automation is the ability to grow cultures on a much smaller scale in a manner reflective of large-scale fermentors or bioreactors, which is where the new strain's productivity or other attributes must ultimately have their impact.

Additional miniature equipment pieces are also available that allow liquid temperature control and automated microwell filtration. The combination of this speed and range of platforms provide the liquid handling robot with great flexibility which can be applied to a range of uses.

1.4 Erythromycin biosynthesis by *S. erythraea*

1.4.1 Actinomycetes

Actinomycetes are primary soil dwelling microorganisms and are widely distributed (Pelczar *et al.*, 1986). In the environment they are important for their ability to degrade a wide variety of organic matter, while industrially they are important for the antibiotics, enzymes and vitamins that they produce. *Actinomycetes* are Gram positive bacteria that form elongated cells or filaments which usually have some degree of branching. *Actinomycete* morphologies vary from simple cocci to complex mycelia which may be pelleted or diffuse. The hyphae extend only at the tips, where the cell wall is not fully matured (Bushell, 1988), branches occur at points of nutrient depletion along the hyphae by the reversal of wall maturation at these points. For the mycelial forms, pelleted growth and fragmentation both reduce antibiotic production, therefore branched diffuse growth is preferred despite the increase in viscosity and complexity of the rheology that results (Bushell, 1988).

1.4.2 Streptomycetes

Streptomyces are the most commonly described genus of the *Actinomycetes*, they are responsible for the majority of commercial secondary metabolite production. Many secondary metabolites are of industrial importance for their antibiotic, anti-cancer, and anti-fungal properties. Streptomyces can be grown on solid substrates or in liquid culture. In liquid culture, the organisms can be found as dispersed mycelia or compact pellets. Dispersed mycelia is considered to be a homogeneous suspension of branched hyphae with no diffusional limitations to the exchange of components in the medium. Pellets are believed to be formed when interactions

occur between hyphae, solid particles and spores. The hyphae are believed to restrict exchange with media components and dissolved gas, such as oxygen (Prosser and Tough, 1991).

1.4.3 Streptomyces metabolism

Organic acids, namely pyruvate and α-ketoglutarate, are excreted from streptomyces as overflow metabolites (Bormann and Herrmann, 1968; Grafe *et al.*, 1975; Ahmed *et al.*, 1984; Hobbs *et al.*, 1992; Madden *et al.*, 1996), similar to acetate excretion in *E. coli* (Holms, 1986; el Mansi and Holms, 1989; Luli and Strohl, 1990). Bormann and Herrmann (1968) found that pyruvate and α-ketoglutarate were excreted by *S. rimosus* in defined medium containing glucose and casamino acids. It was also found that carbonate increased the amount of acid excreted and cultures free of complex nitrogen sources reduced amounts of acids excreted. Increased amounts of ammonia decreased pyruvate excretion, however pyruvate excretion was observed in the presence of ammonia and succinate. They concluded that re-consumed pyruvate was converted to α-ketoglutarate, thus maintaining a constant amount of excreted organic acids (Bormann and Herrmann, 1968). It was shown that production of secondary metabolites in *S. hygroscopicus* interfered with the accumulation of α-ketoglutarate. In *S. venezuelae,* decreased activity of pyruvate dehydrogenase and α-ketoglutarate dehydrogenase resulted in increased amounts of excreted acids (Ahmed *et al.*, 1984). In *S. lividans*, it has been shown that the level of pyruvate and α-ketoglutarate excretion was dependent on the nitrogen source when glucose was the carbon source (Madden *et al.*, 1996). Pyruvate and α-ketoglutarate production has also been observed in *S. coelicolor* (Hobbs *et al.*, 1992).

Streptomyces produces a broad range of secondary metabolites. Although secondary metabolites are naturally produced, the quantities are typically low. Many years of research has been conducted to attempt to understand the mechanisms of secondary metabolite production and control and there remains much to understand about the synthesis and control of these molecules.

Nutrient limitation is one of the most common factors associated with onset of secondary metabolism (Doull and Vining, 1990). Most experimental data support the theory that a inhibitor must be depleted before antibiotic synthesis can occur (Bushell, 1988). However, there is another theory suggesting that an activator must be synthesized before antibiotic synthesis can occur (Martin and Demain, 1980). Carbon catabolite repression has been observed with glucose as the carbon source for several antibiotic producing organisms (Martin and Demain, 1978). It has been shown that repression of antibiotic biosynthesis is caused by increased growth rate due to rapid uptake of carbon (Martin and Demain, 1978), and glucose may have a transient repressive effect on erythromycin synthesis (Escalante *et al.*, 1982).

Typical secondary metabolite production is usually non-growth related where cultures are grown in batch fermentations and secondary metabolite production is initiated by a nutrient limitation. In this respect, there have been several reports on the relationship between growth rate and secondary metabolite production through the use of fed-batch and chemostat fermentation processes. It has been shown, using chemostat fermentation, that a slower growth rate increased clavulanic acid production (Ives and Bushell, 1997). Furthermore, it has also been reported that a slower growth rate induced production of rapamycin and erythromycin in *S. hygroscopicus* and *S. erythraea*, respectively, in batch and fed batch processes

(Wilson and Bushell, 1995; Bushell *et al.*, 1997a). However, actinorhodin production by *S. coelicolor* peaked at the mid-range of dilution rates investigated in chemostat experiments (Melzoch *et al.*, 1997).

Media components have been studied to determine the best combination to produce a given product. In *S. hygroscopicus*, which produces rapamycin, over thirty carbon sources were studied and it was found that 2% sucrose and 0.5% mannose was the best combination to produce rapamycin. By contrast, acetate and propionate which are known to contribute to the carbon ring of rapamycin were not suitable for growth or rapamycin production (Kojima *et al.*, 1995). It appears that high phosphate levels are required for exclusive methylemomycin production by *S. coelicolor*, (Hobbs *et al.*, 1992), which is contrary to other reports suggesting that phosphate inhibits secondary metabolite formation (Lubbe *et al.*, 1985; Obregon *et al.*, 1994). Various studies have shown that the effect of ammonia may be important to understand as it appears to have a changed effect when present in different forms. For example, ammonia inhibits growth in *S. clavuligerus* (Ives and Bushell, 1997), and inhibits erythromycin production by *S. erythraea* (Flores and Sanchez, 1985). In a separate study, it was reported that high levels of ammonium sulfate reduced erythromycin production while ammonium nitrate increased production (Potvin and Peringer, 1994a), which may be due to differences in uptake and utilization of the ammonia form.

Dissolved oxygen is another factor that appears to influence secondary metabolite production. (Chen and Wilde, 1991) reported that high levels of dissolved oxygen are important for production of tylosin by *S. fradiae* as well as for vancomycin produced by *A. orientalis* (Clark *et al.*, 1995). However, it has been reported that

erythromycin can be produced under both oxygen limited (unbaffled shake-flask with dissolved oxygen levels of 0 during growth phase) and oxygen sufficient (baffled shake-flask with dissolved oxygen not dropping below 78%) conditions (Clark *et al.*, 1995; Heydarian *et al.*, 1996).

1.4.4 Saccharopolyspora erythraea

Saccharopolyspora erythraea (S. erythraea), the organism used in this work, is a spore forming member of the classification *Actinomycete*. *S. erythraea* is an aerobic gram positive *actinomycete* with a highly branched filamentous morphology (Seno and Hutchinson, 1986). The wild strain of *S. erythraea*, NRRL2338 (Northern Utilisation Research and Development Division, US Department of Agriculture) was isolated from soil samples collected in the Philippines by Lilly Research Laboratories in 1950. *S. erythraea* produces two known polyketide secondary metabolites; erythromycin and a red pigment, of which little is known (Ushio 2004, Cortes *et al.*, 2002).

1.4.5 Polyketide Antibiotics

Thousands of microbial metabolites have been found to posses a broad range of pharmaceutical activity (Cane, 1997). Therapeutic applications of natural products include antibacterial, antiviral, antitumor, immunosuppressant, antihypertensive and antihypercholesterolemic activity. Polyketides, a class of natural products, comprise a large fraction of the pharmaceutically active metabolites with high commercial value including avermectin, daunorubicin, rapamycin, mevinolin, monensin, tetracycline, FK506, and erythromycin (Ushio 2004).

In a manner similar to fatty acid biosynthesis, polyketides are synthesized by a series of condensation reactions assembling acyl-CoA precursors, which are

activated forms of acetate, propionate, and butyrate. Polyketide synthesis is initiated with a primer unit followed by elongation of the polyketide chain by incorporation of the activated building blocks one at a time. The oxidation level and stereochemistry of the beta-carbonyl are then adjusted through varying degrees of ketoreduction, dehydration and enoylreduction (Cane, 1994). Due to the many variables associated with polyketide synthesis, the structure and properties of polyketides can vary significantly; however, they can be classified into two categories based on their mode of assembly (Katz, 1997):

- Aromatic polyketides: e.g. tetracycline and daunorubicin, are assembled mainly with acetate groups resulting in unreduced beta-keto groups during chain elongation. Folding facilitates aldol condensation resulting in 6-membered rings as chain elongation proceeds or completes. These rings are then reduced through dehydration to produce the final product (Katz, 1997). Aromatic polyketide synthesis is accomplished through Type II polyketide synthases (PKS). Type II PKS consists of discrete enzymes whose activities can be purified

- Complex polyketides: a more diverse group of compounds as compared to aromatic polyketides can be formed by incorporation of activated acetate, propionate and butyrate units into the chain structure. Other differences include the inability of complex polyketides to undergo folding and aromatization due to structural constraints (methyl side chains), beta-carbonyl reduction, and synthesis chemistry. They instead cyclise through lactonization or remain as long acyl chains (Katz, 1997). Some examples of complex polyketides are erythromycin, avermectin, and rapamycin. Complex polyketide synthesis is carried out by Type I PKS which consists

of a single large multifunctional protein with individual activities located in catalytic domains of the protein

1.4.6 Erythromycin synthesis

Erythromycin is the antibiotic product of *S. erythraea* fermentation, it is a secondary metabolite, which is a chemical that is thought important for its survival in its natural habitat. The erythromycins are macrolide antibiotics whose structure consists of a 14 membered lactone and two sugars, one of which contains a basic dimethylamino group. There are six principal forms of erythromycin, A-F, which have slight differences in their alkyl groups but otherwise have similar properties. The most active form of the various erythromycin analogs synthesised is erythromycin A (EA), as shown in Figure 1.5. This has the ability to inhibit polypeptide synthesis in Gram positive bacteria (Corcoran and Omura, 1984, Omura and Tanaka, 1984) and hence has been used clinically for more than 30 years. Some of the key steps involved in the later stages of erythromycin A biosynthesis, together with the corresponding genes, are shown in Figure 1.4. (Carreras *et al.*, 2002). Following cyclisation of the polyketide chain the 14-membered lactone ring, 6-deoxyerythronolide B (6-dEB), is hydroxylated at the C-6 position to form erythronolide B. Mycrose is then attached to yield α-mycrarosylerythronolide B, which is further glycosylated to form erythromycin D (ED). Erythromycin D is then hydroxylated to yield erythromycin C (EC) which in turn is methylated to yield the desired erythromycin A. It is also thought possible that the EryG gene product, methylase, catalyses the formation of erythromycin B (EB) directly from erythromycin D, however, Corcoran and Vygantas (1977), reported that erythromycin B can be considered a shunt metabolite in the erythromycin biosynthetic pathway. In industrial

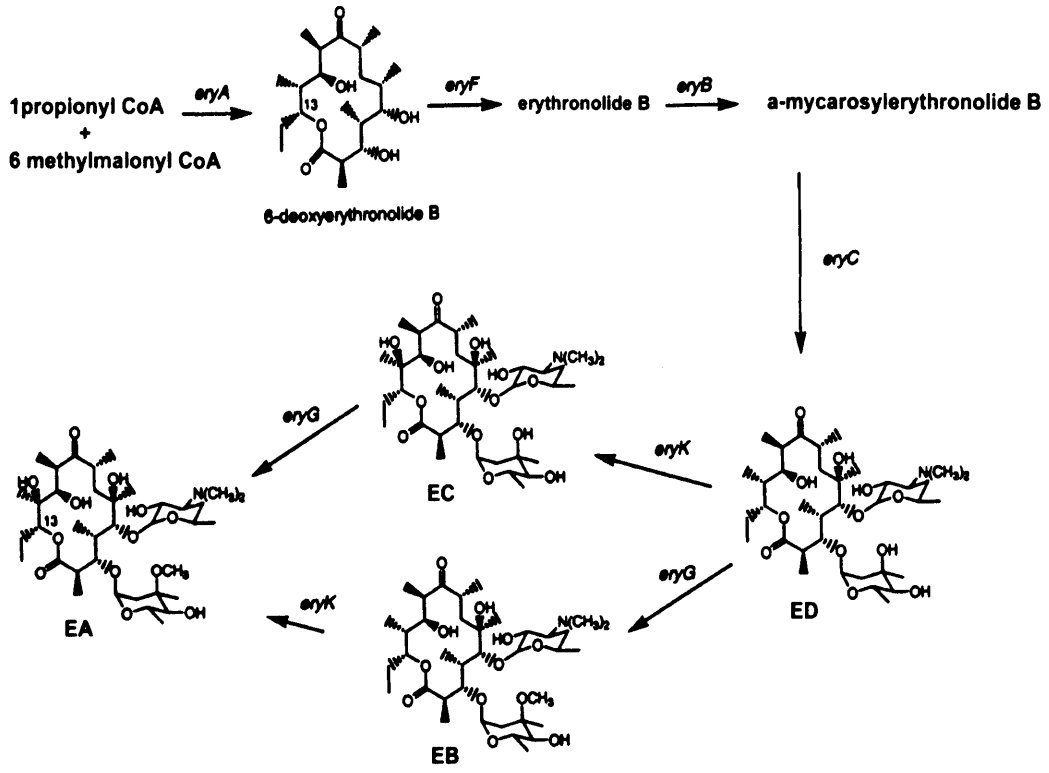

Figure 1.4 Erythromycin biosynthesis in *S. erythraea* CA340, showing the relationship between erythromycin A, B, C, and D. Adapted from Carreras *et al*, (2002).

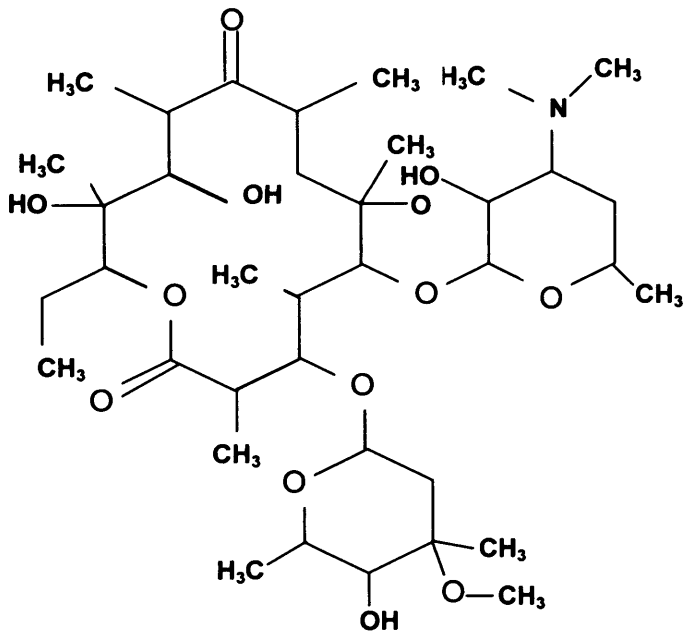

Figure 1.5 Erythromycin A structure

fermentations, careful pH control is used to optimise both erythromycin biosynthesis and the ratios of the various erythromycin analogs produced (Minas *et al.*, 1998).

1.5 Fermentation Process Parameters

1.5.1 Fermentation broth rheology

Liquids and suspensions can be categorised into two rheological groups, Newtonian and non-Newtonian fluids. For Newtonian fluids the viscosity, a measurement of the internal resistance to flow, is independent of the shear rate applied (Atkinson and Mavituna 1991). Non-Newtonian fluids, however, have viscosities that are dependant on the shear rate applied to the system; viscosity can either increase or decrease depending on the shear rate. A problem associated with the measurement of viscosity, is the time dependence of the measurement. Metz *et al.*, (1979) described this phenomenon and suggested a time of 5 seconds after changing the shear rate to take the measurements. The effect of the type of measuring device used should also be considered since several reviews have shown disagreements between the values of viscosity found by different measurement techniques (Bjorkman 1987; Allen and Robinson 1990). These variances can be due to "slip effects", settling of the suspension, or breakage of the solids (Karsheva *et al.*, 1997). Warren *et al.*, (1995) found that for three different species of *Actinomycetes* including *S. erythraea*, viscosity measurements were consistent between two different instruments; a cup and bob viscometer and an impeller viscometer.

Considering the problems of reproducibility when studying biological systems, it becomes difficult to predict how small changes in the fermentation will affect

rheological properties of the broth. There are four main models which have been developed to describe the rheological behaviour of fermentation broths (Karsheva *et al.*, 1997); these are the Newtonian, Power Law, Bingham plastic and Casson plastic models. Researchers have found different rheological models to be more accurate depending on species, strain and medium (Björkman 1987; Allen and Robinson 1990; Warren *et al.*, 1995).

Fermentation broths of *S. erythraea* follow the Power Law model, (Heydarian *et al.*, 1999) which is itself separated into two types, shear thinning (pseudoplastic) and shear thickening (dilatant). In shear thining the flow index (n) is less than 1; and as shear increases the apparent viscosity decreases. In shear thickening (where n is greater than 1), the shear rate increases with the apparent viscosity.

1.5.2 Relationship between media composition, growth and product formation in S. erythraea *fermentations*

The differences in the physiology of *S. erythraea* when grown on complex or defined carbon and nitrogen sources was observed by Smith *et al.*, (1962). They found that when *S. erythraea* was grown on a complex nitrogen source (soybean oil) erythromycin biosynthesis exhibited a non-growth related secondary metabolite profile and production continued until the substrate was depleted. Addition of sucrose caused renewal of erythromycin production; however, if nitrogen was added with sucrose then production was not renewed. It was presumed that the processes of growth consumed the intermediates, energy, or cofactors that would otherwise be used for erythromycin production. Using a defined nitrogen source (glycine) erythromycin production followed a growth related profile. They observed limited growth which may have been due to the inability to fully use media components and, therefore, allowed for simultaneous

erythromycin synthesis. Addition of sucrose and glycine caused renewal of both growth and erythromycin biosynthesis (Smith *et al.*, 1962).

When *S. erythraea* was grown on glucose, a strong but temporary suppression of antibiotic formation was observed. During this antibiotic suppression phase, growth still occurred and the maximum erythromycin suppression occurred at 20 g/L glucose. Glucose only suppressed antibiotic formation when added before the production phase (Escalante *et al.*, 1982). This repression by glucose of antibiotic production has also been observed in other *Actinomycetes* (Martin and Demain, 1978).

The effect of ammonium on erythromycin production was studied by Potvin and Peringer (1994a), who reported that erythromycin production was higher when S. erythraea was grown in a medium containing ammonium nitrate than with one containing ammonium sulphate. A hypothesis was then proposed suggesting that glutamate produced from ammonium could be converted to glutamine via nitrate induced glutamine synthetase where glutamine could then be used as an erythromycin precursor (Potvin and Peringer, 1994b).

1.5.3 Hyphal Morphology

S. erythraea forms long mycelial strands over the course of a fermentation. These morphological changes can adversely affect the mixing within a stirred tank vessel (Li *et al.*, 1995), which can lead to a decrease in erythromycin concentration (Heydarian *et al.*, 1996). Hyphal breakage occurs in shake flasks and fermenters resulting in fragments incapable of producing antibiotics in many filamentous bacteria, this is because secondary metabolites such as erythromycin are only formed once the hyphae reach a certain length (Heydarian *et al.*, 1996; Martin and

Bushell 1996). This may account for the ability to synthesise antibiotics on agar, but not in liquid culture (Pickup *et al.*, 1993).

This is supported by other studies that have reported low productivity in cultures whose hyphae were highly fragmented (Shomura *et al.*, 1979; Roth *et al.*, 1982). Lilly *et al.*, (1992) reported a relationship between morphological changes and the rate of penicillin production by *Penicillium chrysogenum*. As discussed in Section 5.3.5, broth rheology can greatly influence *S. erythraea* fermentation process kinetics. This is a result of a change in the apparent viscosity within the fermenter caused by changes in the morphology of the organism. This will have subsequent effects on subsequent downstream product recovery (Davies *et al.*, 2000).

1.5.4 *Relationship between morphology and erythromycin production by* S. erythraea

There has been several studies on the hyphal strength of *S. erythraea* and the hyphal size at which erythromycin is produced. It was found that hyphal fragments greater than 88 μm, in diameter, exhibit erythromycin production (Martin and Bushell, 1996). This finding was consistent for stirred flasks and for baffled or unbaffled shaken flasks (Bushell *et al.*, 1997b). *S. erythraea* mutants which showed decreased branching frequency also had increased hyphal strength. This increased hyphal strength increased the number of particles with diameters greater than 88 μm and hence increased erythromycin production (Wardell *et al.*, 2002). The strength of hyphae were found to be about 60 % greater during growth phase compared to stationary phase. This is thought to be due to a thinner cell wall during stationary phase as the tensile strength was the same for both phases (Stocks and Thomas, 2001).

1.6 Aims and Objectives

The principal aim of this thesis is to develop an automated pH control system for implementation in microscale fermentations as a means of reducing cost and time scales of fermentation process development. *Saccharopolyspora erythraea* is to be used as a model organism. The specific objectives of this thesis are therefore:

Characterisation of the engineering environment within the shaken microwell (Chapter 3).

The initial objective will be to establish methods for the measurement of liquid phase mixing times (t_m) and oxygen mass transfer coefficients (k_La) in shaken 24-well plates in order to provide an insight into the performance of *S. erythraea* CA340 fermentations operation at the microscale. This will provide criteria for comparison with fermentation results obtained at larger scales and also for the design of a microwell pH control system.

Investigating the effect of pH control on *S. erythraea* fermentations (Chapter 4).

To further characterise the benefits of implementing pH control, a second major objective will be to quantify the benefits of implementing pH control in *S. erythraea* fermentations by applying different strategies of pH control at both the laboratory (7 L) and microscales.

Investigating the effect of fermentation media on *S. erythraea* fermentations (Chapter 5).

In order to select a suitable fermentation medium to be used during automated pH controlled microwell fermentations, the impact of different media types on fermentations of *S. erythraea* will be investigated.

Implementation of automated pH control in batch and fed-batch microrwell fermentations of *S. erythraea* (Chapter 6).

Based on the previous findings, an automated pH control system is designed and integrated with a liquid handling platform to carry out pH control during microwell fermentations of *S. erythraea*. The system will also be used during pH controlled fed-batch fermentations of *S. erythraea*.

A final aim was to consider the practical and economic aspects on microwell technology in industrial fermentation process development. This is a formal part of the EngD programme and so the report is included in Appendix B of this thesis.

2.0 Materials and Methods

2.1 Organisms and Storage Conditions

The main strain used during this study was *saccharopolyspora erythraea* CA340 which was kindly supplied by Abbott Laboratories (Chicago, IL). Spore stocks were initially prepared from *S. erythraea* CA340 grown on agar plates; the medium used contained 20 g L^{-1} agar (technical No. 1), 0.04 g L^{-1} EDTA, 2 g L^{-1} glucose, 5 g L^{-1} soy peptone, 1 g L^{-1} sucrose and 2.5 g L^{-1} yeast extract. The pH was adjusted to 7.0 using 0.1M NaOH prior to autoclaving. Spore suspension was streaked aseptically on the agar plate and incubated for three weeks at 28 °C. Spores were then removed using a sterile loop and collected into a tube. The suspension was aliquoted into 1 mL using 20 % (v/v) glycerol containing 0.1% (v/v) Tween 80 and stored at –80 °C.

An industrial strain of *S. erythraea*, EM5, supplied by Pfizer Ltd (Kent, UK) was also used during parts of this study (Chapter 5). The spore stock and storage conditions were according to the standard industrial guidelines set by the Bioprocess Development Group (BDG), Pfizer Ltd. Since this is an industrial production development strain specific details will not be included in this thesis.

2.2 Chemicals and Media

Chemicals used were all of analytical grade and were purchased from Sigma-Aldrich Chemical Company (Dorset, UK). Reverse osmosis (RO) water was used throughout for medium preparation. The medium mainly used throughout this thesis was a soluble complex medium (SCM) which has been previously used in fermentation studies within this laboratory (Davies *et al.*, 2000; Mirjalili *et al.*; 1999; Heydarian, 1998; Sarra *et al.*, 1996). The components of the SCM are listed

in Table 2.1. To avoid degradation of the nutrient sources, the glucose content of the medium was prepared and sterilised separately from other components. All other medium components were combined and autoclaved together. Prior to inoculation, the salts, glucose and trace elements were aseptically combined to the correct concentrations.

An industrial starch (SBM) and oil-based media (OBM), supplied by Pfizer Ltd (Kent, UK), were also used for some of the experiments described in Chapter 5. These media are currently being used in a production development programme and therefore, details of the chemical composition will not be included in thesis. Sterilisation of the media components was carried out *in situ* prior to inoculation.

Table 2.1 Soluble complex medium (SCM) components composition and concentrations

Component	Concentration (gL^{-1})
Glucose	30
Yeast Extract	6
Bacto-peptone	4
Polypropylene glycol	2.5
Glycine	2
$MgSO_4.7\ H_2O$	0.5
KH_2PO_4	0.68

2.3 Sterility Control

Spore suspensions of *S. erythraea* CA340 and EM5 were streaked aseptically on solid medium (as described in Section 2.1) and incubated at 37 °C for approximately 3 weeks before the spores were collected, during this period plates were checked regularly for growth of microorganisms. Colonies of *S. erythraea*

were visible after 3-4 days, whereas any contaminant would be expected to grow much faster. All manipulations were performed in a biosafety cabinet.

2.4 Stirred tank Fermenters Operating Conditions

2.4.1 7 L fermenter vessel (UCL)

Two fermentation vessels were used during this study. A 7 L stirred tank (LH 7L01 series by Inceltech Ltd., Pangbourne, UK) was used during experiments carried out using the *S. erythraea* CA340 strain at UCL. The vessel comprised two equally spaced top driven 6 bladed Rushton turbine impellers. The impeller shaft was supported by a bush in the bottom plate and the vessel was made from glass with stainless steel top and bottom plates. Heating was controlled by an electric element and cooling by passing chilled water through coils within the vessel. Full dimensions of the 7 L fermentation vessel are given in Table 2.2. Sterilisation was achieved by passing steam at 121 °C for 20 minutes. The pH was measured using a Mettler Toledo probe (Mettler GmbH, Urdork, Switzerland), which was sterilised *in situ* and calibrated outside the vessel using standards at pH 4.01 and pH 7.00 (BDH). The dissolved oxygen tension (DOT) was measured using a probe made by Ingold Messtechnik AG (Urdorf, Switzerland), which was also sterilised in *situ.* The DOT probe was calibrated for a zero reading outside the vessel by passing nitrogen gas (BOC, Surrey, UK) over the membrane and for 100% inside the vessel by sparging air at 2.5 vvm through the sterile medium prior to inoculation. The impeller speed was kept constant at 800 rpm for all 7 L fermentations. The exit gas composition was measured on-line using an MM8-80S mass spectrometer (VG Gas Analysis Ltd., Winsworth, UK). All fermentations were carried out with an aeration rate of 1 vvm at a temperature of 28 °C.

2.4.2 5 L fermenter vessel (Pfizer)

The work carried out with the industrial strain of *S. erythraea* EM5 was performed at Pfizer in a 5 L stirred tank fermenter (Electrolab Limited, Tewkesbury UK). The vessel was made of glass with a stainless steel top plate and agitation was achieved using two equally spaced Ruston turbine impellers. The impellers were top driven via a motor. Heating was achieved by placing the vessel in a thermo matt containing a heating element and cooling by passing chilled water through coils within the vessel. Full dimensions of the 5 L fermentation vessel are given in Table 2.2. The vessel was sterilised by autoclaving in a validated cycle at 121 °C.

The pH was measured using a calibrated Mettler Toledo probe (Mettler, Switzerland) and an Ingold Messtechnick (Switzerland) probe was used to measure the DOT within the vessel. The DOT probe was calibrated outside the vessel using nitrogen gas (0 %) and inside the vessel by passing air at 2.0 vvm (100 %) through the sterile medium prior to inoculation. Again the stirrer speed was kept at 800 rpm during all 5 L fermentations. The exit gas composition was analysed using a Prima 600 (Fisons Instruments, Switzerland) mass spectrometer. All fermentations were carried out with an aeration rate of 1 vvm at an operating temperature of 28 °C. During all fermentations carried out, testing for contamination was regularly made by streaking out, during incubation at 37 °C over 3-4 days period, agar plates with fermentation broth samples prior to visual observation for colonies.

2.4.3 Fermenter inoculation

For inoculation of all fermentations carried out in this study 1 mL of spore stock was first thawed and added to 50 mL nutrient broth (Sigma- Aldrich, Dorset, UK) in a 500 mL conical flask. The flask was then placed in an orbital shaker at 28 °C for 48 h. This culture was then transferred to 450 mL of medium (SCM, OBM,

SBM) in a 2 L conical flask and placed in an orbital shaker at 28 °C for 30 h. The inoculum volume used was always 10 % of the final working volume.

Table 2.2 Dimensions of 7 L and 5 L stirred tank fermenters used in this study

Dimension	Vessel ID LH 7L01	VESSEL ID PF5LMJ
Total volume (L)	7	5
Working volume (L)	5	3
Vessel diameter (mm)	160	145
Vessel Height (mm)	400	370
No. of impellers	2	2
Impeller diameter (mm)	62.3	59
Impeller tip dimensions (mm):		
Length	16	14
Width	2	2
Impeller spacing (mm)	88	85
Sparger No. of holes	6	4
Sparger diameter (mm)	9.5	8.3
Sparger height (mm)	400	370

2.5 Medium buffering capacity

To determine the buffering capacity of the SCM and fermentation broth at different intervals during the course of a fermentation, 10 mL of samples were taken throughout the course of 7 L fermentations (as described in Chapter 4) and titrated with NaOH. The solution to be titrated (whole broth containing cells, a biomass free broth, SCM and water) was placed in a beaker, heated at 28 °C by means of a heating plate and intensively mixed with a magnetic stirrer. The titrants (0.1, 0.2, 0.5, 1 and 5 M NaOH) were added to the solution using a graduated transfer burette. The initial pH of the solution and the titrant was measured using a micro-

combination pH electrode, (Section 2.6.4) and then measured at an interval of 5 minutes following the addition of each portion of the titrant into the solution.

The buffering capacity of the medium during a fermentation was also evaluated as described by Keun Jung and Hur, (2000):

$$\text{Buffering capacity} = {}^{C_{base}}\!/_{\Delta pH} \quad \textbf{(2.1)}$$

where ΔpH is the net change in pH following NaOH addition, and

$$C_{base} = \frac{\text{Base conc.(M)} \times \text{pump feed rate (mL/min)} \times \text{pulse length of pump (min)}}{\text{Total volume(mL)}} \quad \textbf{(2.2)}$$

2.6 Microwell Fermentation Equipment and Operating Conditions

2.6.1 Designed microwell system

Microwell scale fermentations were carried out using a specially designed microtitre plate as shown in Figure 2.1 and Figure 2.2. This design was specific to Pfizer 24-well plate and will be used throughout this thesis. The plate comprised six cylindrical wells; each well has a total capacity of 7 mL and a port for installing a pH or DOT probe at the side (6 mm diameter) 7 mm from the base. The lid has two additional ports on top of each well (3.5 mm id each), one for alkali/glucose addition and the other as an alternative option for insertion of a pH probe. Although this designed microwell system contained only six wells, 24 wells could fit on a standard plate foot print. The microwell block is made of polypropylene.

Sterilisation of the microwell system was carried out by autoclaving the block at 121 °C for 20 minutes.

During microwell fermentations the microtitre plate system was placed on an Eppendorf Thermomixer (Cambridge, UK) shaken at 300-800 rpm with an orbital throw of 3 mm. The temperature was controlled at 28 °C. Testing for contamination was carried out regularly by streaking out, during incubation at 37 °C over 3-4 days period, agar plates with fermentation broth samples prior to visual observation for colonies.

The SCM, SBM and OBM used during microwell fermentations were sterilised separately at 121 °C for 20 minutes, (as described in Section 2.2) prior to aseptically filling each well with the desired amount of the medium (typically 2-4 mL). A sacrificial well approach for sampling the broth was used during the course of each microwell fermentation, whereby the entire liquid volume of a single well was taken for dry cell weight and erythromycin analysis at a particular time during each fermentation. All fermentations were carried out in triplicate.

2.6.2 Inoculation of microwell fermentations

The inoculating procedure used during all microwell fermentations was kept the same as that used for the 7 and 5 L fermentations as described in Section 2.4.3. The final inoculum volume used was 10 % of the final working volume of the well.

2.6.3 Additions during manual microwell fermentations

During some microwell fermentations of *S. erythraea* pH control was carried out manually (Chapter 4), where additions of 80-200 μm of 0.1 M solution of NaOH were made throughout the microwell fermentations in order to control the pH near

a neutral value as shown in Figure 2.2. The frequency of NaOH addition was restricted to twice a day to avoid over filling the wells.

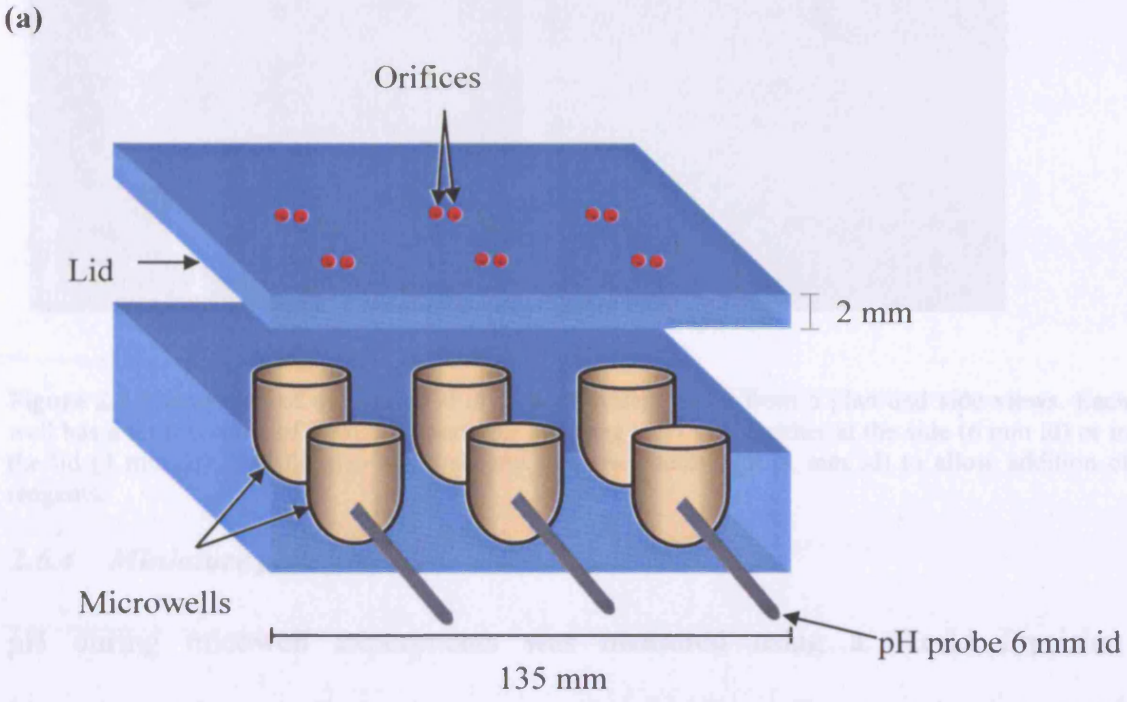

Figure 2.1 Schematic representation of the designed microwell system showing: (a) microwell block, (b) dimensions of a single well.

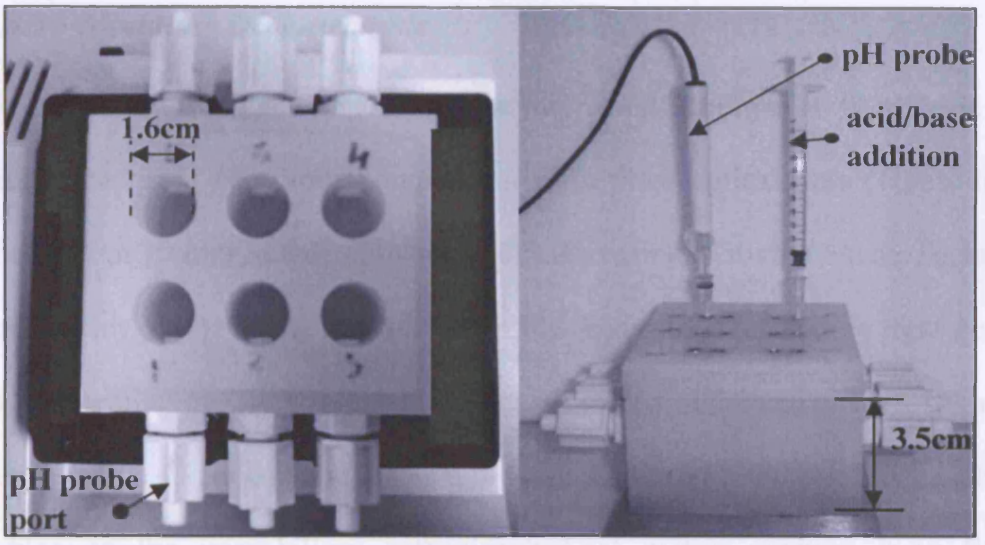

Figure 2.2 Photograph of the designed microwell system taken from a plan and side views. Each well has a total volume of 7 mL and ports for inserting a pH probe either at the side (6 mm id) or in the lid (4 mm id). The lid also has a second port over each well (4 mm id) to allow addition of reagents.

2.6.4 Miniature pH electrode

pH during micowell experiments was measured using a World Precision Instruments (Florida, USA) micro- electrochemical glass pH probe. The probe is 25 mm long and 0.9 mm in outer diameter and comprises a small combination pH electrode mounted in a 20G needle as shown in Figure 2.3. The probe is sterilised before and after use by immersing the end in a solution of sodium hypochlorite and rinsing with sterile water.

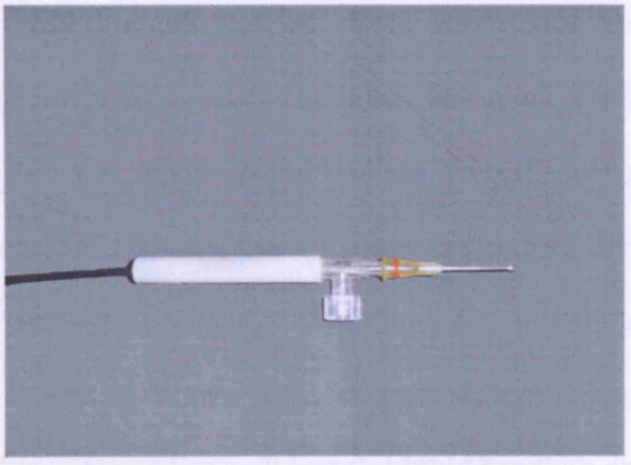

Figure 2.3 Photograph of the miniature pH electrode.

2.6.5 Miniature DOT electrode

To measure the oxygen transfer in the microwell a miniature fibre optic oxygen probe was used. The probe comprises a silica glass optical fibre (1 mm diameter) enclosed in 70 mm length stainless steel tube casing (Knight Optical Technologies Ltd. Surrey, UK). The sensor works on the theory of fluorescence light quenching of a ruthenium dye immobilised on a sol-gel matrix at the end of the working tip of the electrode. Light is passed from a blue LED source (470 nm), through fibre optic cables, to the immobilised ruthenium/sol-gel matrix exciting it to fluoresce. Oxygen molecules diffuse through the sol-gel matrix and interact with the ruthenium causeing the quenching of this florescence (Lamping *et al.*, 2003). The level of fluoresce was analysed using CCD detector array grating spectrometer (AVS-MC2000, Knight Optical Technologies Ltd. Surrey, UK). The dye fluorescence level is related to the oxygen concentration using the Stern Volmer equation (Wang *et al.*, 1999).

2.6.6 Automation of microscale fermentations

An integrated system consisting of Laboratory Virtual Instrument Engineering Workbench (LabVIEW) visual programming package (National Instruments Ltd) and a four tip Packard MultiPobe II Packard robotic arm (Perkin-Elmar Inc, Buchs, U.K) was used to implement automated pH control during microwell fermentations of *S. erythraea* CA340. The system comprises the specially designed microwell plate, a micro-combination pH electrode as the measuring element, a feed-back controller (LabView software package) and a Packard II robotic arm as the final control element as shown in Figure 2.4. Software integration of the different elements was carried out using Microsoft Excel. Liquid handling during automated pH control fermentations

(a)

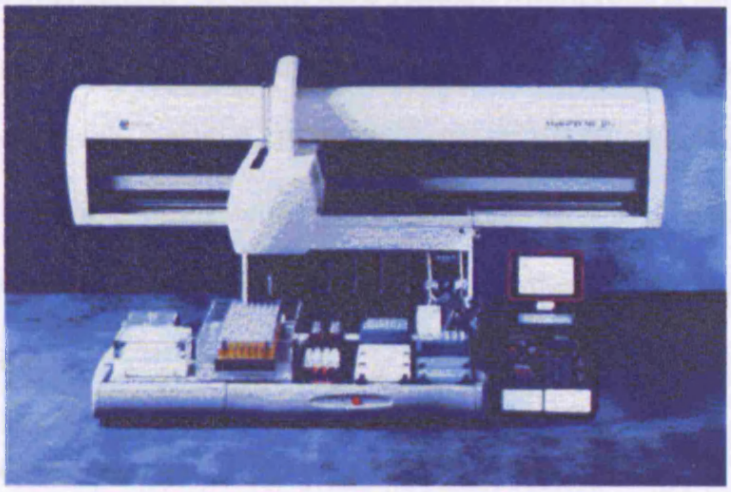

(b)

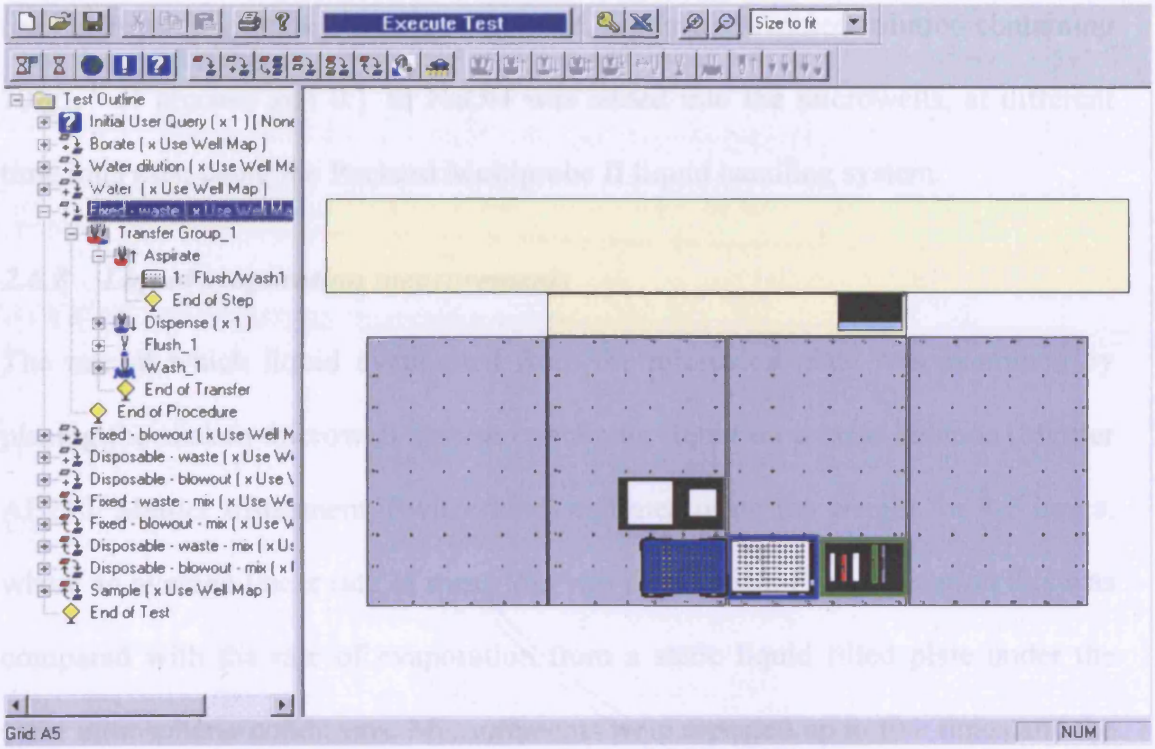

Figure 2.4 Photograph of the robotic Packard Multiprobe II system showing: (a) The Multiprobe II liquid handling robot with various microwell plates and troughs loaded on the platform. (b) The WinPrep software controlling the liquid handling operations.

of *S. erythraea* was carried out using the a Packard Multiprobe II robot as shown in Figure 2.4. Liquid was dispensed directly into the wells of the designed microwell system placed on the orbital Eppendorf thermomixer (Section 2.6.1). The thermomixer was interfaced with the Multiprobe II via a serial port and a programme was written for its manipulation by WinPreb, the software controlling the Multiprobe II.

2.6.7 Fed-batch operations

During automated, pH controlled, microwell fermentations of *S. erythraea* CA340, fed-batch feeding strategy was conducted (Chapter 6). A mixed solution containing 10 gL^{-1} of glucose and 0.1 M NaOH was added into the microwells, at different time intervals, using the Packard Multiprobe II liquid handling system.

2.6.8 Liquid evaporation measurements

The rate at which liquid evaporated from the microwell plate was examined by placing the shaken microwell system containing liquid on a mass balance (Mettler AE240, Mettler Instrument, Switzerland) and measuring the weight for 4-5 hours, where an average linear rate of mass loss was determined. For verification this was compared with the rate of evaporation from a static liquid filled plate under the same atmospheric conditions. Measurements were repeated up to five times and the variability obtained was 8.5 % for a maximum of 75 hours.

2.7 Engineering characterisation of shaken microwell system

2.7.1 Liquid phase hydrodynamics and evaluation of mixing time

Visualisation of the liquid phase hydrodynamics in a mimic of single 24 well was carried out using a high-speed digital camera (NAC Image Technology, Simi

Valley, CA, USA). The model was made from optically clear Perspex, with squarely flat sides to prevent image distortion, and mounted on a base equivalent to the standard microwell footprint to allow shaking in an Eppendorf Thermomixer as described in section 2.6.1. The liquid fill volumes used were 2.5 and 4 mL at different shaking speeds ranging from 300-800 rpm. The liquid phase mixing time (t_m) in the well was analysed by placing a drop of methylene blue dye (50/50 mixture of glycerol and bromophenol, Sigma Chemicals, Dorset, U.K) at the bottom of the well containing 95 % RO water and measuring the time taken for the dye to completely disperse in the liquid once shaking commenced. Complete mixing was achieved when the colour intensity in the solution was uniform. Images were recorded at a speed of 500 frames per second (fps) at a resolution of 496 x 104 pixels and were transferred into a PC for analysis. The mixing time was evaluated from individual frames collected by the video camera during the agitation period of the liquid.

2.7.2 Oxygen mass transfer rate measurements

In order to determine the oxygen mass transfer coefficient in the shaken microwell system (Section 2.6.1) a fibre optic oxygen sensor (as described in Section 2.6.5) was used to measure the dissolved oxygen concentration as a function of time. The oxygen transfer coefficient (k_La) was obtained from dissolved oxygen concentrations of an air-water mixture by using the gassing out technique as described by Van't Riet, (1979). The probe was calibrated at 100 % air saturation by vigorous shaking (300-800 rpm) of the liquid contents (typically 2-4 mL) while open to air, and 0 % air saturation by passing nitrogen gas through the well and waiting until a steady reading of 0 % air saturation was achieved. Nitrogen supply

to the well was then rapidly removed and the subsequent rise in oxygen concentration was then monitored as a function of time.

Experimental k_La values were calculated according to the well-mixed model for liquid and gas phases (Dunn and Einsele, 1975) using the following expression:

$$k_L a = \frac{1}{t} \ln\left(\frac{C^*}{C^* - C}\right) = \frac{1}{t} \ln\left(\frac{1}{C_L}\right) \quad \textbf{(2.3)}$$

where C is the concentration of oxygen in the liquid phase, C^* is the oxygen concentration in the gas phase and (C^* - C) is the driving concentration gradient between gas and liquid phase. C_L, the normalised oxygen concentration is defined as:

$$C_L = \left(\frac{C^* - C}{C}\right) \quad \textbf{(2.4)}$$

The sensor used in this study had a response time, τ_p (the time needed to record 63% of a stepwise change), of 42 s at 20 °C. This was measured using a standard procedure described by Dunn and Einsele, (1975). A fist-order response model described by Badino *et al.*, (2001) was used to account for the sensor response time in the calculations of the mass transfer coefficient k_La, thus:

$$\frac{dC_p}{dt} = \frac{1}{\tau_p}\left(C_L - C_p\right) \quad \textbf{(2.5)}$$

where C_p is the normalised dissolved oxygen concentration measured by the oxygen probe. Substituting for C_L in Equation (2.3) and integrating gives:

$$C_p = \frac{1}{t_m - \tau_p}\left[t_m \exp\left(\frac{-t}{t_m}\right) - \tau_p \exp\left(\frac{-t}{\tau_p}\right)\right] \quad \textbf{(2.6)}$$

where, $t_m = \frac{1}{k_L a}$

k_La values were obtained by solving Equation 2.6 using Microsoft Excel at each time measurement and the results were averaged from triplicate experiments.

2.7.3 Vapour-liquid surface tension

The vapour liquid surface tension (σ) was determined by the Du Nouy ring method, as described by Vazquez *et al.*, (1995), at 25 °C using Kruss K12 tensionmeter (Hamburg, Germany).

2.7.4 Computational fluid dynamics simulations

Theoretical predictions of the overall mass transfer coefficients in the microwell sytem (Section 2.6.1) was carried out using computational fluid dynamics (CFD). The simulations were carried out using a commercial software package CFX-4 (AEA Technology, Oxfordshire, United Kingdom) as described by Zhang *et al.*, (2005). The Reynolds-Averaged-Navier-Stokes (RANS) model was used to solve the three dimensional gas-liquid turbulent flow in the well. The system was modelled as a two fluid, gas-liquid system, where the total liquid volume fraction was based on the experimental liquid fill volume in each well. The total gas volume fraction derived from the simulation was then used to identify the position and structure of the main gas-liquid interface during orbital shaking.

2.8 Analytical methods

2.8.1 Biomass concentration

Biomass concentration of *S. erythraea* grown in SCM (Table 2.1) was measured using a HG53 Halogen Moisture Analyser (Mettler-Toledo, Urdorf, Switzerland) as described by Davies *et al.*, (2000). A 4 mL fermentation sample was vacuum filtered onto a pre-dried 0.2 μm, 25 mm diameter, filter paper (Whatmann Ltd, Surrey U.K). The filter paper containing cells was then dried in the moisture analyzer at 95 °C until a constant weight was achieved. The biomass concentration was determined as the difference of the weight of the cells plus filter and weight of the filter alone. All measurements were carried out in triplicate and the coefficient of variance (CV) was 4.3 %.

2.8.2 Glucose concentration

The assay used was based on the reducing sugar method with dinitrosalicylic acid (DNS) as described by Miller (1959). Fermentation broth samples were diluted by a factor of 10 with RO water, 0.4 mL of diluted samples were then dispensed into test tubes to which 0.5 mL of DNS reagent was added. Samples were incubated in boiling water for 5 minutes. The tubes were then placed on ice and 4 mL of water added, after which the absorbance was read at 540 nm. Glucose concentrations were calculated from a previously prepared standard curve (see Appendix A). All measurements were carried out in triplicate and a CV of 3 % was calculated.

2.8.3 Starch concentration

The concentration of soluble starch was carried out at Pfizer, according to the BDG analytical services guidelines. The method was based on HPLC analysis using an Aminex HPX87H column (Bio-Rad, CA, USA). The following conditions were

used: mobile phase, H_2SO_4 (6 $mmolL^{-1}$), flow rate, 0.8 $mLmin^{-1}$; and temperature, 65 °C. A refractometer (model PU 4026; Philips, Heindoven, Netherlands) was used for detection; with a retention time of 5 minutes.

2.8.4 Oil concentration

The concentration of oil in *S. erythraea* fermentations grown in OBM was carried out using hexane extraction, based on a method described by Junker *et al.*, (1998). A 5 mL sample was mixed with 15 mL of hexane for 3 minutes and then centrifuged at 4000 rpm for 30 minutes to separate the phases. A 1 mL sample of the hexane phase was then dispensed into a pre-weighed aluminium container and dried at 85 °C in a Halogen Moisture Analyser (Mettler-Toledo, Urdorf, Switzerland) to a constant weight. All samples were measured in duplicate and a CV of 4 % was calculated.

2.8.5 Erythromycin concentrations

The concentration of the various forms of erythromycin was determined by HPLC. Fermentation broth samples were centrifuged at 4000 rpm for 20 minutes (Beckman CS-6R centrifuge, Beckman, Buchs, UK) and the supernatant collected. Erythromycin was then concentrated by a factor of 5-10 using C18 bond elute cartridges (Phenomenex, Cheshire UK) as described by Heydarian *et al.*, (1998b). HLPC analysis was subsequently performed on a Beckman model 126 HPLC system equipped with a Beckman model 166 UV detector operated at 215 nm. The column used was a Polymer Laboratories PLR P-S (8 μm). Acetonitrile in 10 mM potassium dihydrogen phosphate (pH 7) was used as the mobile phase, which was pumped isocratically at 1.0 mL min^{-1}. The column temperature was controlled at 70 °C with a block column heater and the sample injection volume was 20 μL. The

chromatogram peaks of erythromycin present on the samples was identified from known standards. A typical standard curve range for the erythromycin assay is shown in Appendix A. All samples were measured in triplicate and a mean and standard deviation calculated. The CV calculated was 3.8 %.

2.8.6 Fermentation broth viscosity

Direct biomass concentration measurements of the OBM fermentation broth (Section 2.2) was not possible due to the presence of undissolved solids. As it has previously been shown by Karsheva *et al.* (1997), biomass concentration is directly proportional to broth viscosity; therefore, the viscosity of the OBM was measured using a rotational viscometer (Haake Rotovisco RV20, Germany). Total sample volume used was 10 mL at a shear rate of 70 s^{-1}. All measurements were carried out in triplicate and a 2.5 % CV was calculated.

2.8.7 Density measurements

Densities of fermentation media and broth samples were carried out by weighing a fixed volume of sample in a sensitive digital balance, Mettler AE240 (Mettler Instrument, Switzerland), and then calculating the density of the sample using:

$$\rho = \frac{m}{v} \tag{2.7}$$

where ρ is the density of the sample and m and v are the mass and volume of the sample, respectively. All measurements were carried out at room temperature in triplicate.

2.8.8 Fermentation media rheology

Fermentation broth rheology was measured at 25 °C using a rotational viscometer (Haake Rotovisco RV20, Germany) with a double concentric cylinder (1.02-1.14 radii ratio range and 0.35-2.6 mm gap range). The rheology of the SCM, OBM and SBM was measured over a shear rate range of 24-1256 s^{-1}. All fermentation media were shown to exhibit non-Newtonian behaviour and adhere to the pseudoplastic Power Law of viscosity (Atkinson and Mavituna, 1991):

$$\tau = K \gamma^n \qquad \textbf{(2.8)}$$

where τ is the shear stress exerted on the system (Pa), γ is the shear rate (s^{-1}) and K and n are the consistency and flow behaviour dimensionless indices respectively. From the values of K and n the viscosity, μ_a (Pa.s) at a given shear rate can be calculated:

$$\mu_a = K \gamma^{n-1} \qquad \textbf{(2.9)}$$

2.8.9 Image Analysis

A method described by Packer and Thomas (1990) and more recently by Heydarian (1998a) was used for image analysis. Fermentation samples of *S. erythraea* CA340 were diluted 400-fold and 40 µL of each sample is transferred to a slide, air dried aseptically in a biosaftey cabinet and stained with mixed solution of ethanol and methylene blue for 1 minute. Images were viewed and processed using a Leica Image Processing and Analysis System (Leicia Imaging Systems Ltd, Cambridge, U.K) which was connected to a Polyvar microscope (Lecia, Cambridge, U.K). The

measured variables were main hyphal length (ML) and branch length (BL), using a 100 x 25 magnification. The number of objects viewed ranged between 20-900. The standard deviation for all measurements taken is presented in Appendix A.

3.0 Engineering Characterisation of Shaken Microwell System

3.1 Introduction

Microwell plates have been widely used in analytical and high throughput screening applications for the past fifty years (Manns, 1999), Recently, shaken microwell systems have been the subject of a growing number of bioprocess studies involving microbial fermentation (Wittmann *et al.*, 2003, John *et al.*, 2003, Dutez *et al.*, 2000) and animal cell culture (Girard *et al.*, 2001). Here the aim is to be able to perform a number of process optimisation experiments in parallel. There is also the implicit assumption that results from the microwell will be predictive of those at larger scales. This necessitates an understanding of the engineering characteristics of shaken culture vessels.

Oxygen transfer is a key parameter for the growth and scale-up of aerobic cultures. As reported by Ulrike and Buchs (2001) and Buchs *et al.*, (2001) the key parameters affecting oxygen transfer rate (OTR) in shaken systems include; (a) vessel shape, size, and surface properties, (b) shaking frequency and diameter, (c) fill volume and (d) the physico-chemical properties of the process fluid such as density, viscosity, and diffusivity. Furthermore, in the case of microorganisms showing filamentous morphology, the complex rheology of the fermentation broth can pose additional challenges for aeration and mass transfer (Pena *et al.*, 2002).

Transport limitations have been regarded as one of the major problems leading to process yield reduction in large-scale bioprocesses (Amanullah *et al.*, 1993). At the laboratory and pilot scales, mixing issues arising from geometrical and operational factors have been extensively studied and documented (Amanullah *et al.*, 2001,

Bouaifi and Roustan, 2001, Nienow, 1998,), as have the distribution of shear stresses throughout various vessels (Alvarez *et al.*, 2002). Various other issues associated with mixing and oxygen transfer have been reported for the operation of industrial scale bioreactors. Recently, Jian Li *et al.*, (2002) reported a large-scale (80 m^3) study involving quantitisation of recombinant enzyme expression at different impeller power supplies in fungal fermentations. Ariff *et al.*, (1997) discussed the effect of mixing on an enzymatic bioconversion reaction, while Vrabel *et al.*, (2001) reported the effect of mixing on top–bottom gradients in glucose concentrations (limiting substrate) in large-scale fermenters. Enfors *et al.*, (2001) have also presented experimental evidence of the complex physiological responses of microorganisms when exposed to the more inhomogenous conditions frequently encountered in larger scale bioreactors.

For the *S. erythraea* CA340 to be studied here the generation of an adequate mixing environment within each microwell is vital in order to assure homogeneous conditions for cell growth, and to minimise any negative impact on the functionality of shear-sensitive cells. In addition, during microwell fermentations, it is the intention that liquids are added throughout to regulate pH and to control the supply of nutrients. These must also be rapidly mixed within the well contents to minimise the formation of gradients. Finally, quantification of mixing times and oxygen transfer rates will be important from the point of view of process design and scale-up.

3.2 Aims and Objectives

The aim of this chapter is to precisely characterise the engineering environment in shaken 24 well plates. This will provide insight to the performance of *S. erythraea* CA340 fermentations operation at this scale and also provide criteria for

comparison with fermentation results obtained at larger scales. The specific objectives of this chapter are therefore:

1. Establish methods for the measurement of liquid phase mixing times (t_m) and oxygen mass transfer coefficients (k_La) in shaken 24-well plates.
2. Quantify t_m and k_La as a function of well shaking frequency and fill volume and explore the use of parallel computational fluid dynamics (CFD) to predict these key process variables.
3. Carry out preliminary microwell fermentations of *S. erythraea* CA340 to show how the engineering environment of a microwell impacts on cell growth kinetics and hyphal morphology of *S. erythraea* CA340.

3.3 Results and Discussion

3.3.1 Visualisation of liquid phase hydrodynamics in shaken 24-well plates

Knowledge of liquid phase mixing underpins the engineering characterisation of shaken microwells. This is a complex phenomenon due to the variation of different factors governing fluid motion, including vessel geometry, fill volume, hydromechanical forces and fluid properties (Maier and Buchs, 2001). Initial Experiments to observe the liquid hydrodynamics and to quantify the liquid phase mixing times during shaking were carried out as described in Section 2.7.1 using high speed video photography.

Figure 3.1 shows representative examples of high speed video camera frames taken during orbital shaking of a single well mimic from a 24-well plate (Section 2.7.1). Images were obtained with a liquid fill volume of 2.5 mL at different shaking frequencies. The liquid meniscus remains largely undisturbed at shaking frequencies lower than 500 rpm; the surface of the liquid is almost stationary at a

shaking frequency of 300 rpm both at fill volumes of 2.5 mL and also 4 mL (images not shown for larger fill volume). At shaking frequencies of 500 rpm and above the liquid starts moving around the walls of the well and a vortex is created. The depth of the vortex increases with increasing shaking frequency. Hermann *et al.*, (2002) reported that a critical shaking frequency of 450 $Lmin^{-1}$ must be exceeded in a 96-round deepwell plate in order to overcome the surface tension of the liquid within each well. A similar critical shaking frequency of 500 rpm appears to exist for the larger wells used here. The trend shown in Figure 3.1 of an increase in the surface area available for gas-liquid mass transfer with increasing shaking frequency will be discussed later in Section 3.3.3.

It should be noted that it was not possible to agitate microwells with liquid fill volumes of 2.5-4.0 mL at shaking frequencies higher than 800 rpm since the surface of the liquid was broken and liquid was thrown out of the well.

The impact of different process fluids (water, soluble complex medium (SCM) and oil base medium(OBM)) on liquid phase hydrodynamics at a fill volume of 2.5 mL and a shaking frequency of 800 rpm are shown in Figure 3.2. Vortex formation and deformation are seen to be similar for water and SCM. However, with the more viscous oil based medium OBM (Table 3.1), the liquid surface shows little deformation since the applied centrifugal forces are unable to overcome the higher surface tension of this viscous fluid (Hermann *et al.*, 2002). Again, the impact of the process fluid on oxygen mass transfer will be observed later in Section 3.3.3.

3.3.2 Quantification of liquid phase macro-mixing times

During agitation of the well mimic containing 2.5 mL of water, shaken at 800 rpm, it was observed that shortly after agitation commenced (t = 6 s), the liquid begins to rotate around the walls of the well while the added trace dye remained unmoved at the base of the well. Progressively, the maximum height of the liquid increases and a vortex is created at 2.3 seconds. At this point an axial motion is established in the fluid, and the liquid containing the tracer dye is lifted off the base of the well and begins to disperse throughout the liquid in the well. Homogeneity is reached after 4.8 seconds as determined by the colour intensity of the tracer dye being uniform along the main axis of the well mimic.

Table 3.1 Values of the vapour-liquid surface tension, density and viscosity for different process fluids. All measurements were carried out at 28 °C. Measurements were carried out as described in Sections 2.7.3, 2.8.7 and 2.8.6.

Process fluid	Density (ρ) ($kg\ m^{-3}$)	Viscosity (μ) (mPa.s)	Surface tension (σ) (mNm^{-1})
Water	1000	1	72.6
SCM	1200	1.3	72.7
OBM	15000	6.2	80.5

Table 3.2 summarises liquid phase mixing times measured using water and SCM as function of shaking frequency and fill volume. There is an increase in t_m from 5-840 s, for a water fill volume of 2.5 mL at 800 and 300 rpm as compared to 17-2280 s for fill volume of 4 mL at shaking frequencies of 300 and 600 rpm. For the SCM again, the mixing time generally increased with increasing fill volume and decreasing shaking frequency. These mixing times are in good agreement with those reported by Weiss *et al* (2002) on a recent experimental study on liquid phase mixing in agitated microplates.

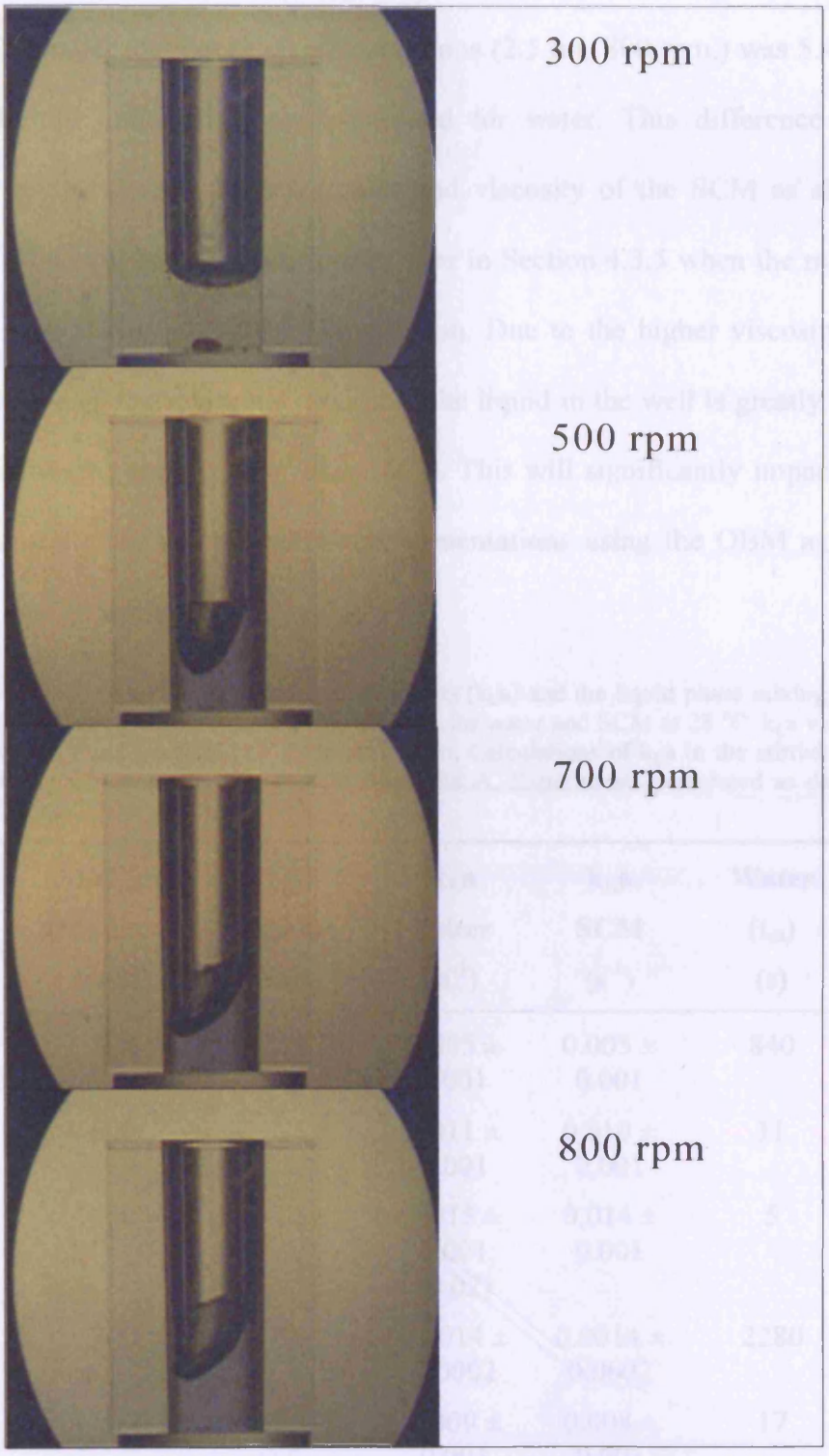

Figure 3.1 High speed video camera images showing the effect of shaking frequency on liquid phase hydrodynamics in the microwell system. Example indicates images obtained using water at a fill volume of 2.5 mL and a shaking diameter of 3 mm, as described in Section 2.7.1. Images were taken 6 seconds after shaking commenced once a stable fluid motion was established.

Compared to water as the process fluid, the liquid phase mixing time determined for the SCM under identical shaking conditions (2.5 mL 800 rpm,) was 5.4 s. This is only slightly longer than t_m determined for water. This difference can be explained by the slightly higher density and viscosity of the SCM as shown in Table 3.1. This will be discussed further later in Section 4.3.5 when the microwell system is used during microbial fermentation. Due to the higher viscosity of the OBM (6.2 mPa.s), the rotational motion of the liquid in the well is greatly reduced resulting in mixing times higher than 200 s. This will significantly impact on the oxygen transfer rates during microwell fermentations using the OBM as will be described later in Section 5.2.6.

Table 3.2 Measured oxygen mass transfer coefficients (k_La) and the liquid phase mixing times (t_m) as a function of shaking frequencies and fill volumes for water and SCM at 28 °C. k_La values given in parenthesis are those predicted by CFD simulation. Calculations of k_La in the stirred tank were carried out using a correlation described in Appendix A. Experiments performed as described in Sections 2.7.2 and 2.7.3.

Geometry	Shaking frequency (rpm)	Fill volume (mL)	k_La water (s^{-1})	k_La SCM (s^{-1})	Water (t_m) (s)	SCM (t_m) (s)
24-well	300	2.5	0.005 ± 0.001	0.005 ± 0.001	840	843
24-well	600	2.5	0.011 ± 0.001	0.010 ± 0.001	11	10
24-well	800	2.5	0.015 ± 0.001 (0.02)	0.014 ± 0.001	5	5
24-well	300	4.0	0.0014 ± 0.0002	0.0014 ± 0.0002	2280	2284
24-well	600	4.0	0.009 ± 0.001 (0.01)	0.008 ± 0.001	17	18
Stirred-tank	800	5000	0.038	0.036	N.D	N.D

ND: not determined.

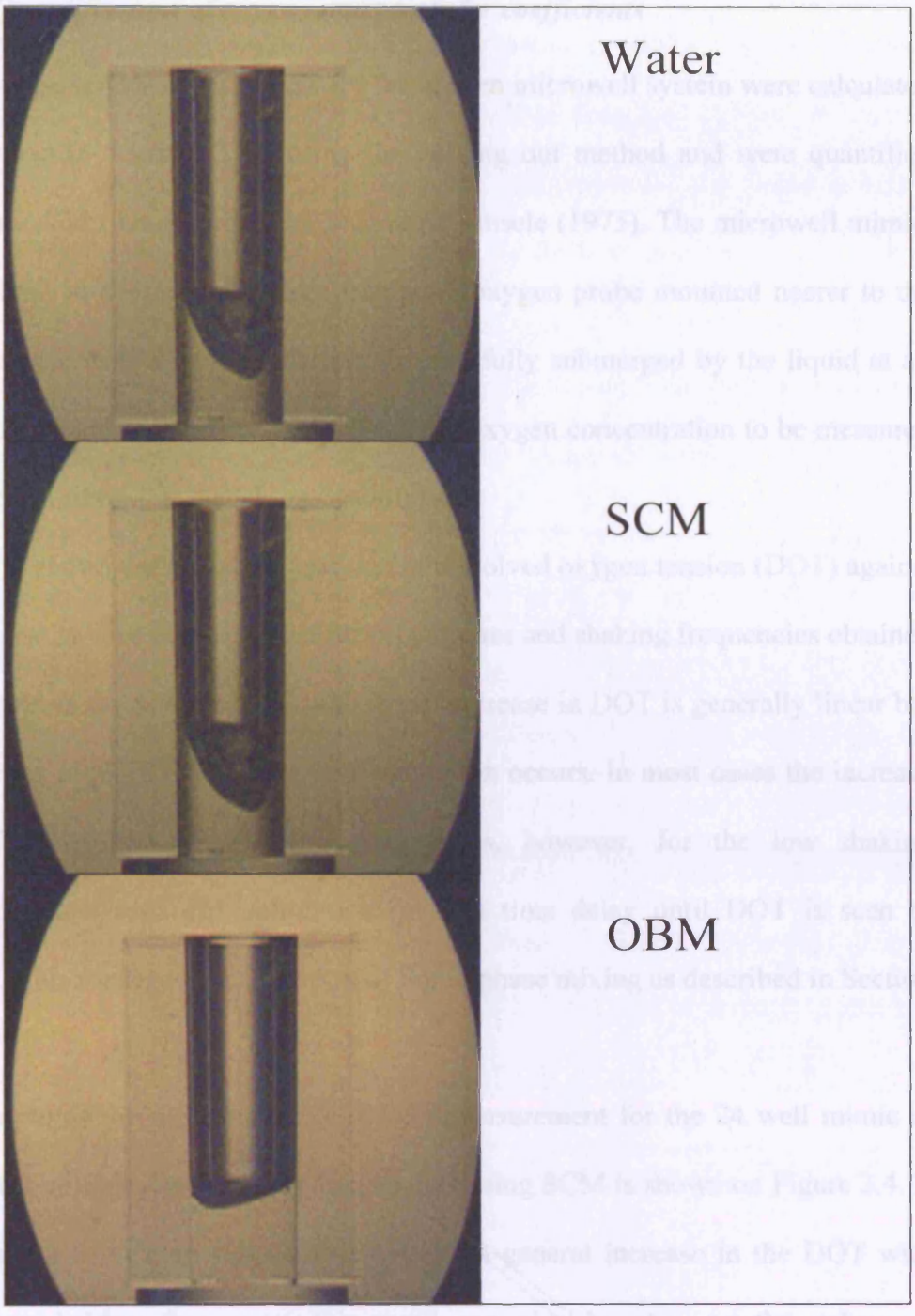

Figure 3.2 Images from high speed video camera showing the effect of shaking frequency on liquid hydrodynamics within the microwell system for different process fluids: water, soluble complex medium (SCM) and oil based medium (OBM). Experiments carried out with fill volumes of 2.5 mL shaken at 800 rpm and a shaking diameter of 3 mm, as described in Section 2.7.1. Images were taken 6 seconds after shaking commenced once a stable fluid motion was established.

3.3.3 Quantification of oxygen mass transfer coefficients

Oxygen mass transfer coefficients for the shaken microwell system were calculated as described in Section 2.7.2 using the gassing out method and were quantified using a method first described by Dunn and Einsele (1975). The microwell mimic, as described in Section 2.6, had a miniature oxygen probe mounted nearer to the bottom of the well to ensure that the tip was fully submerged by the liquid at all times. This enabled the increase in dissolved oxygen concentration to be measured as a function of time and shaking conditions.

Figure 3.3 shows the measured increase in dissolved oxygen tension (DOT) against time for the 24 well mimic at various fill volumes and shaking frequencies obtained using water as the process fluid. The initial increase in DOT is generally linear but decreases at higher DOT values until saturation occurs. In most cases the increase in DOT is rapid once shaking commences, however, for the low shaking frequencies and high fill volumes there is a time delay until DOT is seen to increase. This relates to the initiation of liquid phase mixing as described in Section 3.3.1.

An example of the oxygen uptake (OUR) measurement for the 24 well mimic at various fill volumes and shaking frequencies using SCM is shown on Figure 3.4. It is noticeable from both figures that there is a general increase in the DOT with increasing shaking frequency; this trend can also be seen on the values of calculated k_La shown in Table 3.2 as discussed on Section 3.3.2.

Calculated k_La values for experiments with water carried out with 2.5 and 4.0 mL fill volumes at different shaking frequencies are presented in Table 3.2. A maximum k_La value of 0.015 s^{-1} is observed at a shaking frequency of 800 rpm and a fill volume of 2.5 mL. At a fill volume of 4 mL and a shaking frequency of 300

rpm the k_La value is ten times lower than that obtained with 2.5 mL fill volume at 800 rpm. In general there is a trend of increasing k_La with increasing mixing frequency and decreasing fill volume similar to that described in Section 3.3.2 for liquid phase mixing times. This trend in k_La values is related to an increase in gas-liquid interfacial areas seen with decreasing fill volume and increasing shaking frequencies as shown in Section 3.3.1. This suggest that the specific surface area, a, is the dominant parameter, rather than the mass transfer coefficient, k_L, which controls the oxygen transfer capability of shaken microwell systems.

As well as mixing, the geometry of the microwell can also be expected to have an influence on the oxygen mass transfer coefficients. As represented in, Figure 2.1, the 24 well geometry used here is cylindrical with a hemispherical base, which can result in the liquid within this area to remaining unmoved while there is a circulation in the bulk of the liquid. Hermann *et al.*, 2002 and Kato *et al.*, (1996) have reported an increase in interfacial area available for mass transfer in box-shaped shaken vessels and microwells caused by the square corners of the box acting as baffles.

3.3.4 CFD predictions of liquid hydrodynamics and oxygen transfer rates

In addition to the experimental approaches described previously CFD was also used to predict fluid motion in shaken microwells and predict k_La values. The basis of CFD simulation is described in Section 2.7.4. Initially it is important to verify that the CFD approach reasonably predicts the location and structure of the interface between gas and liquid within a well.

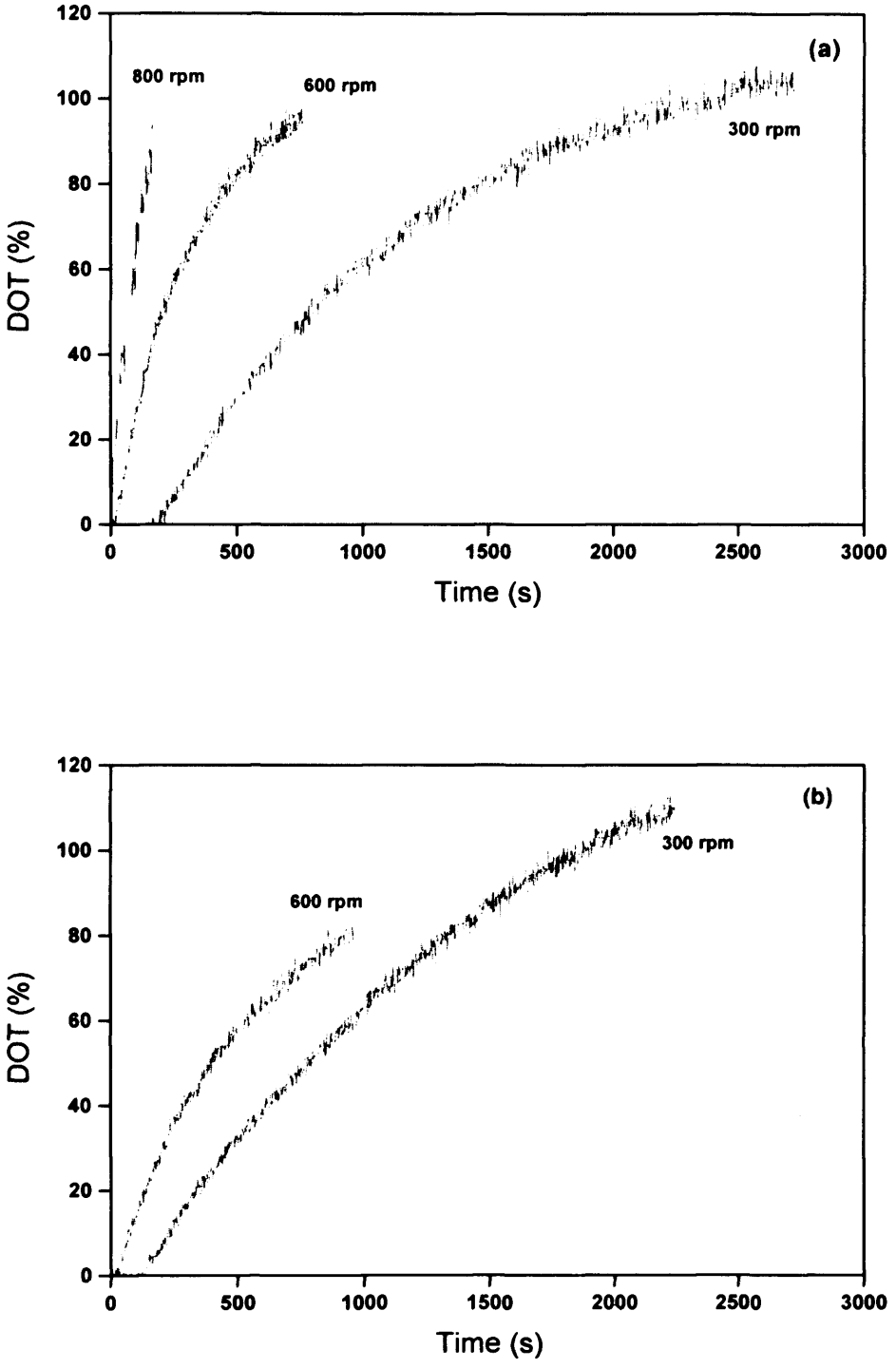

Figure 3.3 Example of oxygen uptake kinetics for water shaken at different shaking frequencies at fill volumes of (a) 2.5 mL (b) 4 mL. Experiments carried out as described in Section 2.7.2.

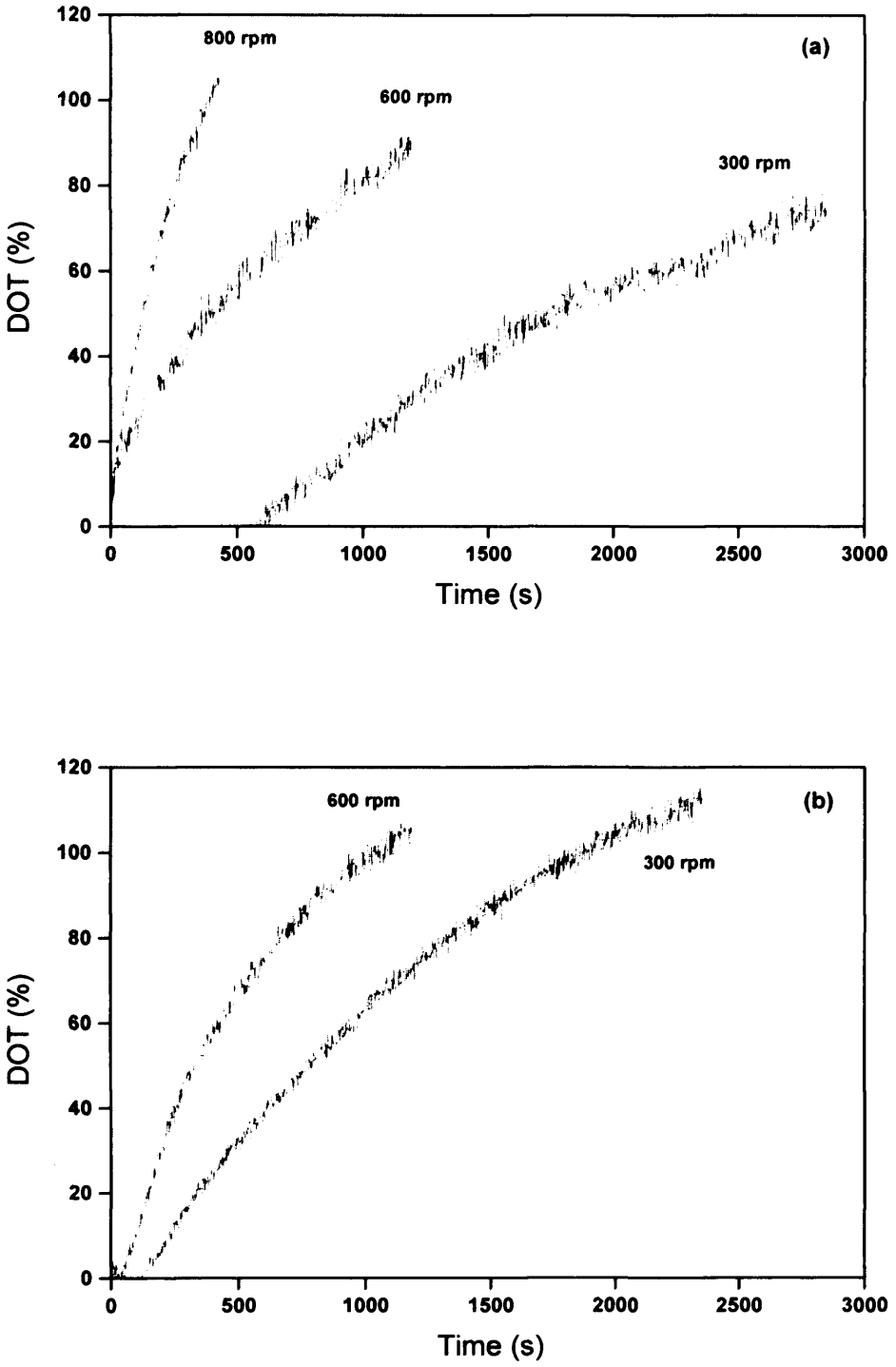

Figure 3.4 Example of oxygen uptake kinetics for SCM shaken at different shaking frequencies at fill volumes of (a) 2.5 mL (b) 4 mL. Experiments carried out as described in Section 2.7.2.

Figure 3.5 shows an example of the CFD predictions of the gas–liquid interface pattern during shaking of a microwell. The images are cross sections of the y plane under two operating conditions. It can be observed that the location and structure of the gas-liquid interface changes with the point in a rotational cycle (0-360 degrees) under the action of centrifugation, gravity and surface tension forces. The surface of the liquid is taken to be under the predicted local gas-liquid volume fraction in the range of 0-1. In this case there is a reasonable agreement with the high speed video images shown in Figure 3.1, which verifies the CFD predictions of fluid motion. The CFD simulation predicted an increase in interfacial area with increasing the shaking frequency and decreasing the fill volume, this is in good agreement with high speed video images shown in Figure 3.1 In Table 3.2 k_La values predicted from the CFD simulations are shown in brackets for the conditions of shaking a 2.5 mL and 4 mL fill volumes of water at 800 and 600 rpm respectively. These results also correlate well with those obtained experimentally as discussed previously in Sections 3.3.2 and 3.3.3.

3.3.5 Impact of engineering environment on microwell S. erythraea *CA340 fermentation kinetics*

It was shown previously in Sections 3.3.2 and 3.3.3 how key engineering parameters such as t_m and k_La varied as a function of fluid fill volume and shaking frequency. In this section the results of preliminary microwell fermentations are reported and it is shown how they relate to the measured oxygen transfer values. For comparison, results from a 7 L stirred bioreactors are also shown.

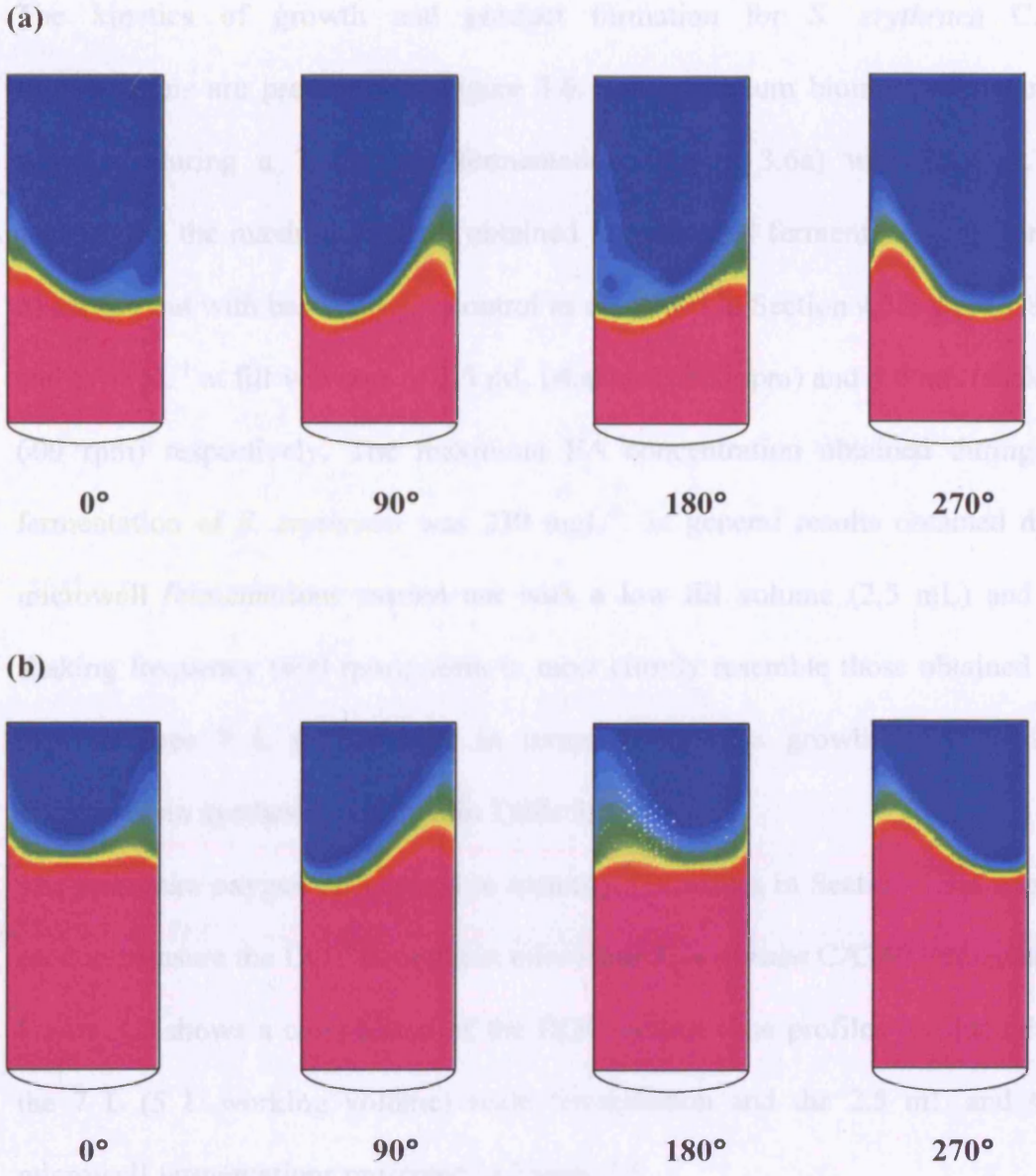

Figure 3.5 CFD simulation of gas-liquid volume fraction in the shaken microwell system at different degrees of rotation with (a) fill volume of 2.5 mL shaken at 600 rpm, (b) fill volume of 4 mL shaken at 600 rpm. The red and green colours represent the homogenous (volume fraction =1) liquid and gas phases respectively. Simulations were conducted as described in Section 2.7.4.

The kinetics of growth and product formation for *S. erythraea* CA340 fermentations are presented in Figure 3.6. The maximum biomass concentration achieved during a 7 L scale fermentation (Figure 3.6a) was 9.45 gL^{-1}. In comparison the maximum values obtained in microwell fermentations (Figure 3.6 b) carried out with base only pH control as described in Section 4.3.5 were 7.8 gL^{-1} and 6.90 gL^{-1} at fill volumes of 2.5 mL (shaken at 800 rpm) and 4.0 mL (shaken at 600 rpm) respectively. The maximum EA concentration obtained during 7 L fermentation of *S. erythraea* was 230 mgL^{-1}. In general results obtained during microwell fermentations carried out with a low fill volume (2.5 mL) and high shaking frequency (800 rpm); seem to most closely resemble those obtained from the reference 7 L fermentation in terms of biomass growth rate, yield and erythromycin synthesis as shown in Table 3.3.

The miniature oxygen probe used to quantify k_La values in Section 3.3.3 was also used to measure the DOT throughout microwell *S. erythraea* CA340 fermentations. Figure 3.7 shows a comparison of the DOT against time profiles obtained during the 7 L (5 L working volume) scale fermentation and the 2.5 mL and 4 mL microwell fermentations presented in Figure 3.6.

Table 3.3 Comparison of growth and product formation in batch 7 L and microwell scale fermentations of *S. erythraea* CA340. Fermentations were performed as described in Sections 2.4.1 and 2.6.1 respectively.

Geometry	Shaking/Mixing Frequency (rpm)	Fill Volume (mL)	μ_{max} (h^{-1})	X_{max} (gL^{-1})	EA_{max} (mgL^{-1})	DOT_{min} (%)
24-well	600	4.0	0.03	6.9	134	5
24-well	800	2.5	0.06	7.8	173	20
Stirred-tank	800	5000	0.09	9.5	230	36

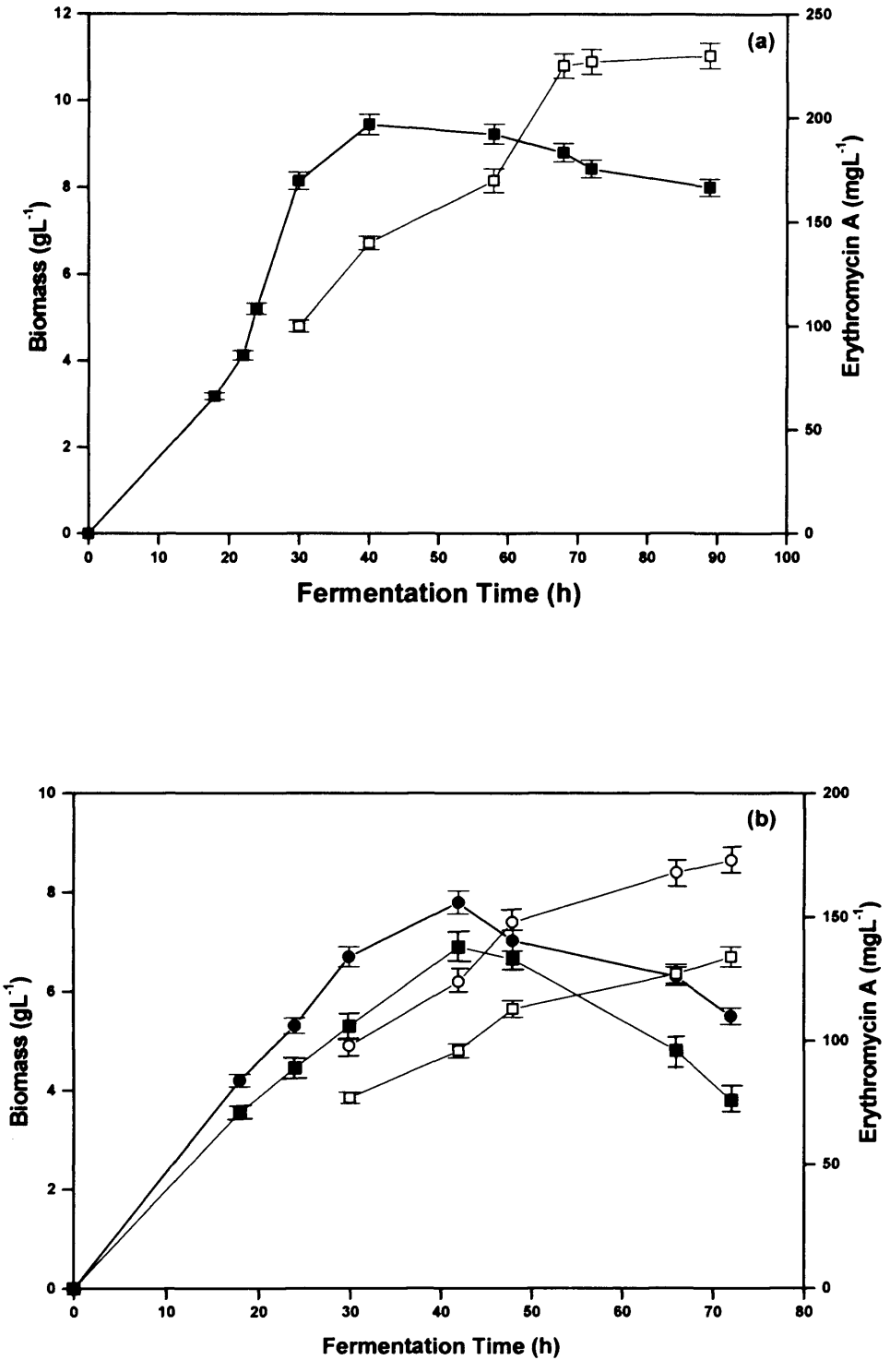

Figure 3.6 Growth (■) and erythromycin formation (□) kinetics for a typical *S. erythraea* CA340 fermentations at: (a) 7 L scale, agitated at 800 rpm (b) Growth (■) and erythromycin formation (□) kinetics for 4.0 mL microwell scale, shaken at 600 rpm and growth (♦) and erythromycin formation (○) kinetics for 2.5 mL shaken at 800 rpm. Fermentations were carried out as described in Sections 2.4.1 and 2.6.1 respectively.

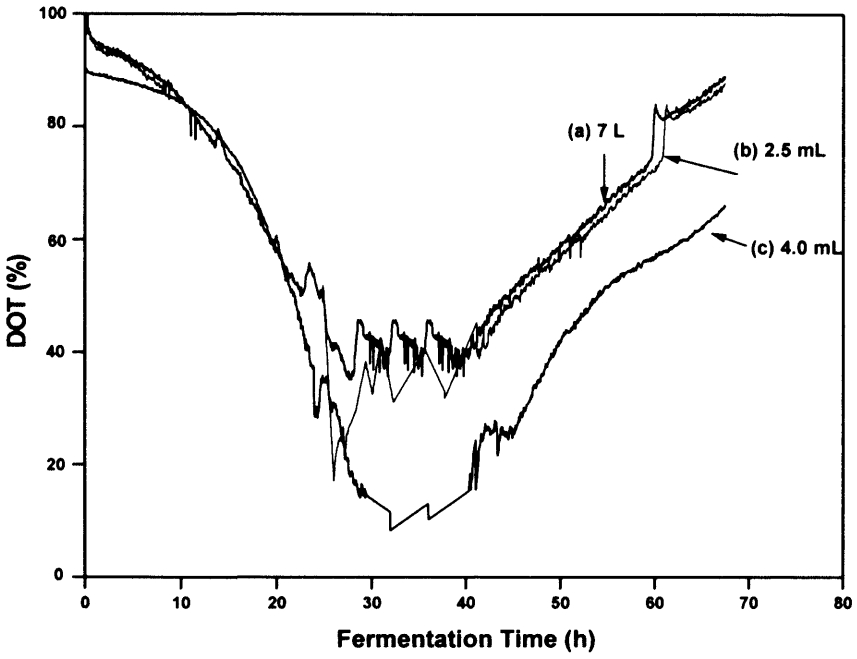

Figure 3.7 Typical on-line DOT profiles obtained during: (a) 7 L scale fermentation, mixed at 800 rpm, (b) 2.5 mL microwell fermentation, shaken at 800 rpm, (c) 4 mL microwell fermentation, shaken at 600 rpm. Experiments were carried out as described in Sections 2.4.1 and 2.6.1.

As shown in Table 3.2, for the 7 L scale bioreactor mixed at 800 rpm, with a superficial gas velocity of 1 vvm the calculated k_La (Appendix A) was 0.038 s^{-1}. This is about twice that for the 2.5 mL microwell fermentation shaken at 800 rpm but 4 times higher than that obtained for a 4.0 mL shaken at 600 rpm. It therefore, seems that k_La and hence the ability to supply oxygen to the microwell culture is a key parameter in determining *S. erythraea* CA340 growth and erythromycin production. The slightly higher growth rates and erythromycin levels obtained in the 7 L bioreactor compared to the 2.5 mL microwell fermentation shaken at 800 rpm are due to the higher k_La that can be obtained in stirred vessels.

The impact of pH on *S. erythraea* CA340 growth and erythromycin biosynthesis at batch microwell and 7 L scales fermentations will be described further in Chapter 4.

3.3.6 Impact of engineering environment on S. erythraea *CA340 morphology*

As shown in the previous section a limitation of using microtitre plates for cultivation of aerobic microorganisms is the low aeration rate and its possible consequences on the physiology of the organism, Duetz and Witholt, 2001., Enfors *et al.*, 2001. It is therefore important to study the interaction between the fluid dynamics of shaken microwells and the physiological responses of an organism, especially one with a filamentous nature like *S. erythraea.*

The morphology of *S. erythraea*, has been shown to be an important factor in erythromycin biosynthesis (Bushell *et al.*, 1997; Heydarian *et al.*, 1998a) and would influence the rheology and mass transfer properties of the fermentation broth. Dispersed filamentous growth, while favourable for erythromycin biosynthesis (Heydarian, 1998a) may lead to a highly viscous and pseudoplastic behaviour, resulting in poor mixing, and broth inhomogeneities (Duetz and

Witholt, 2001, Treskatis *et al.*, 1996). On the other hand, when subjected to intensively turbulent flows the mycelia structure can be adversely affected by the action of flow forces resulting from the normal surface pressure and shear stresses (Heydarian *et al.*, 1999; Ayazi Shamlou *et al.*, 1994). Previous studies by Davies (2001) and Heydarian (1998a) have reported that in a stirred fermentation vessel the higher the impeller speed, the smaller is the average size of the mycelia produced in the fermenter.

Figure 3.8 shows typical images of *S. erythraea* CA340 morphology captured during the microwell scale (2.5 mL and 4 mL fill volume) and a 7 L scale fermentations shown in Figure 3.6. Image analysis was carried out using a method described by Packer and Thomas, (1990, Section 2.8.9).

In all fermentations carried out, no pellets formation was observed and the images taken for up to 25 hours are from the lag phase of the fermentation where the existence of both individual and highly branched mycelia can be seen, as shown in Figure 3.8. The mean main length of the freely dispersed mycila, shown in Figure 3.9, tended to increase during the exponential growth phase reaching a maximum of 48 μm and then decreasing towards the end of the fermentation in the 7 L stirred vessel. The maximum ML measured during microwell fermentations was 42 μm (2.5 mL, 800 rpm) and 28 μm (4 mL, 600 rpm) and the general trend resembled that seen with the 7 L scale fermentation.

The mean branch length also increased during the exponential growth phase for all the fermentations, reaching a maximum of 10.6 μm and 8.5 μm for the 7 L and 2.5 mL (shaken at 800 rpm) microwell fermentations respectively. During fermentations with 4 mL fill volume at 600 rpm it was observed that the branching phase was somewhat slower, this might be due to the slower growth kinetics in this

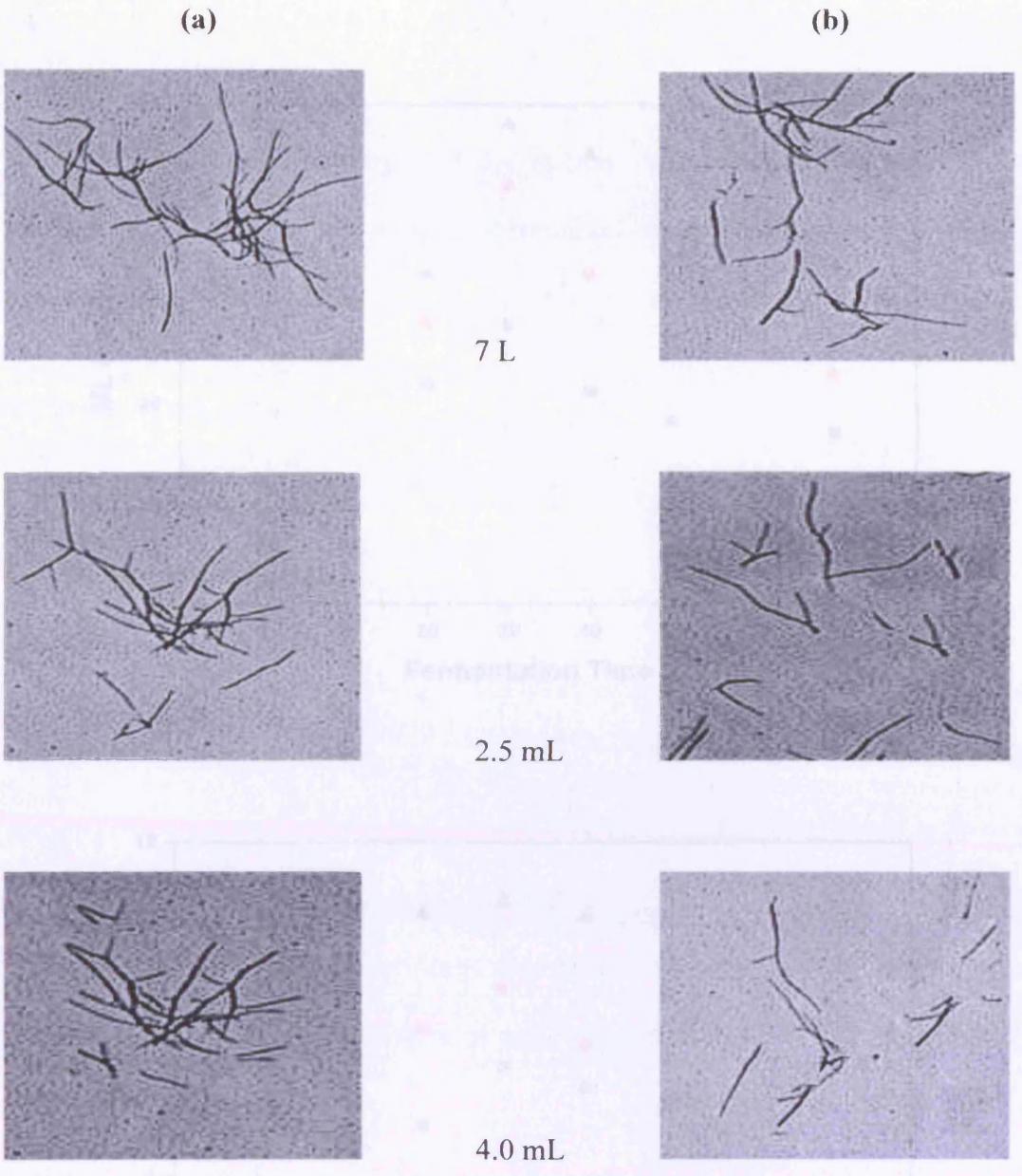

Figure 3.8 Representative images of *S. erythraea* CA340 hyphae during: 7 L fermentation mixed at 800 rpm, 2.5 mL fermentation shaken at 800 rpm and, 4 mL fermentation shaken at 600 rpm showing: (a) mycelial clumps, (b) freely dispersed mycelia. (Scale, 1mm = 2μm). All samples prepared at the same dilution rate. Image analysis carried out as described in Section 2.8.9. Fermentations correspond to the profiles seen in Figure 3.6.

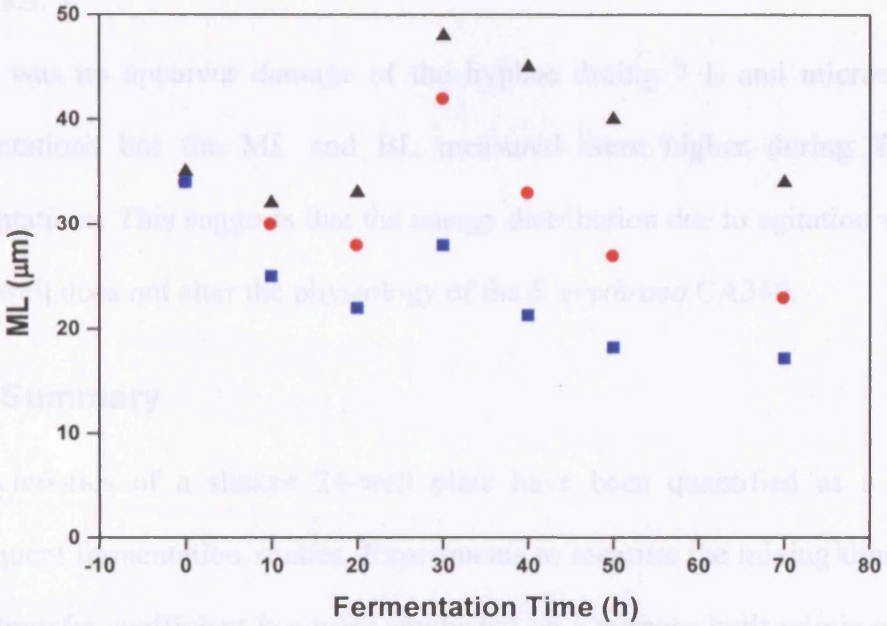

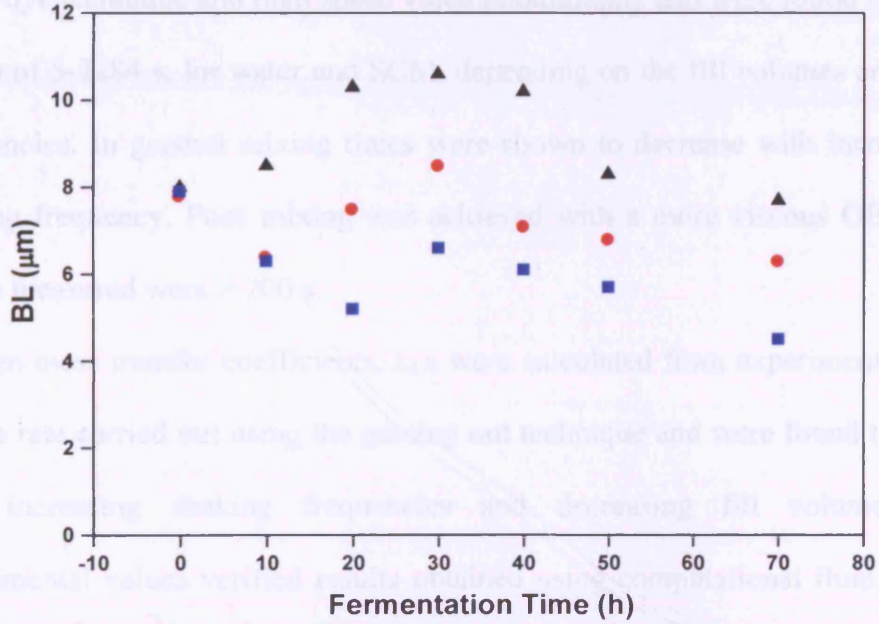

Figure 3.9 Example of morphological measurements showing the variation of ML and BL with time for fermentations carried out at: (▲) 7 L scale fermentation, mixing speed 800 rpm, (●) 2.5 mL microwell fermentation, shaken at 800 rpm, (■) 4 mL microwell fermentation, shaken at 600 rpm. Data corresponds to fermentation profiles shown in Figure 3.6. Image analysis and quantification were carried out as described in Section 2.8.9. Standard deviation of repeated measurements shown in Appendix A.

case and the poor mixing and aeration rates as discussed earlier in Sections 3.3.2 and 3.3.3.

There was no apparent damage of the hyphae during 7 L and microwell scale fermentations but the ML and BL measured were higher during 7 L scale fermentations. This suggests that the energy distribution due to agitation within the microwell does not alter the physiology of the *S. erythraea* CA340.

3.4 Summary

Characteristics of a shaken 24-well plate have been quantified as a basis for subsequent fermentation studies. Experiments to measure the mixing time (t_m) and mass transfer coefficient k_La were conducted on a purpose built mimic of a single well. Experiments carried out to measure t_m within the well were conducted using a tracer-dye technique and high speed video photography and were found to be in the region of 5-2284 s, for water and SCM, depending on the fill volumes and shaking frequencies. In general mixing times were shown to decrease with increasing the shaking frequency. Poor mixing was achieved with a more viscous OBM and t_m values measured were > 200 s.

Oxygen mass transfer coefficients, k_La were calculated from experimental oxygen uptake rate carried out using the gassing out technique and were found to increase with increasing shaking frequencies and decreasing fill volumes. These experimental values verified results obtained using computational fluid dynamics simulations of the microwell geometry to predict the fluid flow behaviour and oxygen mass transfer coefficients.

The kinetics of growth and product formation for *S. erythraea* CA340 during micowell fermentations were found to be higher at low fill volumes and higher shaking frequencies. This is thought to be due to the higher oxygen transfer rates

available during fermentations carried out at higher shaking speeds and lower fill volumes.

The impact of the engineering environment within the microwell on the morphology of *S. erythraea* was examined and the results showed that the hyphae length obtained during microwell fermentations were shorter than those obtained during 7 L scale fermentations. No apparent damage to the hyphae was observed during microwell fermentations

4.0 Effect of pH Control on *S. erythraea* Fermentation

4.1 Introduction

The creation of microscale fermentation procedures could have significant benefits at all stages of fermentation process development from discovery through to process optimisation (Doig *et al.*, 2004). For both microbial and mammalian fermentations pH is a vital process parameter as it has a marked affect on cell growth rate, viability and product synthesis. The effect of fermentation pH on the growth kinetics of microorganisms has been examined previously by a number of authors including Elibol *et al.*, (2002); Amanullah *et al.*, (2001) and Tang *et al*, (1989), all have concluded that pH is one of the most important environmental factors for cell growth and product formation. The action of the enzymes that catalyse all metabolic reactions are themselves governed by a range of chemical and environmental conditions, especially pH, which can exert a marked control on enzyme activity (Moat and Foster, 1988). Fermentation pH can also determine complex physiological parameters such as membrane permeability and cell morphology.

Recently there has been growing interest in microscale fermentation processes carried out in microtitre (microwell) plate formats, Lye *et al.*, (2003). The small volumes required and the use of parallel, automated experimentation has the potential to greatly reduce fermentation development times compared to conventional shake flask approaches. Published examples to date involve the growth of *E. Coli* (Weuster-Botz *et al.*, 2001; Kostov *et al.*, 2001) and *Streptomycete* species (Duetz *et al.*, 2000; Minas *et al.*, 2000) with some data reported on pH profiles during microwell or miniature scale fermentations

(Lamping *et al.*, 2003; Harms *et al.*, 2002). However, there has been no attempt so far, to actually control important process parameters such as pH and dissolved oxygen tension (DOT) in microscale fermentations.

Given the importance of fermentation pH its measurement and control is a fully automated process in virtually all laboratory and large-scale bioreactors. The basis of this on-line control is the point measurement of pH using a pH probe followed by a pulse injection of acid or base in response to a deviation from the set point (Amanullah *et al.*, 2001; Singh *et al.*, 1986).

In this chapter the influence of various pH control strategies on growth and erythromycin synthesis by *S. erythraea* CA340 is described at the 7 L and microwell scales. The results presented in this chapter have also been published as Elmahdi, I., Baganz, F., Dixon, K., Harrop, T., Sugden, D., Lye, G.J. **2003.** pH control in microwell fermentations of *S. erythraea* CA340: Influence on biomass growth kinetics and erythromycin biosynthesis. Biochem. Eng. J. **16**, 299-310.

4.2 Aims and Objectives

Having previously characterised the engineering environment within the shaken designed microwell (Chapter 3), the aim of the work carried out in this chapter is to demonstrate the benefits of implementing pH control in microwell fermentations. The specific objectives are:

1. To quantify the influence of pH on *S. erythraea* CA340, grown on SCM (Table 2.1), on cell growth and erythromycin biosynthesis.
2. Establish quantitative data on pH changes occurring during *S. erythraea* CA340 fermentations and the buffering capacity of the medium as a basis for developing manual pH control.

3. Demonstrate the utility of manual pH control in microwell scale fermentation. This will form the basis for designing an automated pH control system in the microwell as will be described later in Chapter 6.

The organism used in this study is *Saccharopoyspora erythraea* CA340, which produces the polyketide antibiotic erythromycin as a secondary metabolite. The most active form of the various erythromycin analogs synthesised is erythromycin A (EA) as described on Section 1.4.6.

4.3 Results and Discussion

4.3.1 Effect of pH control strategy in 7 L S. erythraea *CA340 fermentations*

In order to justify the development of a pH control system for microscale fermentations it is first necessary to establish the practical benefits. These could be related to both the kinetics of biomass growth and the biosynthesis of erythromycin A and its analogs (Section 1.4.6). As a reference for subsequent results, Figure 4.1(a) shows a typical profile for a batch 7 L scale fermentation of *S. erythraea* CA340 carried out with full pH control as described in Section 2.4.1. Replicate fermentations under the same conditions routinely produced similar results. The biomass concentration is seen to reach a maximum of 10 gL^{-1} at around 40 h while the erythromycin A concentration reaches a peak of 230 mgL^{-1} after approximately 70 h. The maximum volumetric rate of glucose utilisation was 0.94 $gL^{-1}h^{-1}$ coinciding with the exponential growth phase of the cells. The main carbon source in the SCM fermentation is glucose and the relatively low concentration of 30 gL^{-1} in this batch medium formulation is likely to be the limiting factor in relation to the biomass and antibiotic levels achieved (Davies, 2001).

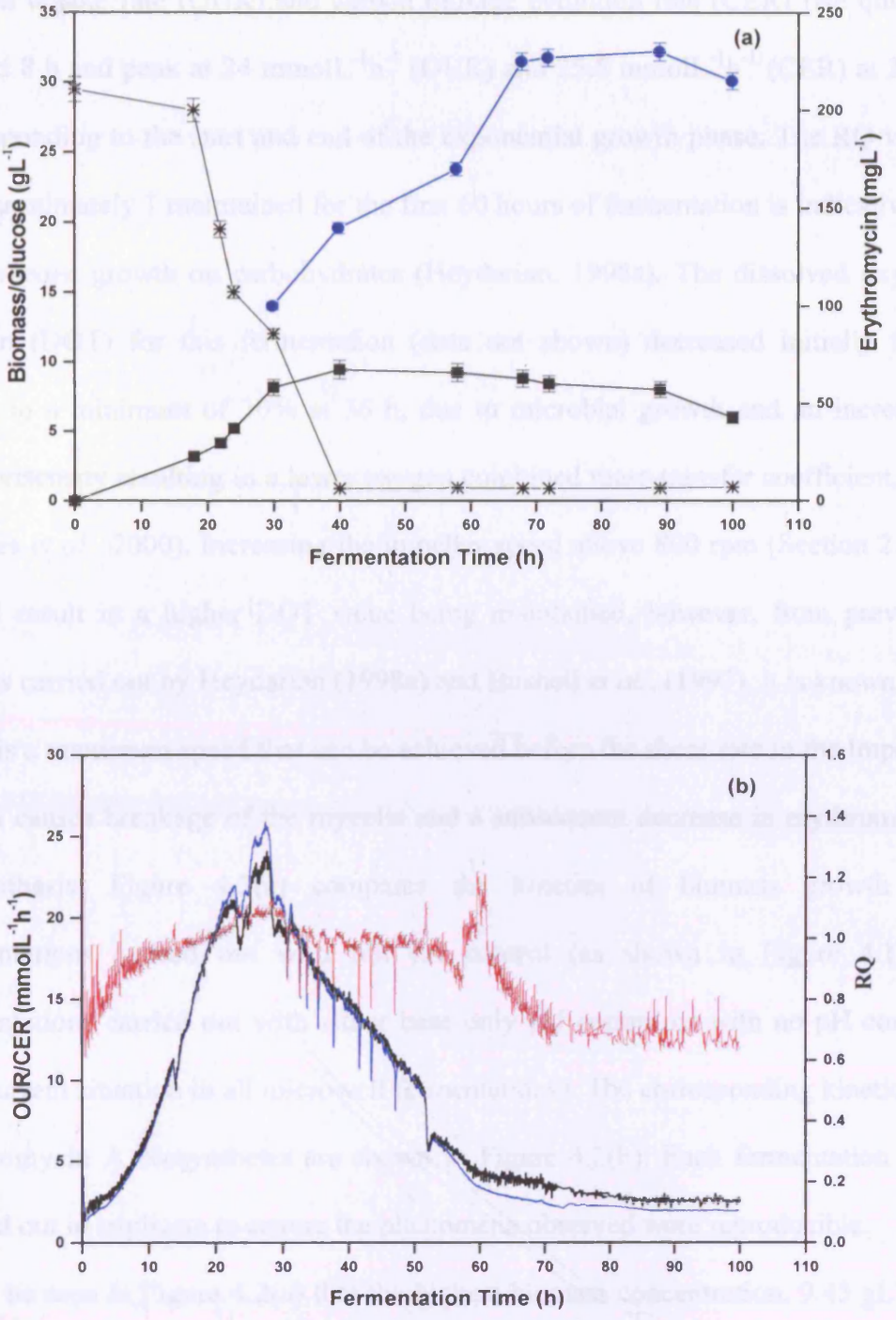

Figure 4.1 Profile of typical 7 L batch fermentation of *S. erythraea* CA340 grown on a SCM with full pH control showing: (a) biomass concentration (■), glucose concentration (*) and erythromycin A concentration (●). (b) on-line exit gas data: carbon dioxide evolution rate (CER:-), oxygen uptake rate (OUR: -), and respiratory quotient (RQ: -). Error bars represent standard deviation of triplicate measurements. Fermentation performed as described in Section 2.4.1.

The on-line exit gas profiles for this fermentation are shown in Figure 4.1(b). The oxygen uptake rate (OUR) and carbon dioxide evolution rate (CER) rise quickly around 8 h and peak at 24 $mmolL^{-1}h^{-1}$ (OUR) and 25.6 $mmolL^{-1}h^{-1}$ (CER) at 30 h, corresponding to the start and end of the exponential growth phase. The RQ value of approximately 1 maintained for the first 60 hours of fermentation is indicative of *S. erythraea* growth on carbohydrates (Heydarian, 1998a). The dissolved oxygen tension (DOT) for this fermentation (data not shown) decreased initially from 100% to a minimum of 30% at 36 h, due to microbial growth and an increased broth viscosity resulting in a lower oxygen combined mass-transfer coefficient, k_La (Davies *et al.*, 2000). Increasing the impeller speed above 800 rpm (Section 2.4.1) would result in a higher DOT value being maintained, however, from previous studies carried out by Heydarian (1998a) and Bushell *et al.*, (1997), it is known that there is a maximum speed that can be achieved before the shear rate in the impeller region causes breakage of the mycelia and a subsequent decrease in erythromycin biosynthesis. Figure 4.2(a) compares the kinetics of biomass growth for fermentations carried out with full pH control (as shown in Figure 4.1) to fermentations carried out with either base only pH control or with no pH control (the current situation in all microwell fermentations). The corresponding kinetics of erythromycin A biosynthesis are shown in Figure 4.2(b). Each fermentation was carried out in triplicate to ensure the phenomena observed were reproducible.

It can be seen in Figure 4.2(a) that the highest biomass concentration, 9.45 gL^{-1}, is obtained in fermentations with full pH control while the maximum obtained without pH control, 5.93 gL^{-1}, is almost two fold lower. In the case of base only pH control the maximum biomass concentration obtained is about 8 gL^{-1}, 60% higher than that obtained with no pH control.

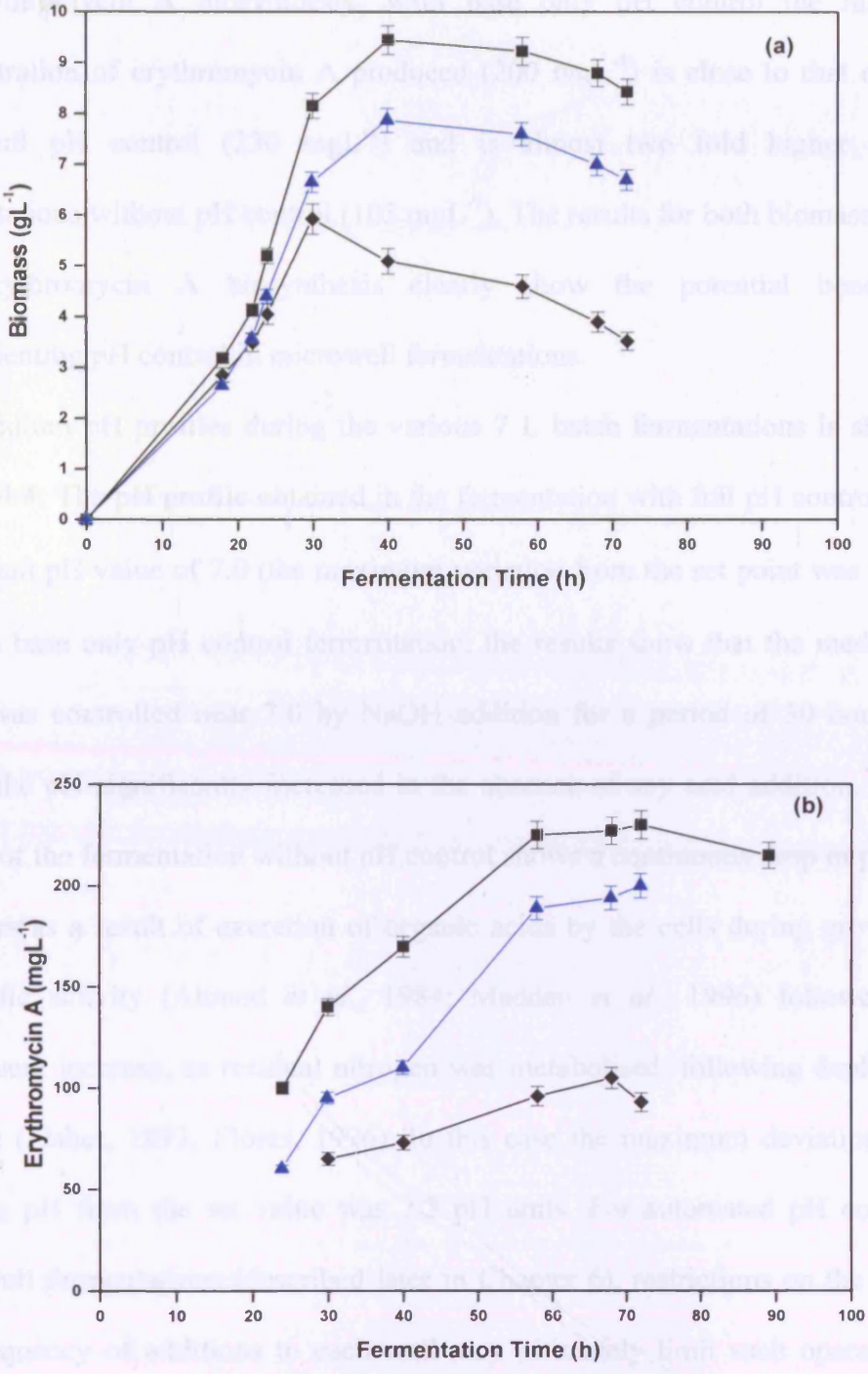

Figure 4.2 Comparison of 7 L batch fermentation of *S. erythraea* CA340 carried out with various pH control strategies: (a) biomass concentration: full pH control (■), base only pH control (▲), no pH control (♦). (b) corresponding erythromycin A concentration (EA). Error bars represent standard deviation of triplicate analytical measurements. Fermentations were performed as described in Section 2.4.1.

A similar effect to that seen with the biomass concentration is seen in Figure 4.2(b) for erythromycin A biosynthesis. With base only pH control the maximum concentration of erythromycin A produced (200 mgL^{-1}) is close to that obtained with full pH control (230 mgL^{-1}) and is almost two fold higher than in fermentations without pH control (105 mgL^{-1}). The results for both biomass growth and erythromycin A biosynthesis clearly show the potential benefits of implementing pH control in microwell fermentations.

The medium pH profiles during the various 7 L batch fermentations is shown in Figure 4.4. The pH profile obtained in the fermentation with full pH control shows a constant pH value of 7.0 (the maximum variation from the set point was ± 0.03). For the base only pH control fermentation, the results show that the medium pH value was controlled near 7.0 by NaOH addition for a period of 30 hours after which the pH significantly increased in the absence of any acid addition. The pH profile of the fermentation without pH control shows a continuous drop in pH up to 60 hours as a result of excretion of organic acids by the cells during growth and metabolic activity (Ahmed *et al.*, 1984; Madden *et al.*, 1996) followed by a subsequent increase, as residual nitrogen was metabolised, following depletion of glucose (Fisher, 1993; Flores, 1996). In this case the maximum deviation of the medium pH from the set value was 2.2 pH units. For automated pH control in microwell fermentations (described later in Chapter 6), restrictions on the volume and frequency of additions to each well may ultimately limit such operations to either base only or acid only addition. In the case of *S. erythraea* CA340 fermentation it is clear that base only pH control will be the most useful in terms of enhanced biomass production and erythromycin biosynthesis.

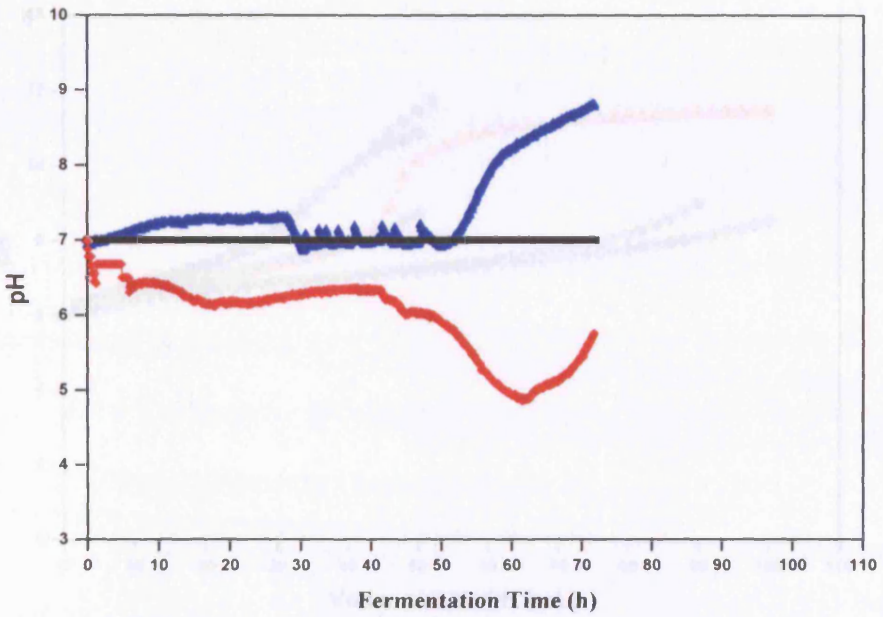

Figure 4.3 Variation of medium pH values with time during 7 L batch fermentations of *S. erythraea* CA340 carried out with full pH control (-), base only pH control (-), no pH control (-). Fermentations carried out as described in Section 2.4.1.

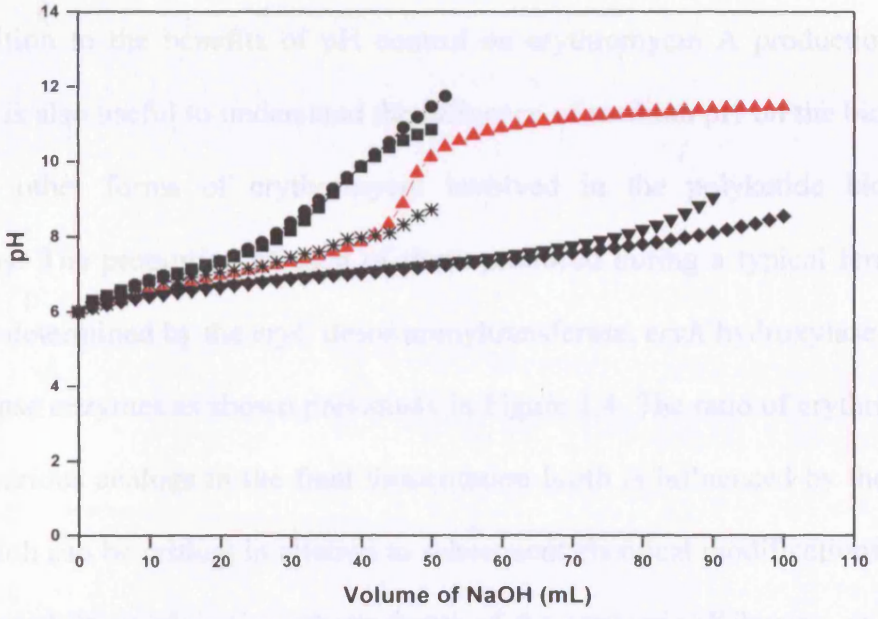

Figure 4.4 Titration curves for media fractions from the 7 L *S. erythraea* CA340 base only pH control fermentation as shown in Figure 4.2. Whole broth after 48 h (♦), whole broth after 64 h (▼), medium prior to inoculation (*), SCM (▲), biomass free broth after 48 h (■), biomass free broth after 64 h (●).Titration curves determined as described in Section 2.5.

4.3.2 Influence of pH control strategy on erythromycin biosynthesis

In addition to the benefits of pH control on erythromycin A production (Figure 4.2), it is also useful to understand the influence of medium pH on the biosynthesis of the other forms of erythromycin involved in the polyketide biosynthetic pathway. The proportion of each of these produced during a typical fermentation will be determined by the *eryC* desosaminyltransferase, *eryK* hydroxylase and *eryG* methylase enzymes as shown previously in Figure 1.4. The ratio of erythromycin A to its various analogs in the final fermentation broth is influenced by the medium pH which can be critical in relation to subsequent chemical modifications involved in the production of semi-synthetic forms of the antibiotic (Kibwage, *et al.*, 1987; Carreras *et al.*, 2002).

Table 4.1 shows the variation in the different erythromycins produced during the time course of each of the 7 L fermentations described in Section 4.3.1. It is noticeable that erythromycin C is present in small quantities at pH values near neutral (6.40-7.01) but increases at higher pH values. The maximum ratio of erythromycin A to C in the fermentation with full pH control (11:1) is significantly higher than for base only pH control (6:1) which is three times greater than that in the absence of pH control (2:1). The concentration of erythromycin B in all fermentation samples was lower than the detection limit of the HPLC assay (Section 2.8.5). The formation of this erythromycin analogue is reported to take place during oxygen limitation when the DOT levels are close to zero. (Carreras *et al.*, 2002).

Table 4.1 Kinetics of erythromycin A (EA), and C (EC) formation in 7 L batch fermentations of *S. erythraea* CA340 operated with various pH control strategies. Fermentations as described in Figure 4.2. Erythromycin concentrations analysed as described in Section 2.8.5.

(i) Full pH control			
Time (h)	**pH**	**EA (mgL^{-1})**	**EC (mgL^{-1})**
24	7.00	100.00	ND
30	7.00	140.00	ND
40	7.01	170.00	ND
58	7.01	225.00	69.00
68	7.00	227.00	34.00
72	7.00	230.00	21.00
89	7.00	215.00	20.00
(ii) Base only pH control			
Time (h)	**pH**	**EA (mgL^{-1})**	**EC (mgL^{-1})**
24	6.99	60.00	ND
30	6.96	95.00	ND
40	7.40	110.00	ND
58	7.20	189.00	58.00
68	7.60	194.00	55.00
72	7.50	200.00	32.00
(iii) No pH control			
Time (h)	**pH**	**EA (mgL^{-1})**	**EC (mgL^{-1})**
30	7.00	65.00	ND
40	6.40	73.00	ND
58	6.30	96.00	52.00
68	7.45	105.00	63.00
72	8.90	93.00	41.00

ND = below detection limit of HPLC assay (< 15 mgL^{-1}).
No erythromycin B was detected

4.3.3 Summary of kinetic parameters in 7 L fermentations of S. erythraea *CA340*

The results presented in Table 4.1, together with other key parameters for the three types of fermentation performed in Section 4.3.1, are summarised in Table 4.2. The specific yield of erythromycin A produced during 7 L fermentations with full and base only pH control was significantly higher (~25 $mg_{EA}mg^{-1}_{cells}$) than that obtained in fermentations without pH control (18 $mg_{EA}mg^{-1}_{cells}$), showing that the increased erythromycin production was due to enhanced biosynthetic activity under defined pH conditions rather than simply due to an increased biomass production.

Table 4.2 Comparison of growth and product formation parameters in 7 L batch fermentations of *S. erythraea* CA340, carried out with various pH control strategies. Fermentations as described in Section 4.3.1.

Fermentation parameter	Full pH control	Base only pH control	No pH control
X_{max} (gL^{-1})	9.45	7.87	5.93
μ_{max} (h^{-1})	0.09	0.08	0.07
EA_{max} (mgL^{-1})	230	200	105
Maximum ratio EA:EC	11:1	6:1	2:1
Maximum glucose utilisation rate (gL^{-1} h^{-1})	0.94	0.88	0.71
Biomass yield on glucose ($Y_{x/s}$)	0.28	0.22	0.12
Specific EA yield ($mg_{EA}mg^{-1}_{cells}$)	25	25	18

4.3.4 Buffering capacity of the SCM

For the implementation of pH control in microwell fermentations (described later in Section 4.3.5) it is important to understand how the buffering capacity of the fermentation broth varies during the course of the fermentation and also which medium components have the greatest buffering effect. Figure 4.4 compares titration curves carried out with various fermentation broth fractions at different times during the course of a fermentation (all samples were taken from fermentations conducted with base only pH control, as shown in Figure 4.2). By definition, it also indicates the volume of NaOH required to bring the pH of the fermentation broth back to a neutral value. It is clear that the whole broth, containing microbial cells, is more resistant to pH change than either the clarified supernatant or SCM (control). This is most likely due to the surface charge on the cells as a result of specific ion pumps in the cell membrane (Bulgakova *et al.*, 1994).

The maximum buffering capacity of the whole fermentation broth was determined from Equations 2.1 and 2.2, to be 5.0 mM pH^{-1}. This is in good agreement with the buffering capacity determined from the on-line data collected during the 7 L base only pH control fermentation (Figure 4.4(b)) which was 5.4 mM pH^{-1}. During the course of the fermentation the buffering capacity of the whole broth varied from 0.8 $mMpH^{-1}$ at 10 hours to 5.4 $mMpH^{-1}$ at 48 hours and was directly proportional to the increase in biomass over this time period. In the absence of biomass, the maximum buffering capacity of the medium was just 0.5 mM pH^{-1}. This information on the buffering capacity of the medium over time has subsequently been used as the basis for implementing manual pH control in microwell fermentations as will be described later in Section 6.3.2.

4.3.5 Identification of manual pH control in microwell fermentations

Based on the information described in Sections 4.3.1 and 4.3.4 a system for the manual implementation of pH control in microwell fermentations of *S. erythraea* CA340 was carried out as described in Section 2.6.1. The actual measurement of pH during microwell fermentations was done using a combination micro-pH probe (20G needle tip) as described in Section 2.6.4. This type of probe is widely used for the *in-situ* measurement of blood pH in physiological studies. In relation to the microwell fermentations performed here, the mico-pH probe could be introduced to the individual microwells via ports in either the side of each well or in the top plate as shown in Figure 2.2.

"optode" technology has been previously used by a number of researchers (Kostov *et al.*, 2001; Lamping *et al.*, 2003; Doig *et al.*, 2005) for the measurement of dissolved gases during microwell fermentations. These sensors rely on the variable fluorescence quenching of certain dyes immobilised on the end of a fibre optic

cable. In the case of pH measurement, however, an indicator dye is usually placed directly in the growth medium with the risk that it might interfere with cell growth and metabolism (Harms *et al.*, 2002; Kostov *et al.*, 2001; John and Heinzle, 2001).

In order to initially demonstrate the benefits of implementing pH control in microwell fermentations the results reported here were obtained using manual alkali additions as described in Section 2.6.3. Base only pH control was implemented because the *S. erythraea* strain, like other *Streptomyces* related organisms, has a higher demand for alkali rather than acid due to production of keto-acids as overflow metabolites during rapid growth (Bulgakova *et al.*, 1994). This phenomenon is clearly seen on Figure 4.3 where the pH profile obtained during base only pH control and no pH control fermentations of *S. erythraea* CA340 is shown. It is also necessary to establish the number, frequency and volume of additions for a given concentration of NaOH. In this case additions of between 80-200 μL of 0.1 M NaOH solution were made throughout the microwell fermentations in order to control the pH near a neutral value. The frequency of NaOH addition was restricted to twice a day to avoid over filling the wells.

As discussed previously in Section 3.3.2, liquid phase mixing time in the microwell was in the range of 5-2284 s for SCM, shaken at different frequencies. Recent experimental studies on liquid phase mixing in shaken microplates have also shown mixing times to be of the order of 5 – 312 s (Weiss *et al.*, 2002). In relation to this, these time constants are significantly less than those associated with cell growth (Figure 4.2(a)), hence any effects of mixing time on pH control can be neglected. An increase in liquid volume also has a tendency to reduce the combined oxygen mass transfer coefficient, k_La, measured in microwells due to a decrease in mixing efficiency as discussed previously in section 3.3.3. The total number of additions

per individual well was thus limited to six resulting in a maximum 18.5% increase in liquid volume. Allowing for the rate of evaporation (Section 2.6.8) which ranged between 4.5 to 8 % v/v during the 72 h period of fermentation, the actual increase was just 10.5 % v/v of the initial volume.

Typical biomass and erythromycin A profiles obtained during microwell fermentations of *S. erythraea* CA340, with and without pH control, are shown in Figure 4.5(a). These were performed in triplicate to ensure the phenomena observed were reproducible. The maximum biomass concentration obtained in the microwell fermentation with base only pH control was 7 gL^{-1} compared to 5 gL^{-1} obtained without pH control. The corresponding erythromycin A production curves, corrected for dilution effects brought about by NaOH addition, are shown in Figure 4.5(b). The maximum amount of erythromycin A produced in the base only pH control fermentation (134 mgL^{-1}) is nearly 50 % higher than that obtained without pH control (90 mgL^{-1}). The decreased levels of both biomass production and erythromycin A biosynthesis in these microwell experiments compared to those obtained in the 7 L fermentation (see Figure 4.2(a) and (b) respectively) is probably due to the reduced rate of oxygen transfer in the microwell system (John *et al.*, 2003; Hermann *et al*, 2003). The volumetric oxygen mass transfer coefficient in the 7 L vessels is of the order 0.036 s^{-1} (Table 3.2), while that measured in the microwell system under similar conditions is significantly lower at 0.014 s^{-1} as discussed previously in Section 3.3.3. The DOT levels observed during microwell fermentations with operating conditions similar to those reported here were significantly lower than those obtained during 7 L scale fermentations, as discussed in Section 3.3.5.

Figure 4.5(a) shows the measured pH during each microwell fermentation. The maximum variation in pH during the pH controlled fermentation was initially 7.0 ± 0.06 units due to the manual addition of NaOH. However, after approximately 60 h of fermentation time the pH of the broth increased due to lack of any acid addition. Table 4.3 shows the variation in erythromycin analogs produced during each of the microwell fermentations. Erythromycin C is again present in small quantities at pH values near neutral and no erythromycin B is detected, agreeing with the data obtained in the 7 L fermentations (Table 4.1).

Table 4.3 Kinetics of erythromycin A (EA), B (EB) and C (EC) formation in microwell batch fermentations of *S. erythraea* CA340, carried out with (i) base only pH control or (ii) no pH control. Fermentations profiles as shown in Figure 4.5(a).

(i) Microwell fermentation: Base only pH control			
Time (h)	**pH**	**EA (mgL^{-1})**	**EC (mgL^{-1})**
30	7.00	75.00	ND
43	7.06	94.00	ND
48	7.30	108.00	ND
66	7.00	120.00	40.00
72	6.98	134.00	30.00
(ii) Microwell fermentation: No pH control			
Time (h)	**pH**	**EA (mgL^{-1})**	**EC (mgL^{-1})**
30	6.90	52.00	ND
43	7.30	68.00	ND
48	7.40	75.00	ND
66	7.50	84.00	ND
72	7.78	90.00	42.00

The maximum specific growth rate and the yield of biomass on substrate for the fermentation without pH control were 0.01 h^{-1} and 0.10 g (biomass) g^{-1} (glucose) respectively compared to 0.03 h^{-1} and 0.16 g (biomass) g^{-1} (glucose) for the microwell fermentation with base only pH control. The ratio of EA:EC produced increased two fold from 2:1 (no pH control) to 4:1 (base only pH control). These results for the implementation of base only pH control in microwell

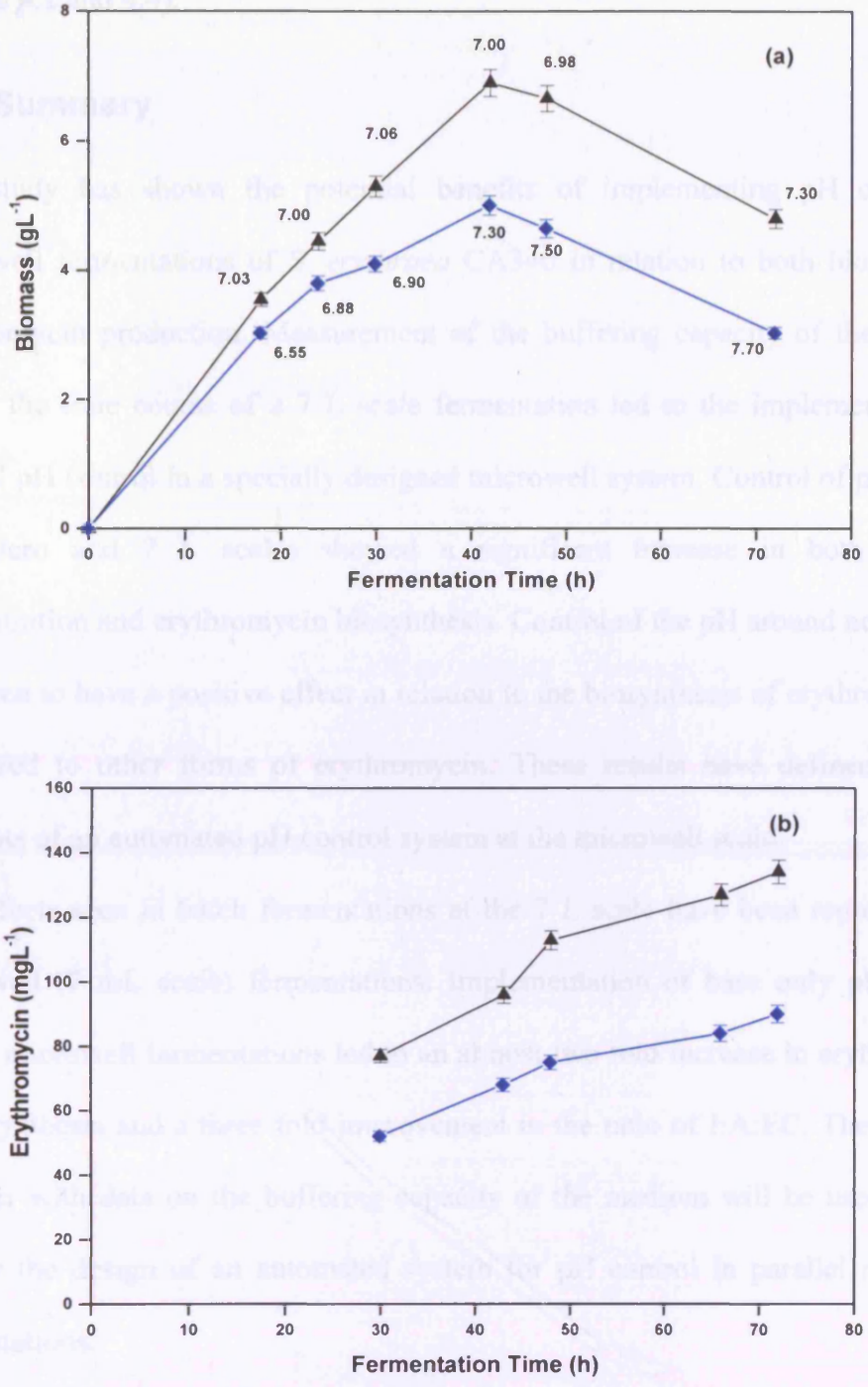

Figure 4.5 Microwell (7 mL) batch fermentation kinetics of *S. erythraea* CA340: (a) biomass concentration: base only pH control (▲), no pH control (♦). Values alongside each data point show the measured pH. (b) Erythromycin A concentration. Error bars represent standard deviation of triplicate measurements. Experiments were carried out as describes in Section 2.6.1.

fermentation corresponds well to those seen previously in the 7 L fermentations (Tables 4.2 and 4.4).

4.4 Summary

This study has shown the potential benefits of implementing pH control in microwell fermentations of *S. erythraea* CA340 in relation to both biomass and erythromycin production. Measurement of the buffering capacity of the medium during the time course of a 7 L scale fermentation led to the implementation of manual pH control in a specially designed microwell system. Control of pH at both the micro and 7 L scales showed a significant increase in both biomass concentration and erythromycin biosynthesis. Control of the pH around neutral was also seen to have a positive effect in relation to the biosynthesis of erythromycin A compared to other forms of erythromycin. These results have defined the key elements of an automated pH control system at the microwell scale.

The effects seen in batch fermentations at the 7 L scale have been reproduced in microwell (7 mL scale) fermentations. Implementation of base only pH control during microwell fermentations led to an almost two fold increase in erythromycin A biosynthesis and a three fold improvement in the ratio of EA:EC. These results together with data on the buffering capacity of the medium will be used later to specify the design of an automated system for pH control in parallel microwell fermentations.

In the following chapter 5 L and microwell scale fermentations of two *S. erythraea* strains cultivated in three different media formulations will be examined to select a suitable medium to be used during automated pH controlled micowell fermentations (Chapter 6).

5.0 Effect of Media and Strain Type on *S. erythraea* Fermentation Kinetics

5.1 Introduction

As described in Section 1.1.1, the selection of appropriate carbon and nitrogen sources in fermentation media can play an important role in determining the titre of secondary metabolites and hence fermenter productivity. The media used during fermentations can also influence broth rheology and consequently the initial stages of down stream product recovery (Davies *et al.*, 2000).

As seen in Chapter 3, for the particular case of shaken microwell fermentations, the physical properties of a fermentation medium will influence key engineering properties such as liquid phase mixing and gas-liquid mass transfer. In the absence of any direct mechanical agitation, as in the microwell, the physical properties of the fluid will dominate the performance of a particular fermentation process. An important characteristic to consider in the design of a system for automated pH control in microwell fermentations will be broth viscosity and its influence on liquid phase mixing times during the addition of acid or base to achieve pH control (Chapter 6). Consequently, in this Chapter two different *S. erythraea* strains were grown on various forms of media and the effect on growth kinetics and erythromycin biosynthesis were investigated in batch stirred tank and microwell fermentations.

5.2 Aims and Objectives

The primary aim of this chapter is to investigate a range of different medium formulations that might be used during microwell fermentations of *S. erythraea*

with automated pH control. Three very different media compositions will be used during this study, a completely soluble SCM where glucose is the main carbon and energy source, an OBM, which uses a second liquid phase (oil) as a carbon and energy source and SBM, where a solid phase is used as a carbon and energy source (Section 2.2). In each case the effect of broth physical properties on fermentations kinetics of two *S. erythraea* strains will be investigated. The *S. erythraea* strains investigated are the CA340 strain used previously in Chapter 4 and an industrial strain, EM5, provided by Pfizer Ltd (Kent, U.K) as described previously in Section 2.2. Commercial considerations prevent the disclosure of actual quantitative data or a direct public comparison of the industrial strain with the CA340 strain. All data related to the EM5 strain has therefore been normalised.

5.3 Results and Discussion

5.3.1 5 L fermentations of S. erythraea

To enable a direct comparison, all fermentations were performed in the PF5LMJ stirred vessel at Pfizer as described in Section 2.4.2. The EM5 strain of *S. erythraea*, the OBM and SBM are currently being used in a production development programme as mentioned previously in Sections 2.1 and 2.2, and therefore data related to these fermentations can only be presented in a normalised form.

All fermentations in this chapter were carried out as described previously in Section 2.4.1. Each fermentation was maintained until the process was past the stage of maximum erythromycin production. Table 5.1 shows the nomenclature used to describe each of the fermentations from which data are presented.

Table 5.1 Details of 5 L *S. erythraea* fermentations carried out using CA340 and EM5 strains grown on SCM, OBM and SBM media. All fermentations were carried out as described in Section 2.4.2.

Fermentation	Description
SCM5LCA340	5 L CA340 fermentation on, SCM. Details in Section 5.3.2
SCM5LEM5	5 L EM5 fermentation on, SCM. Details in Section 5.3.2
OBM5LCA340	5 L CA340 fermentation on, OBM. Details in Section 5.3.3
OBM5LEM5	5 L EM5 fermentation on, OBM. Details in Section 5.3.3
SBM5LCA340	5 L CA340 fermentation, on SBM. Details in Section 5.3.4
SBM5LEM5	5 L EM5 fermentation, on SBM. Details in Section 5.3.4

All fermentations were carried out in duplicate with typical fermentation profiles shown in Figure 5.1-Figure 5.6.

5.3.2 Growth of S. erythraea *on SCM*

The SCM investigated here has been previously used by a number of researchers in this laboratory (Sarra *et al.*, 1996; Heydarian, 1998; Mirjalili *et al.*, 1999; Davis *et al.*, 2000). This is a complex medium which is completely soluble in water with glucose (30 gL^{-1}) being the primary carbon and energy source (Table 2.1). Yeast extract, bactopeptone and minerals supply the nitrogen and trace elements demands of the organism. The medium also contains potassium di-hydrogen phosphate (0.68 gL^{-1}) which acts as a source of phosphate ions as well as providing some buffering capacity (Martin and Demain, 1977).

Figure5.1(a) shows a typical fermentation profile for a *S. erythraea* CA340 grown on SCM. The biomass increases rapidly, reaching a maximum of 8.5 gL^{-1} at around 35 hours, during the log phase of growth. As a result of exhausting the carbon source, the growth rate slows and then declines after 40 hours. The erythromycin A concentration reached a maximum of 200 mgL^{-1} at approximately 65 hours then

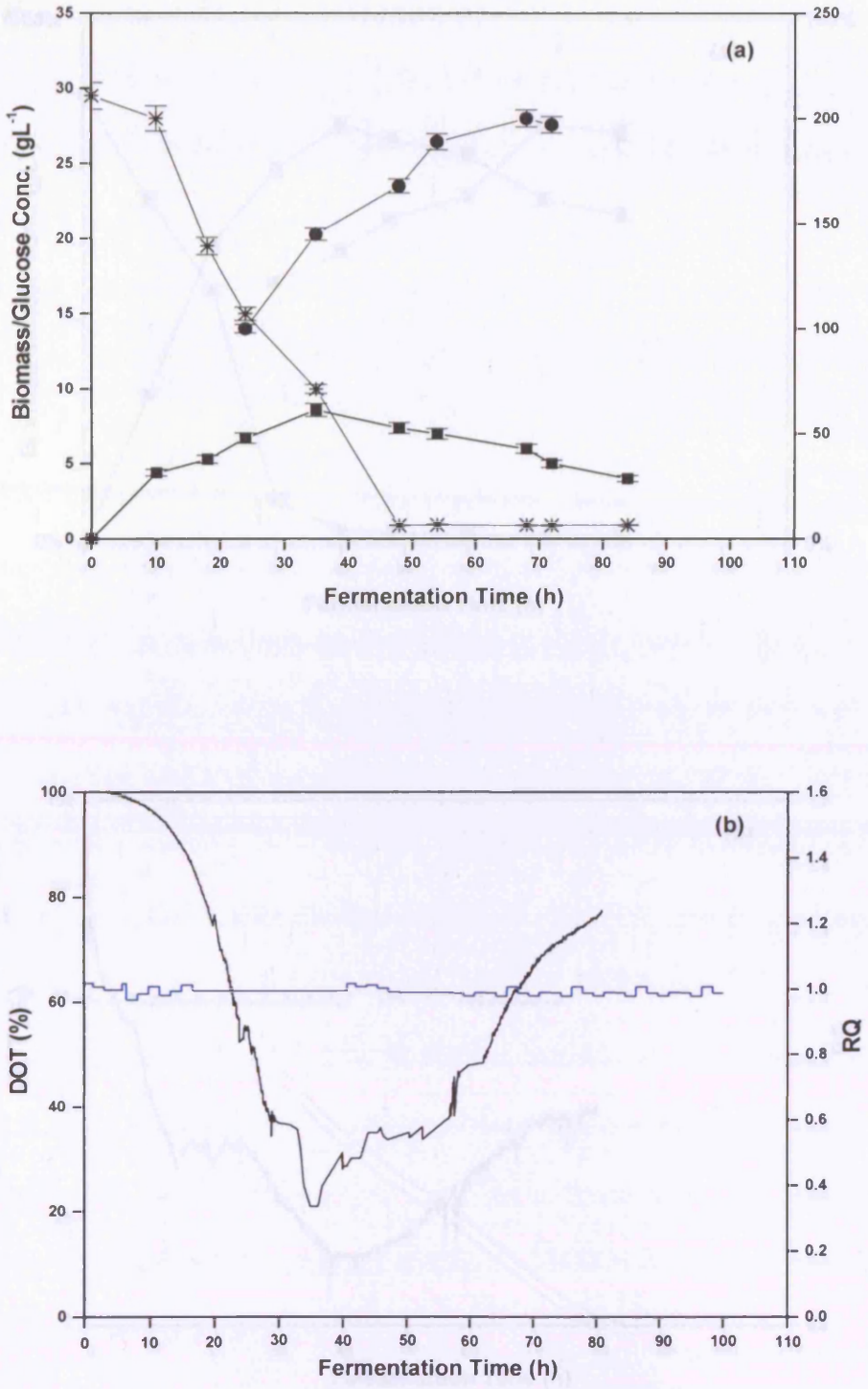

Figure 5.1 Fermentation kinetics of a 5 L *S. erythraea* CA340 fermentation on SCM medium (SCM5LCA340) (a) Biomass concentration (■), glucose concentration (*), erythromycin A concentration (●). (b) DOT (-), RQ (-). Fermentations carried out as described in Section 2.4.2. Error bars represent standard deviation of triplicate measurements.

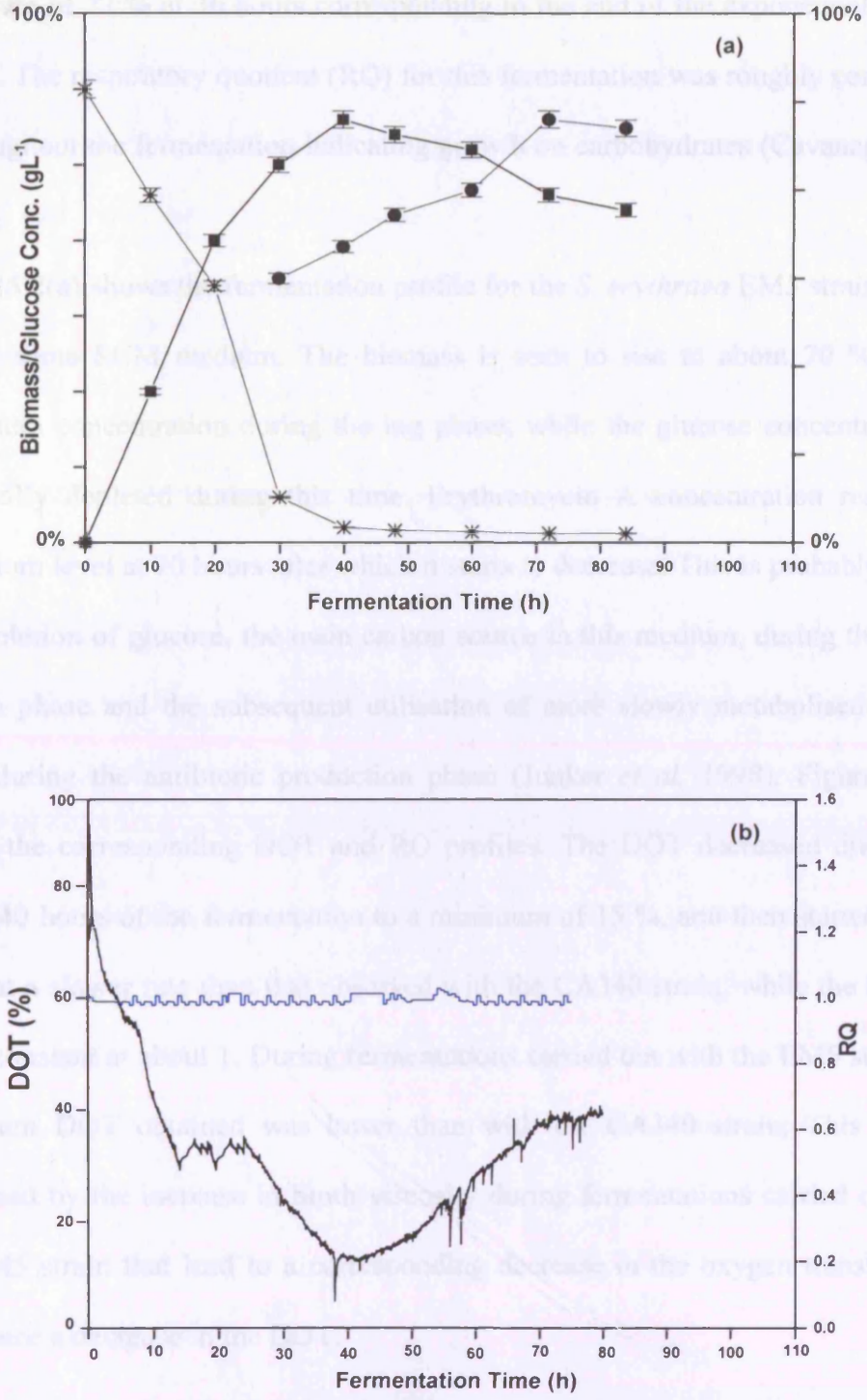

Figure 5.2 Fermentation kinetics of a 5 L *S. erythraea* EM5 on SCM medium (SCM5LEM5) (a) Biomass concentration (■), glucose concentration (*), erythromycin A concentration (●). (b) DOT (+), RQ (-). Fermentations carried out as described in Section 2.4.2. Error bars represent standard deviation of triplicate measurements.

declined. The corresponding DOT profile, shown on Figure 5.1(b), decreased to a minimum of 22 % at 36 hours corresponding to the end of the exponential growth period. The respiratory quotient (RQ) for this fermentation was roughly constant at 1 throughout the fermentation indicating growth on carbohydrates (Cavanagh *et al*, 1994).

Figure 5.2(a) shows the fermentation profile for the *S. erythraea* EM5 strain grown on the same SCM medium. The biomass is seen to rise to about 70 % of the maximum concentration during the log phase, while the glucose concentration is practically depleted during this time. Erythromycin A concentration reached a maximum level at 70 hours after which it starts to decrease. This is probably due to the depletion of glucose, the main carbon source in this medium, during the initial growth phase and the subsequent utilisation of more slowly metabolised amino-acids during the antibiotic production phase (Junker *et al,* 1998). Figure 5.2(b) shows the corresponding DOT and RQ profiles. The DOT decreased during the initial 40 hours of the fermentation to a minimum of 15 %, and then started to rise again at a slower rate than that observed with the CA340 strain, while the RQ was again constant at about 1. During fermentations carried out with the EM5 strain the minimum DOT obtained was lower than with the CA340 strain. This can be explained by the increase in broth viscosity during fermentations carried out with the EM5 strain that lead to a corresponding decrease in the oxygen transfer rate, and hence a decrease in the DOT.

5.3.3 Growth of S. erythraea on *OBM*

OBM is an industrial medium supplied by Pfizer Ltd (Kent, UK), and as mentioned previously in Section 2.2, information related to the composition of this medium can not be divulged as it is currently being used during a production development

programme. The medium comprises oil as the main carbon and energy source and a number of other components which are immiscible or partially dissolve in the aqueous phase. It was not possible to directly measure the biomass concentration of this broth as the medium contained insoluble components; therefore the growth profile was monitored by measuring the apparent viscosity of the broth as described by Karsheva *et al.* (1997), Section 2.8.4).

The variations of broth viscosity and oil concentration during fermentation of *S. erythraea* CA340 grown on OBM are presented in Figure 5.3(a). It can be seen that the increase in growth, indicated by an increase in broth viscosity to a maximum of 0.18 Pa.s at 76 hours. Erythromycin A concentration reached a peak of 400 mgL^{-1} at 176 hours. The RQ was constant at approximately 1 for 20 hours following inoculation after that, the organism switched to utilising oil, the main carbon source, and the RQ dropped to an average value of about 0.7. Figure 5.3(b) shows the corresponding DOT profile, which decreased gradually reaching a minimum of 8 % after 70 hours, corresponding to the maximum growth period. At this point, the impeller speed was increased to 900 rpm and the air flow rate was raised to 1.5 vvm in an attempt to support the oxygen demand of the organism. However, at this point foaming occurred, highlighting a problem of poor gas-liquid mixing and circulation in this viscous broth (almost five times more viscous than SCM) and the risk of a decrease in the gas-liquid oxygen mass transfer rate as described previously in Chapter 3.

It was observed that not all of the oil was used during this fermentation, as has been previously reported by Davies *et al.*, (2000) and Mirjalili *et al.*, (1999). This is thought to be the result of inadequate mass transfer at the lipid-aqueous interface,

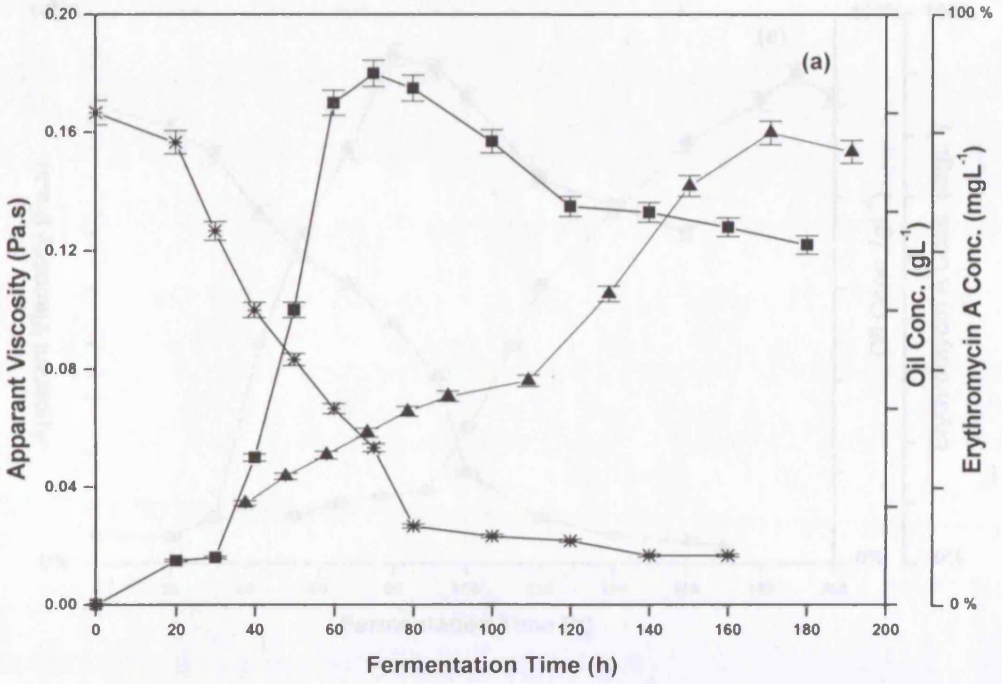

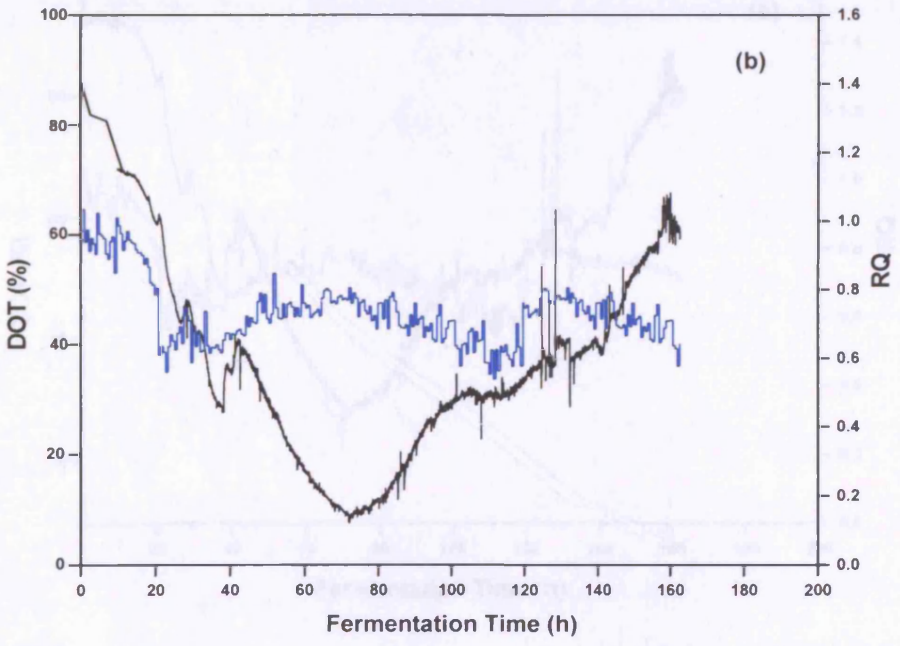

Figure 5.3 Fermentation kinetics of a 5 L *S. erythraea* CA340 on OBM (OBM5LCA340). (a) Viscosity (■), oil concentration (*), erythromycin A concentration (▲). (b) DOT (+), RQ (-). Fermentations carried out as described in Section 2.4.2. Error bars represent standard deviation of triplicate measurements.

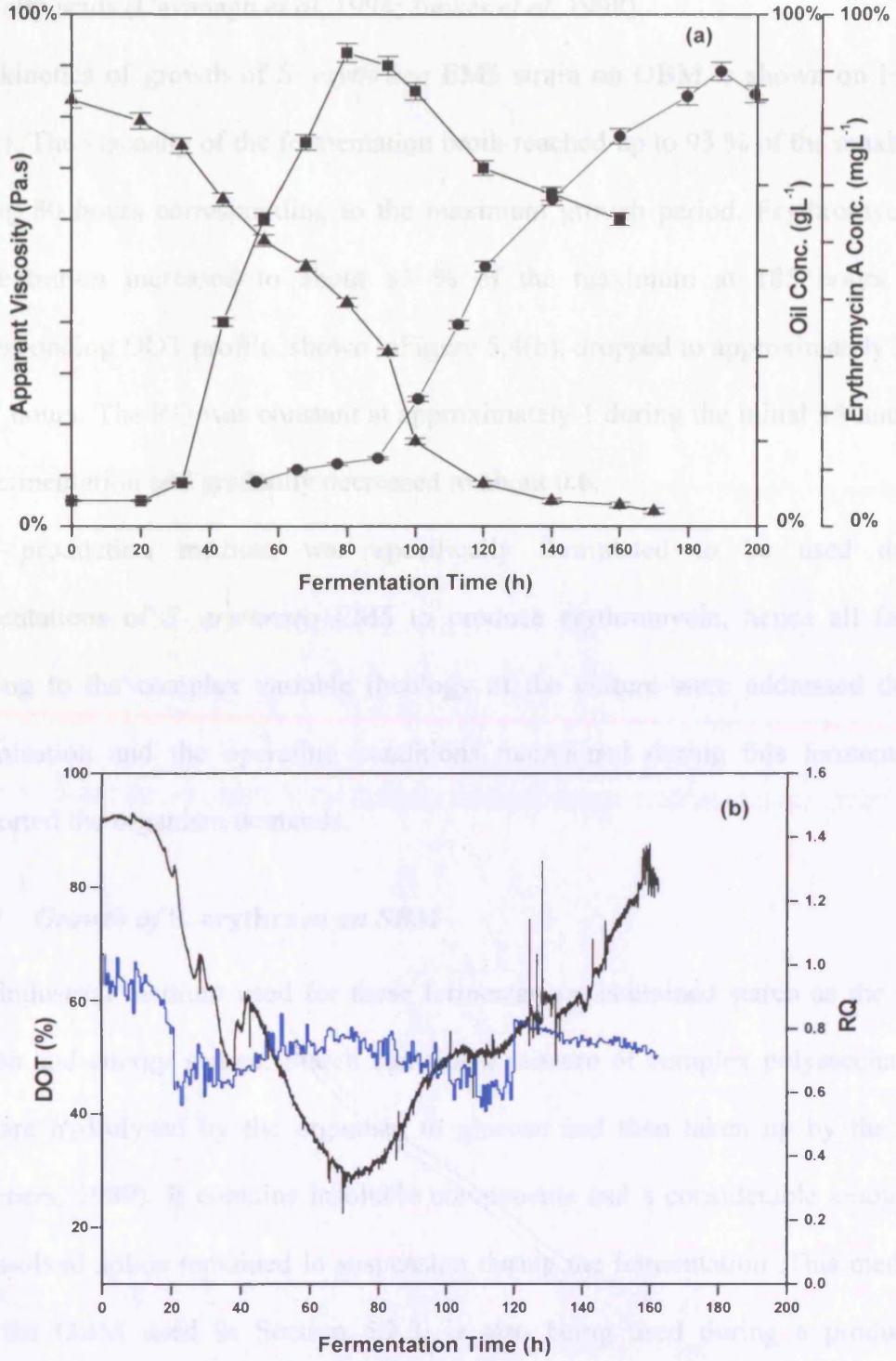

Figure 5.4 Fermentation kinetics of a 5 L *S. erythraea* EM5 on OBM (OBM5LEM5). (a) Viscosity (■), oil concentration (▲), erythromycin A concentration (●). (b) DOT (+), RQ (-). Fermentations carried out as described in Section 2.4.2. Error bars represent standard deviation of triplicate measurements.

resulting in a decline of the lipase activity, which hydrolyses oil to form glycerol and fatty acids (Cavanagh *et al*, 1994; Junker *et al*, 1998).

The kinetics of growth of *S. erythraea* EM5 strain on OBM is shown on Figure 5.4(a). The viscosity of the fermentation broth reached up to 93 % of the maximum during 80 hours corresponding to the maximum growth period. Erythromycin A concentration increased to about 85 % of the maximum at 185 hours. The corresponding DOT profile, shown inFigure 5.4(b), dropped to approximately 24 % at 77 hours. The RQ was constant at approximately 1 during the initial 15 hours of the fermentation and gradually decreased to about 0.6.

This production medium was specifically formulated to be used during fermentations of *S. erythraea* EM5 to produce erythromycin, hence all factors relating to the complex variable rheology of the culture were addressed during optimisation and the operating conditions maintained during this fermentation supported the organism demands.

5.3.4 Growth of S. erythraea *on SBM*

The industrial medium used for these fermentations contained starch as the main carbon and energy source. Starch contains a mixture of complex polysaccharides that are hydrolysed by the organism to glucose and then taken up by the cells (Manners, 1989). It contains insoluble components and a considerable amount of undissolved solids remained in suspension during the fermentation .This medium, like the OBM used in Section 5.3.3, is also being used during a production development programme and hence all information related its composition can not be divulged.

The kinetics of growth of the *S. erythraea* CA340 in SBM are shown on Figure 5.5 (a). The biomass concentration reached a maximum of 9 gL^{-1} at about 35 hours

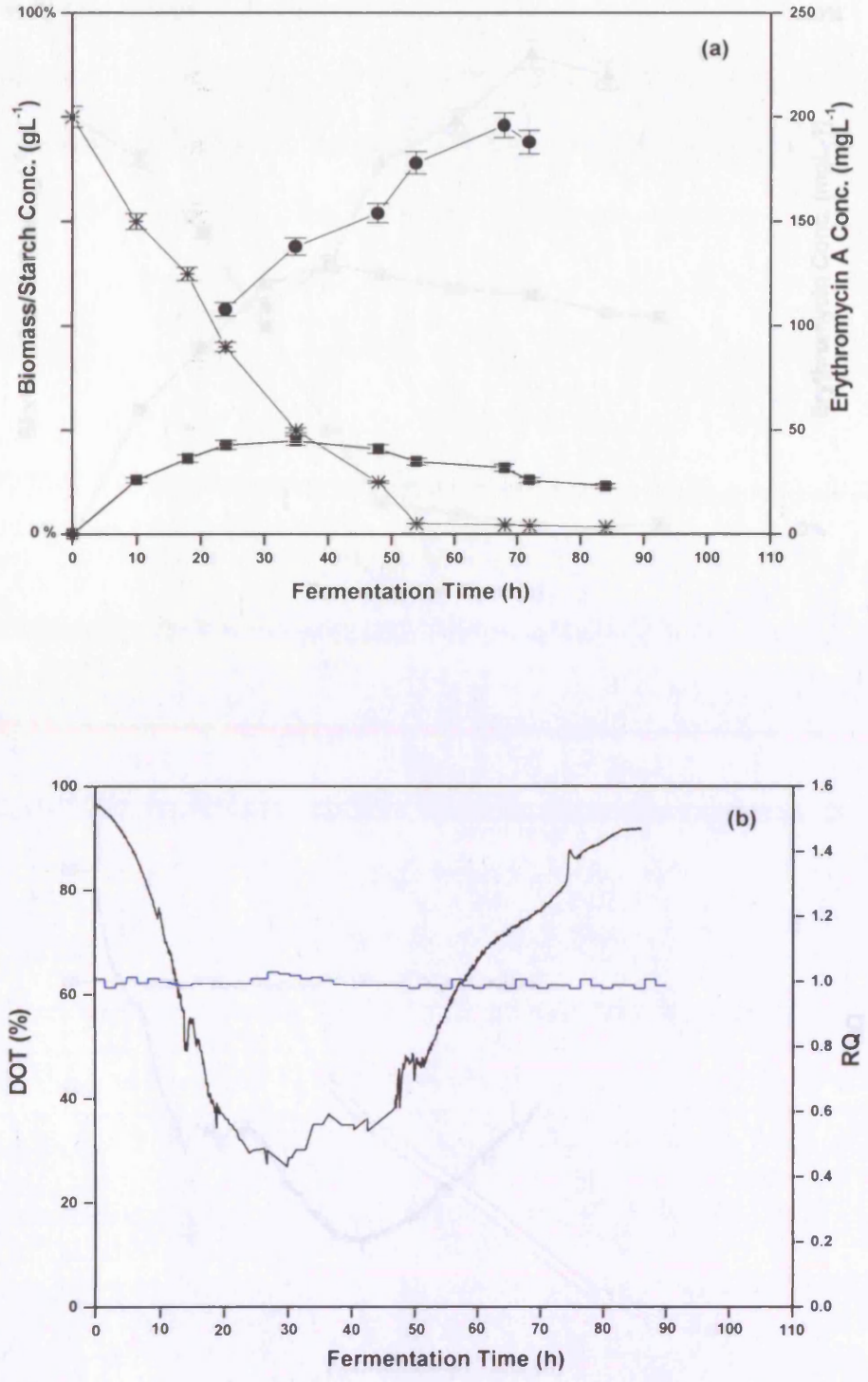

Figure 5.5 Fermentation kinetics of a 5 L CA340 on SBM (SBM5LCA340). (a) Biomass concentration (■), starch concentration (*), erythromycin A concentration (●). (b) DOT (+), RQ (-). Fermentations carried out as described in Section 2.4.2. Error bars represent standard deviation of triplicate measurements.

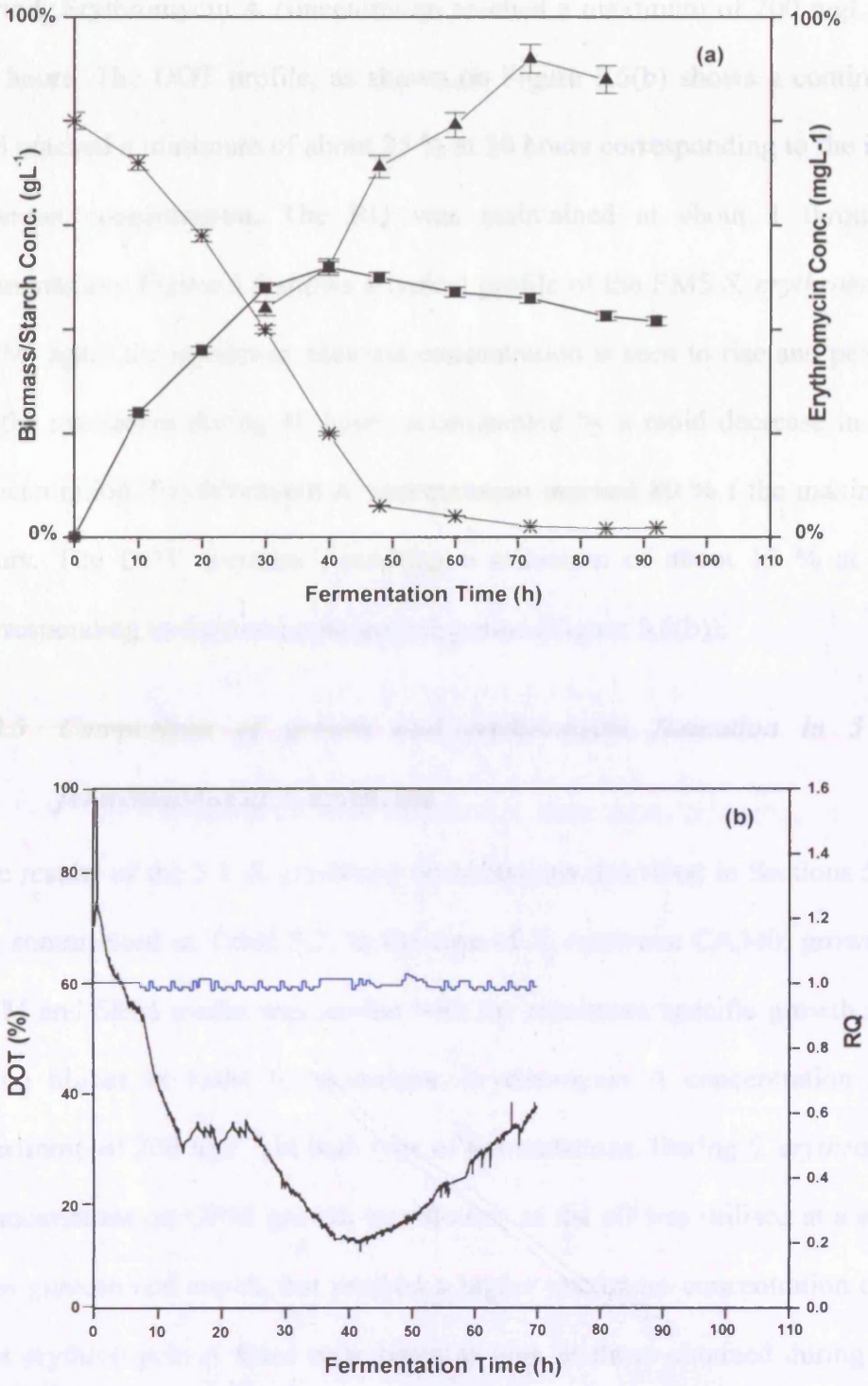

Figure 5.6 Fermentation kinetics of a 5 L *S. erythraea* EM5 on SBM (SBM5LEM5). (a) Biomass concentration (■), starch concentration (*), erythromycin A concentration (●). (b) DOT (+), RQ (-). Fermentations carried out as described in Section 2.4.2. Error bars represent standard deviation of triplicate measurement.

following inoculation, while the starch concentration depleted rapidly at this period. Erythromycin A concentration reached a maximum of 200 mgL^{-1} at about 68 hours. The DOT profile, as shown on Figure 5.5(b) shows a continuous drop and reached a minimum of about 25 % at 30 hours corresponding to the increase in biomass concentration. The RQ was maintained at about 1 throughout the fermentation. Figure 5.6 shows a typical profile of the EM5 *S. erythraea* grown in SBM; again the maximum biomass concentration is seen to rise and peak at 55 % of the maximum during 40 hours accompanied by a rapid decrease in the starch concentration. Erythromycin A concentration reached 80 % f the maximum at 72 hours. The DOT decreased, reaching a minimum of about 15 % at 40 hours, corresponding to the maximum growth period (Figure 5.6(b)).

5.3.5 Comparison of growth and erythromycin formation in 5 L batch fermentations of S. erythraea

The results of the 5 L *S. erythraea* fermentations described in Sections 5.3.2-5.3.4 are summarised in Table 5.2. In the case of *S. erythraea* CA340, growth on both SCM and SBM media was similar with the maximum specific growth rate (μ_{max}) being higher in SBM fermentations. Erythromycin A concentration reached a maximum of 200 mgL^{-1} in both type of fermentations. During *S. erythraea* CA340 fermentations on OBM growth was slower, as the oil was utilised at a slower rate than glucose and starch, but reached a higher maximum concentration of 13 gL^{-1}. The erythromycin A titres were twice as high as those obtained during SCM and SBM fermentations.

Little quantitative data can be disclosed in the case of *S. erythraea* EM5 fermentation, however, significantly higher erythromycin A titres were obtained during fermentations carried out on the OBM than on SCM or SBM.

5.3.6 Microwell S. erythraea *CA340 fermentations on SCM, OBM and SBM media*

As seen in Sections 5.3.2-5.3.4 the media tested during this study supported the growth of *S. erythraea* CA340 and EM5 strains. The *S. erythraea* EM5 strain could not be removed from the Pfizer site which prevented any further use at UCL with the automated pH control system (Chapter 6). Consequently growth and erythromycin production of *S. erythraea* CA340 during microwell fermentations with each media was examined. All fermentations were carried out as described in Section 2.6.1 and the pH was not controlled in these initial fermentations.

Table 5.2 Comparison of growth and erythromycin formation in 5 L *S. erythraea* fermentations carried out using different media compositions. Kinetic parameters derived from Figures 5.1-5.6. Biomass and erythromycin A concentrations are measured as described in Sections 2.8.1 and 2.8.3 respectively.

Fermentation	X_{max} (gL^{-1})	μ_{max} (h^{-1})	EA_{max} (mgL^{-1})
SCM5LCA340	8.6	0.09	200
SCM5LEM5	NA	0.13	NA
OBM5LCA340	13	0.03	400
OBM5LEM5	NA	0.06	NA
SBM5LCA340	9.0	0.12	200
SBM5LEM5	NA	0.16	NA

NA: Not able to disclose

Figure 5.7(a) summarises cell growth on each of the three media used, while the corresponding erythromycin A biosynthesis is shown in Figure 5.7(b). In the case of the SCM, as seen previously in Section 4.3.5, the maximum biomass concentration reached was 5 gL^{-1} obtained at 40 hours. The corresponding erythromycin A concentration reached a peak of 88 mgL^{-1} at approximately 72 hours. During the SBM fermentation, it can be seen that the biomass concentration gradually increased between 8-40 hours of fermentation time, reaching a maximum

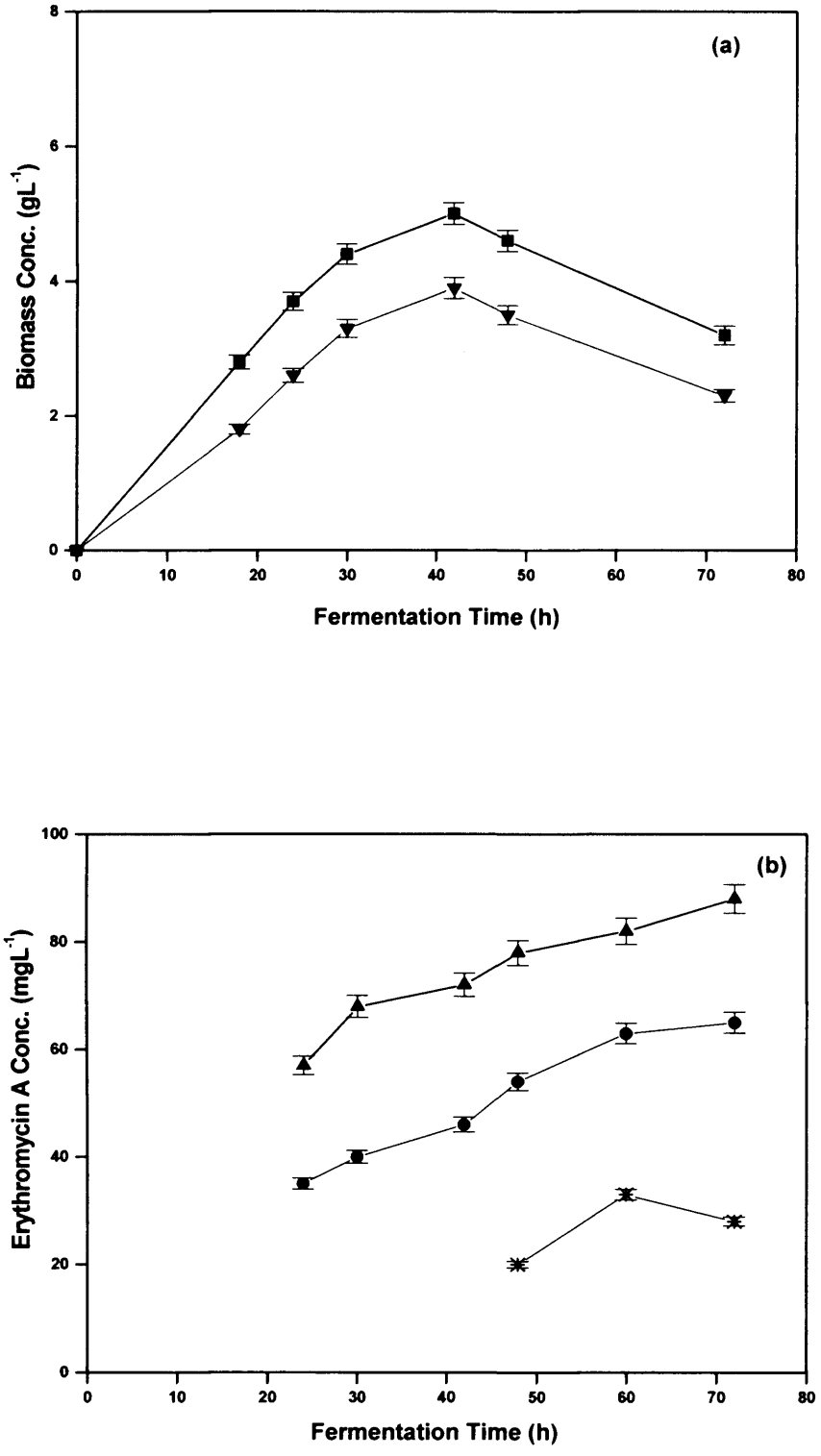

Figure 5.7 Microwell fermentation of CA340 *S. erythraea* strain carried out using different media (a) Biomass concentration: SCM (■), SBM (▼). (b) Erythromycin A concentration: SCM (▲), SBM (●), OBM (*). Fermentations were carried out as described in Section 2.6.1. Error bars represent standard deviation of triplicate measurement.

of 3.9 gL^{-1} at 40 hours. Precipitation of the solid components of the SBM at the bottom of the well was observed during this experiment from about 5 hours onwards, suggesting that solid-liquid mixing was not sufficient to achieve homogeneity in the fermentation broth. The impact of this was observed on the lower growth rates and erythromycin A titres obtained. The biomass concentrations obtained during fermentations carried out on the OBM were determined from viscosity measurements (data not shown) the growth rate was very low, with the maximum biomass concentration reaching a maximum of 2.2 gL^{-1}, as shown in Table 5.3, at about 48 hours, similarly the erythromycin A concentrations reached only 33 gL^{-1} at about 60 hours.

Table 5.3 Comparison of microwell CA340 *S. erythraea* fermentation kinetics using SCM, OBM and SBM media.

Fermentation parameter	SCM	OBM	SBM
X_{max} (gL^{-1})	5.0	2.2	3.9
μ_{max} (h^{-1})	0.01	0.002	0.007
EA_{max} (mgL^{-1})	88	30	65
Biomass yield ($Y_{x/s}$)	0.09	NA	NA

NA: Not able to disclose

5.4 Summary

In this study it has been demonstrated that the fermentation medium composition can greatly influence fermentation process productivity. Three very different types of media, SCM, OBM and SBM were used and the effect on growth and product formation of *S. erythraea* CA340 and EM5 strains was investigated. For comparative stirred tank fermentations at the 5 L scale, the growth of *S. erythraea* CA340 was shown to be quickest on the SCM, however, this rapid growth was at the expense of erythromycin titre. Similar performance was obtained with the

SBM. Best performance, in terms of erythromycin A titres, was obtained with the OBM, where the maximum erythromycin A concentration was twice that of the other fermentations. For all three media mixing in the tank was sufficient to scatter the extra solid and liquid phases present in the SBM and OBM respectively. Due to commercial considerations, little can be revealed regarding the *S. erythraea* EM5 cultures.

For the microwell fermentations, cell growth rates obtained during *S. erythraea* CA340 were faster with SCM and SBM. However, the growth kinetics was slower during SBM fermentations and the erythromycin A concentrations were lower than those obtained during SCM fermentations. Due to the high viscosity of the OBM, microwell fermentation of CA340 *S. erythraea* could not be achieved under the conditions described in Section 2.6.1 as a result very low growth rates and erythromycin titres were obtained. The mixing time achieved during shaking of the microwell containing OBM was >200 s, as measured previously in Section 3.5, making this medium unsuitable for use during microwell fermentations with automated pH control

The work discussed in this chapter showed that SCM is the most suited medium for microwell fermentations in terms of liquid phase mixing and oxygen transfer. Similarly, data presented in Chapter 4 showed the benefits of manually implementing pH control in microwell fermentations of *S. erythraea* CA340. In Chapter 6 the design and implementation of an automated pH control system, using SCM as the fermentation growth medium, will be described.

6.0 Automation of pH Control in Batch and Fed-batch Microwell Fermentations

6.1 Introduction

The use of automated microwell systems in fermentation process development could enable the parallel evaluation of many process variables simultaneously such as, pH, temperature, medium composition *etc*. Whilst the technology for measuring process parameters such as pH, dissolved oxygen tension (DOT) and optical density (OD) at the microwell scale is widely available, it is still difficult to monitor these critical parameters (Kumar *et al.*, 2004), and few attempts have been made to accurately control them. In an attempt to develop complete systems for monitoring and control of important process variables at microwell scale, Nealon *et al.*, (2005), reported the use of an automated liquid handling robot integrated with a microwell plate reader for fast acquisition of bioprocess kinetic data. Integrated automation platforms have been previously shown to present a powerful process development tool over traditional experimental methods used for bioprocess development (Doig *et al.*, 2002). The small volumes required and the use of parallel, automated experimentation has the potential to greatly reduce fermentation development times as well as maintain reproducibility and sensitivity (Lye *et al.*, 2003).

Now days a common way to enhance the productivity of larger scale microbial fermentations is to use fed-batch or semi-batch techniques (Andersson *et al.*, 1996). In these processes one or more nutrients are supplied to the bioreactor during the fermentation at a controlled rate based upon a continuously measured process parameter e.g. glucose feeding based on oxygen uptake measurement. Such

approaches enhance productivity by overcoming substrate inhibition, catabolite repression or overflow metabolism (Westgate *et al.*, 1991). Other reasons for implementing fed-batch operations are to switch from growth to metabolite overproduction by limitation of a autotrophic nutrient or to control cell-specific oxygen consumption rates to achieve high cell densities in cases where the oxygen transfer rate of the reactor is limited (Altenbach-Rehm *et al.*, 1999).

In the case of fermentations performed in shaken flasks, Weuster-Botz *et al.*, 2001 have developed an automated system for pH control during a 16 parallel *E. coli* fermentation at the 100 ml scale. While significant improvements in biomass production and enzyme expression levels were obtained, such an approach requires dedicated hardware and instrumentation and lacks the throughput achievable in parallel microwell fermentations. The potential benefits for implementing pH control in microwell fermentations of *S. erythraea* CA340, in relation to both biomass and erythromycin production has been previously shown in this work (Chapter 4). It has also been shown that when using a SCM, (Chapter 5), the characteristics of shaken microwells liquid mixing and gas-liquid mass transfer (Chapter 3) is sufficient to enable good cell growth and erythromycin production. The results obtained so far during this study have thus helped to define the key elements of an automated pH control system at the microwell scale and the potential benefits for a fermentation development programme.

6.2 Aims and Objectives

The aim of this chapter is to design and implement an automated pH control system on a liquid handling robotic platform for performing pH controlled microwell fermentations of *S. erythraea* CA340. The specific objectives of this chapter are:

1. To integrate the operation of a Packard MultiProbe II liquid handling robot with a LabView PID controller for data acquisition and control of pH during fermentations performed in the designed microwell system described in Chapter 4.
2. To evaluate the sensitivity of the automated system in terms of speed of response and the minimisation of pH fluctuations.
3. To utilise the system as a tool for parallel additions of pH controlling reagent during batch *S. erythraea* CA340 fermentations.
4. To operate the system as a means for parallel pH control and feeding of growth limiting nutrients, such as glucose, during fed-batch microwell fermentations of *S. erythraea* CA340 .

6.3 Results and Discussion

6.3.1 pH data acquisition and control system setup

The experimental setup of the automated pH control system was described briefly in Section 2.6.6. The pH in each microwell is measured using a miniature combination pH electrode (Section 2.6.4). The analogue signal from the probe is converted through a terminal block into a digital form and logged into the PC (Figure 6.1) running the control software via a PCI bus multifunction data acquisition (DAQ) device (National Instruments, Newbury, UK). The DAQ system is supplemented with signal conditioning for increased measurement accuracy. pH control, based on the measured input, was carried out using a Proportional Integral Derivative (PID) control programme written in LabView software as described in Section 2.6.4. A schematic representation of the feed-back control system is shown in Figure 6.2. The pH control system comprises the designed microwell system

(Chapter 4), the miniature pH probe, the LabView data logger and controller and the Packard II liquid handling robot system controlled by the MultiProbe™ WinPreb software.

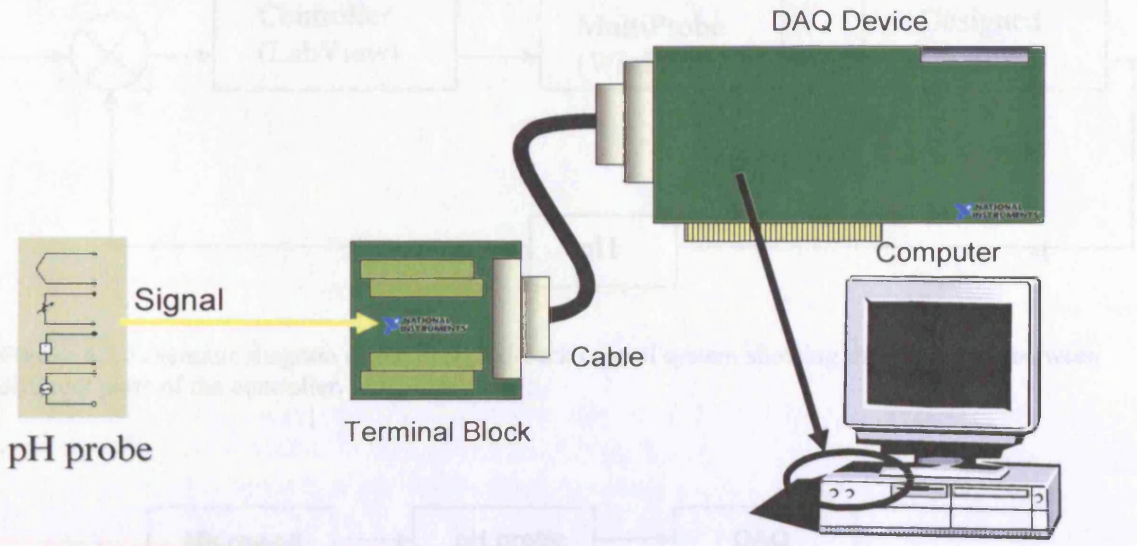

Figure 6.1 Diagrammatic representation of pH data acquisition, showing the hardware set-up.

The details of the automated pH control system are shown in Figure 6.3. The pH is measured during the fermentation in a single well and data is logged into the PID controller. The controller compares the measured pH with the desired value of the set point (pH 7) and an error is produced. The PID controller uses this error to calculate a change to the manipulated variable, the pH, driving the error to zero. The process was assumed to be first order with a gain of 1. Equation 6.1 shows the controller algorithm.

$$J = J_0 + K_C\varepsilon + K_I \int_0^t \varepsilon dt + K_D \frac{d\varepsilon}{dt} \qquad (6.1)$$

Where, J is the controller output signal, J_0 is the controller output when ε is zero, ε is the system error, K_C, K_I and K_D are constants. The controller was tuned by varying the values of K_C, K_I and K_D to minimise oscillation from the set-point.

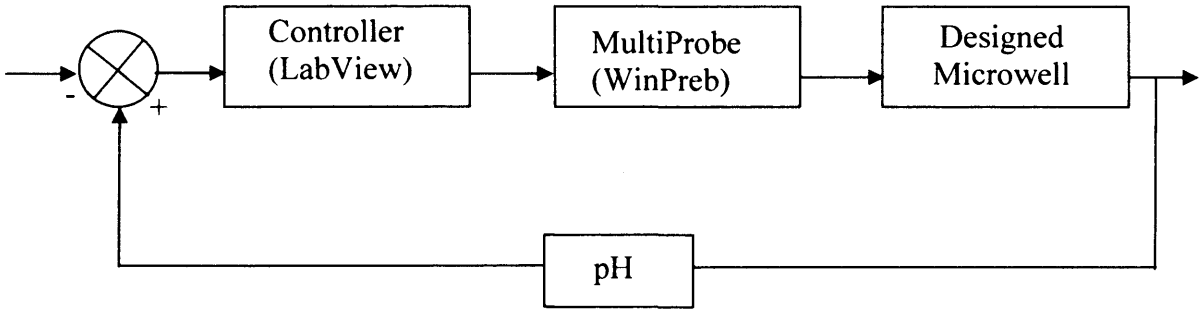

Figure 6.2 Schematic diagram of the PID feed-back control system showing the interaction between different parts of the controller.

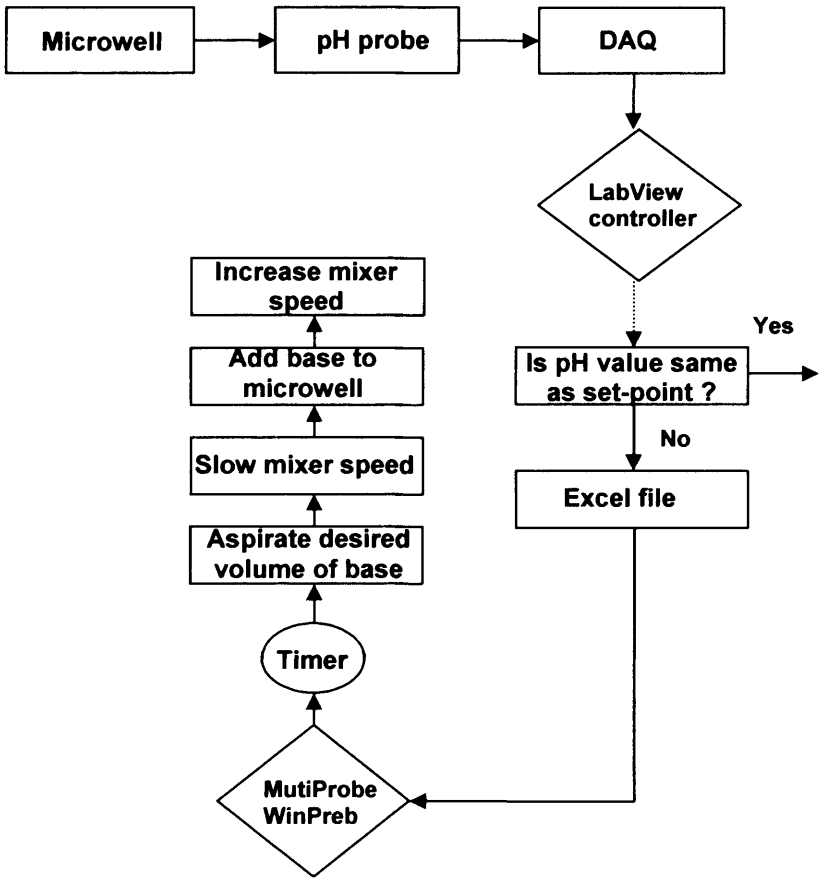

Figure 6.3 Schematic sequence of the automated pH control system showing the steps carried out in pH controlled microwell fermentations of *S. erythraea* CA340. System set up as described in Section 2.6.6.

The output of the controller i.e. the volume of the base to be added to return the pH to the set point is then passed into the WinPreb software controlling the Packard robotic liquid handling arm via a programme written in Windows Excel. The liquid handling system responds by aspirating the required amount of NaOH, and slowing the Eppendorf mixer (Section 2.6.1) to enable accurate positional dispensing into the specific microwell, while continuing rapid mixing of the solution.

6.3.2 Liquid handling parameters

As described in Section 4.3.5, the kinetics of growth of *S. erythraea* CA340 on SCM is relatively slow, with a maximum specific growth rate of 0.03 h^{-1}, and the viscosity of the fermentation broth does not exceed 1.8 mPa.s (Davies, 2001). It was therefore unnecessary to carry out real-time pH control during microwell fermentations of *S. erythraea* CA340 since the medium pH would not change significantly over very short time periods; consequently, the DAQ device was set up for a pH detection period of 40 seconds. To avoid overfilling the well, additions of the 0.1 M NaOH solution used to control the pH were set to minimum and maximum values of 20 µL and 600 µL respectively.

6.3.3 Performance and sensitivity analysis of automated pH control system

The pH-set point for the PID controller was kept at 7, this is the optimum pH selected for *S. erythraea* fermentation as indicated by results shown in Chapter 4. In order to test the system response to sudden deviations of the pH, sulphuric acid solutions with various concentrations were added during the course of a typical fermentation and the system response was recorded.

Table 6.1 summarises the system response to changes in the pH during a fermentation over 60 hours with various acid additions at intervals. Overall, the pH of the system was maintained at approximately pH 7. The response time of the PID controller was longer when an acid with a high concentration (5M H_2SO_4) was added into the well, this was to allow sufficient amounts of NaOH to be added by the robotic liquid handling system to neutralise the pH.

Table 6.1 Response of automated pH control system to artificially induced variations of pH during microwell fermentations of *S. erythraea* CA340. Fermentations were carried out as described in Section 2.6.6. NaOH with an equal concentration to the acid solution was used to control the pH at set-point 7.

Parameter	0.2 M H_2SO_4	0.5 M H_2SO_4	1 M H_2SO_4	5 M H_2SO_4
Volume of acid added (μL)	50	50	50	50
Volume of base added (μL)	48	53	49	55
Initial pH reading after acid addition	6.2	6.0	5.4	3.6
Average response time (s)	10	10	12	20
Final pH reading after control action	7.00	6.99	7.02	7.03

6.3.4 Automated pH control in batch microwell fermentations

As described previously in Section 2.6.1, a sacrificial well approach, that assumes that the fermentations in individual wells are identical, is used to develop a complete representation of the microwell fermentation kinetics over time. This is necessary because of the volumes of broth required for biomass and erythromycin analysis (Sections 2.8.1 and 2.8.5). To further confirm this, the automated pH control system was first used to just monitor the pH profiles in all wells of the designed microwell plate during the course of CA340 *S. erythraea* fermentations

on SCM. The pH in each individual well was measured using the miniature pH probe as described in Section 2.6.6. The optimum pH for growth and product formation for *Streptomyces* is pH 7 (Glazebrook and Vining, 1992) and all microwell fermentations were adjusted to pH 7 at the start of each fermentation run. As discussed in Section 4.3.5 pH control in microwell fermentations of *S. erythraea* was carried out using 0.1 M NaOH to regulate the pH as the organism has a higher demand for alkali rather than acid. Figure 6.4 shows the pH profile measured over time without applying pH control. The pH in all the wells is seen to decrease rapidly during the initial 30 hours of the fermentation corresponding to the period of maximum cell growth. During this time the carbon and energy source, glucose, is broken down into primary intermediates through the action of catabolic enzymes (Drew and Demain, 1977) as discussed earlier in Section 4.3.1. After 40 hours, the pH of the fermentation broth begins to increase gradually as the addition of an acid solution is required. Importantly, the data in Figure 6.4 confirms the pH profiles in all wells are practically identical (± 0.05 pH unit), supporting the sacrificial well approach.

Figure 6.5(a) shows the pH profile measured in a microwell fermentation in which automated pH control has been implemented. Data from microwell fermentation without pH control is also shown for comparison. During fermentations carried out with automated pH control, additions of NaOH commenced between 4-5 hours and continued until 58 hours to satisfactorily maintain the pH at 7 but, eventually the broth became too alkaline and the pH started to rise. The corresponding cell growth and erythromycin fermentation kinetics are shown in Figure 6.5(b). The biomass and erythromycin concentrations obtained during fermentations carried out with

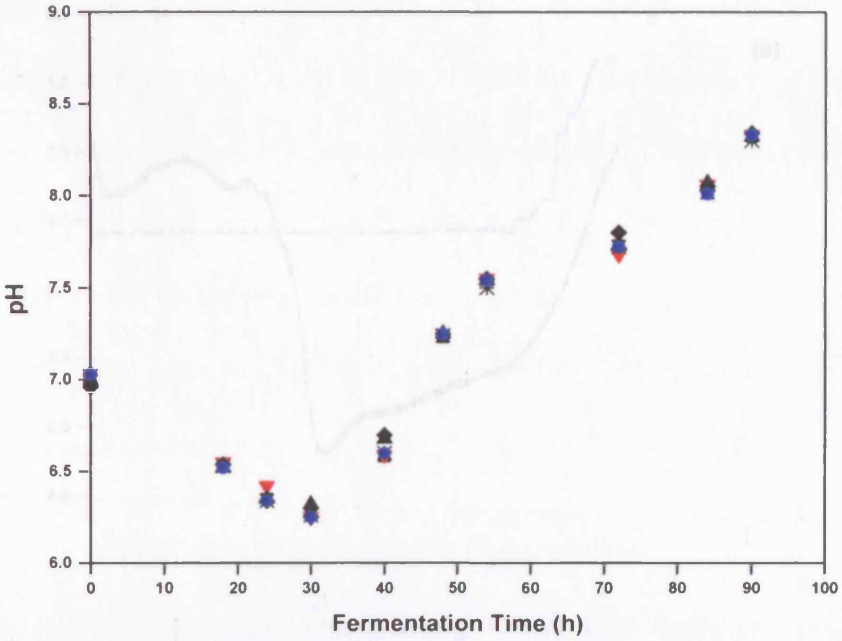

Figure 6.4 pH profiles in individual wells during microwell fermentations of *S. erythraea* in shaken microwell system carried out without pH control implementation: well 1 (■), well 2 (▼), well 3 (♦), well 4 (*), well 5 (▲), well 6 (●). Fermentations were carried out in duplicate as described in Section 2.6.1.

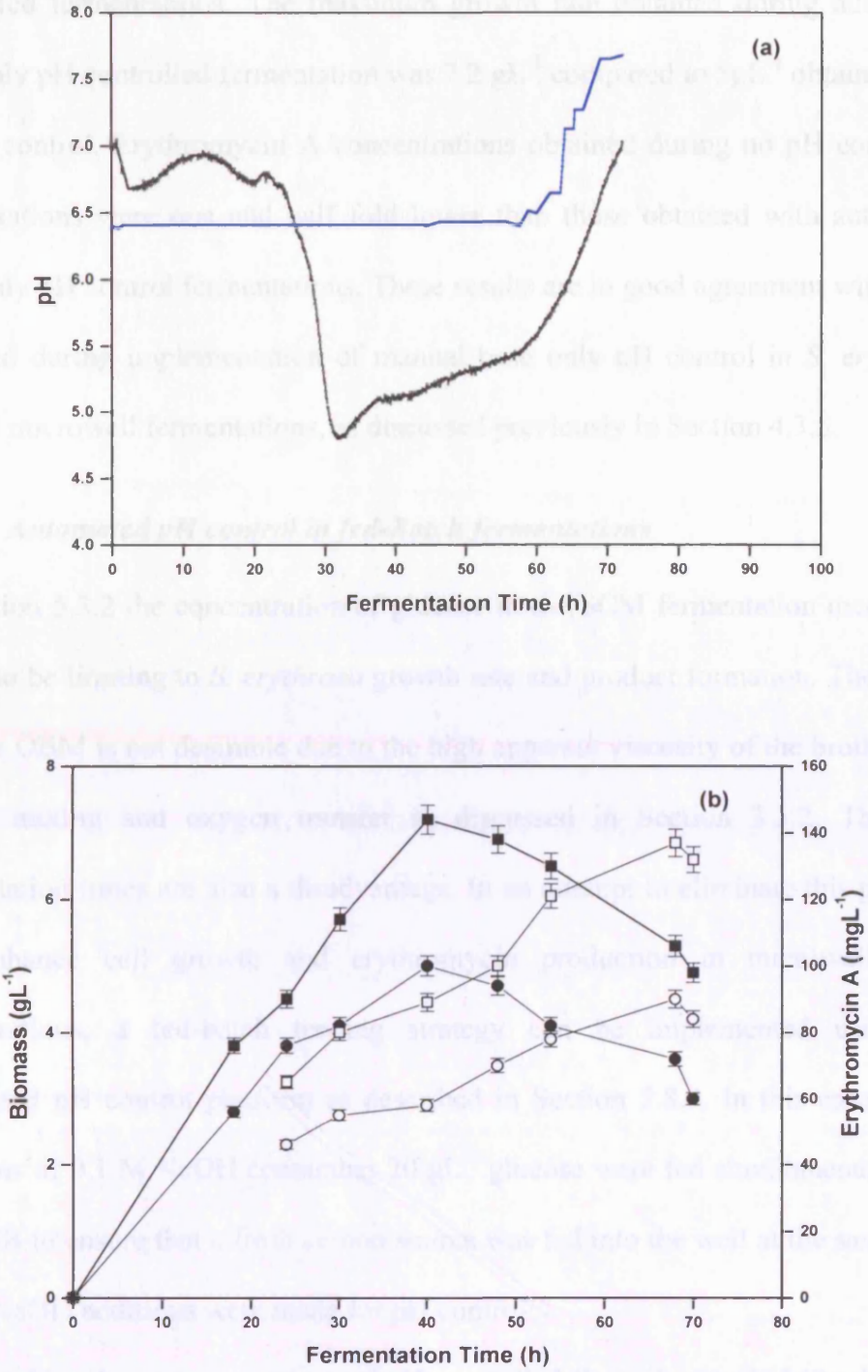

Figure 6.5 Kinetics of a typical ***S. erythraea*** CA340 microwell fermentation showing: (a) pH profiles in single microwells operated with: automatic base only pH control (-), and no pH control (-). (b) Biomass concentration during fermentation operated with automatic base only pH control (■) and no pH control (●). Erythromycin A concentration during a fermentation carried out with base only pH control (□), no pH control (○). Fermentations were carried out in duplicate as described in Section 2.6.1.

automated pH control showed a greater increase than those obtained during no pH controlled fermentations. The maximum growth rate obtained during automated base only pH controlled fermentation was 7.2 gL^{-1} compared to $5gL^{-1}$ obtained with no pH control. Erythromycin A concentrations obtained during no pH controlled fermentations were one and half fold lower than those obtained with automated base only pH control fermentations. These results are in good agreement with those obtained during implementation of manual base only pH control in *S. erythraea* CA340 microwell fermentations, as discussed previously in Section 4.3.5.

6.3.5 Automated pH control in fed-Batch fermentations

In Section 5.3.2 the concentration of glucose in the SCM fermentation media was found to be limiting to *S. erythraea* growth rate and product formation. The use of a richer OBM is not desirable due to the high apparent viscosity of the broth which affects mixing and oxygen transfer as discussed in Section 3.3.2. The long fermentation times are also a disadvantage. In an attempt to eliminate this problem and enhance cell growth and erythromycin production in microwell SCM fermentations, a fed-batch feeding strategy can be implemented using the automated pH control platform as described in Section 2.8.4. In this case mixed solutions of 0.1 M NaOH containing 20 gL^{-1} glucose were fed simultaneously into the wells to ensure that a fresh carbon source was fed into the well at the same time as the NaOH additions were made for pH control.

Figure 6.6(a) shows a comparison of pH controlled *S. erythraea* CA340 microwell fermentations carried out with batch and fed-batch operation. Little difference can be seen in the biomass concentration during the two feeding operations. However, during the batch fermentations, the erythromycin A concentration reached a

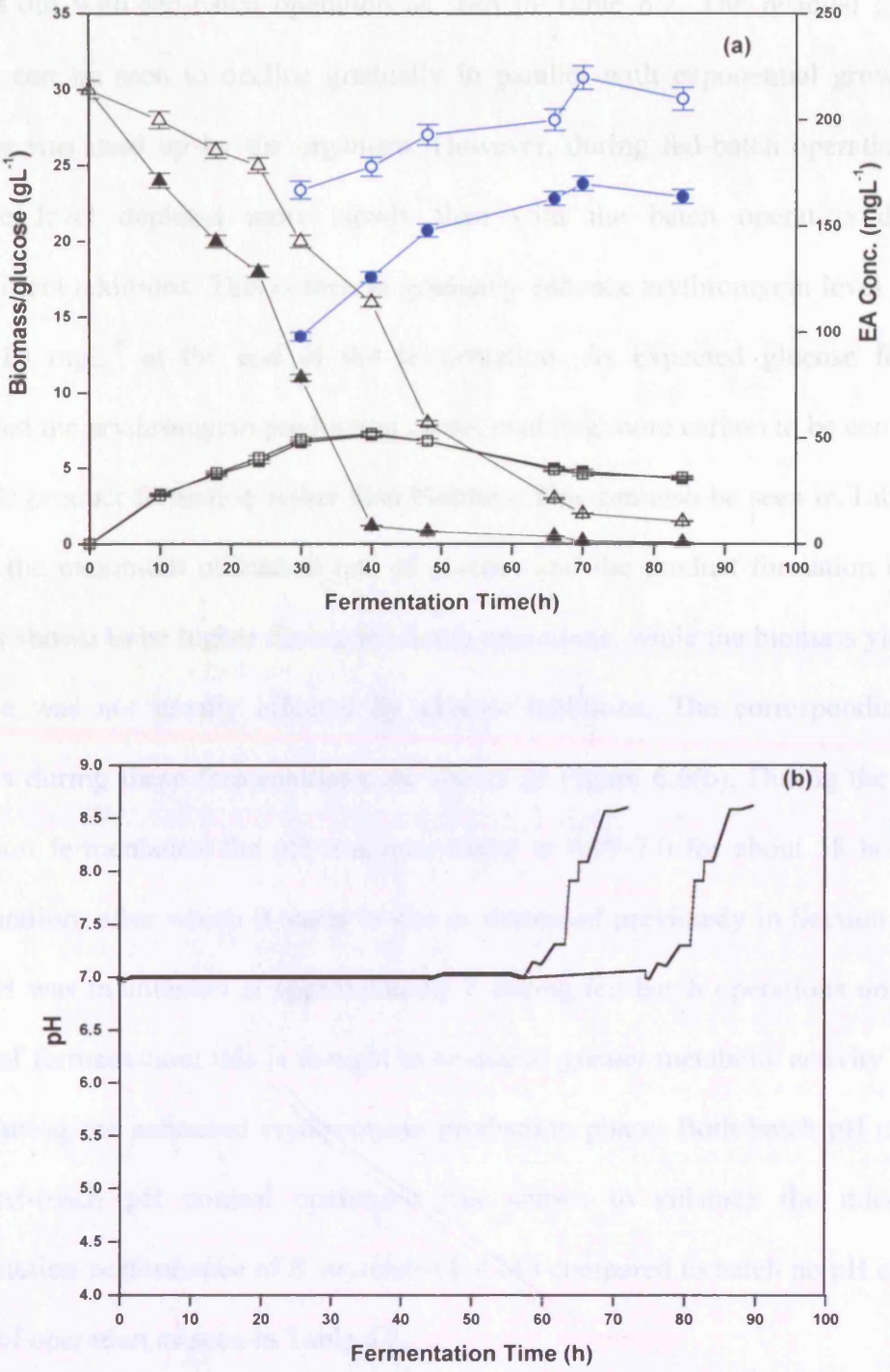

Figure 6.6 Batch and fed-batch operation of pH controlled microwell fermentations of *S. erythraea* CA340 on SCM medium: (a) Fermentation kinetics, symbols: (□, ■) biomass concentration, (▲, Δ) glucose concentration, (●, ○) erythromycin A concentration. Closed symbols represent data obtained during batch fermentation, while open symbols represent data obtained during fed-batch fermentation, (b) pH profiles, (+) batch fermentations, (-) fed-batch fermentations. Error bars represent deviation of triplicate measurements. Fermentations were carried out in duplicate as described in Sections 2.6.1 and 2.6.7

maximum of 170 mgL^{-1} as compared to 220 mgL^{-1} obtained during fermentations carried out with fed-batch operation as seen in Table 6.2. The residual glucose curves can be seen to decline gradually in parallel with exponential growth, as glucose was used up by the organism. However, during fed-batch operation, the glucose level depleted more slowly than with the batch operation due to intermittent additions. This is seen to gradually enhance erythromycin level which was 210 mgL^{-1} at the end of the fermentation. As expected glucose feeding extended the erythromycin production phase, enabling more carbon to be converted towards product formation rather than biomass. This can also be seen in Table 6.2 where the maximum utilisation rate of glucose and the product formation by the cells is shown to be higher during fed-batch operations, while the biomass yield on glucose was not greatly affected by glucose additions. The corresponding pH profiles during these fermentations are shown in Figure 6.6(b). During the batch operation fermentation the pH was maintained at 6.99-7.0 for about 58 hours of fermentation, after which it starts to rise as discussed previously in Section 6.3.4. The pH was maintained at approximately 7 during fed-batch operations up to 72 hours of fermentation; this is thought to be due to greater metabolic activity of the cells during the enhanced erythromycin production phase. Both batch pH control and fed-batch pH control operations has shown to enhance the microwell fermentation performance of *S. erythraea* CA340 compared to batch no pH control mode of operation as seen in Table 6.2.

Table 6.2 Comparison of fermentation kinetics of *S. erythraea* CA340 microwell fermentation carried out with different feeding operations. Fermentations were carried out as described in Sections 2.6.1 and 2.6.8.

Fermentation parameter	Batch no pH control	Batch pH control	Fed-batch pH control
Total glucose added (gL^{-1})	30	30	25
Maximum glucose utilisation rate ($gL^{-1}\ h^{-1}$)	0.59	0.74	0.87
X_{max} (gL^{-1})	5.01	6.9	7.0
Biomass yield on glucose ($Y_{x/s}$)	0.1	0.16	0.17
EA_{max} (mgL^{-1})	90	134	220
Specific EA yield ($mg_{EA}mg^{-1}_{cells}$)	18	19	24

6.4 Summary

In this work an automated system for controlling pH during microwell fermentations of *S. erythraea* CA340 was designed and built. It consisted of a specially designed microwell plate, a micro-combination pH probe, a LabView data acquisition device, a PID controller and a Packard II robotic liquid handling system. Previous experimental data obtained from fermentations of *S. erythraea* CA340 obtained in Chapter 4 was used to define the volume and frequency of NaOH additions by the automated pH control system. The system responded well to radical variations of the pH from the set-point and maintained an accurate control of the pH.

The system was used to monitor and control the pH during batch microwell fermentation of *S. erythraea* CA340 and the results showed that erythromycin A titres and the growth rate were greatly enhanced during fermentations carried out with automated pH control than those obtained with no implemented pH control. The results obtained were in good agreement with previous data attained in Chapter 4 during manual base only pH control operations.

The liquid handling capability of the system was adopted for additions of glucose during fed-batch microwell fermentations of *S. erythraea* CA340. This mode of operation has enhanced the titres of erythromycin A by more than two fold.

7.0 Summary and Future Work

7.1 Overall Summary and Conclusions

Here the main findings of this thesis are summarized with respect to the aims and objectives identified in Section 1.6. As a basis for predictive scale-up the initial focus of this research was to define the engineering environment in a shaken 24-well microtitre system (Chapter 3). This involved the determination of oxygen mass transfer coefficients and liquid phase mixing times at different shaking frequencies and fill volumes in a purpose built mimic of a single well from a 24-well plate (Figure 2.1). Measurements of the dissolved oxygen tension (DOT) in the shaken microwell using water and soluble complex medium (SCM) as process fluids were carried out using a miniature fiber optic oxygen probe. Corresponding volumetric mass transfer coefficients, k_La, values were calculated from the DOT profiles obtained (e.g. Figure 3.3) as a function of time using the gassing out technique (Van't Riet, 1979). It was discussed that there was a general trend of an increase in k_La with increasing shaking frequencies and decreasing fill volumes due to an increase in the gas-liquid interfacial area (Section 3.3.3.) This suggests that the specific surface area, a, is the main parameter governing oxygen transfer capability in shaken microwells.

High speed video was also used to visualise the liquid hydrodynamics in the shaken microwell system. It was observed that the surface of the liquid was almost stationary during shaking of water and SCM at shaking frequencies lower than 500 rpm, while at 500 rpm and higher speeds a rotational vortex is created and its depth increased with increasing the shaking frequency (Figure 3.1). These observations confirmed an increase in the interfacial area available for mass transfer with an

increase in shaking frequency and a decrease in fill volume as discussed in Section 3.3.2. During shaking of the more viscous OBM, the surface of the liquid remained generally unmoved during all the shaking conditions applied leading to much lower k_La values. Liquid phase mixing times during shaking of the microwell were measured using a tracer dye technique (Figure 3.1) placed in microwells containing water, SCM and OBM as process fluids (Section 3.3.2). Mixing times to achieve homogeneity were determined in the water and SCM as 4.8 s and 5.4 s respectively for shaking at 800 rpm; the mixing times measured in the OBM, were higher than 200 s due to the high viscosity of the fluid hindering its movement within the well. These experimental results verified computational fluid dynamics (CFD) predictions of the fluid motion and gas-liquid interface (Figure 3.5) during shaking of the microwell.

The impact of the main engineering parameters within the shaken microwell on fermentation process kinetics was subsequently investigated using *S. erythraea* CA340 grown in SCM. The results were compared to experiments performed in 7 L stirred bioreactor. Measured k_La values in the microwell system were about half those calculated in the stirred bioreactor (Table 3.2). However, the growth rate and erythromycin production levels determined in the microwell fermentation were only slightly lower (Figure 3.6). The DOT profile of the microwell fermentation, carried out with a fill volume of 2.5 mL and shaken at 800 rpm, closely resembled that of the 7 L scale fermentation. This suggested that the oxygen transfer was not limiting in the fermentation and that other parameters like shear, or lack of pH control, were responsible for the reduced performance of the microwell fermentations. To investigate possible shear effects on the physiology of the organism, image analysis was also used to investigate the morphology of the *S.*

erythraea, during microwell and 7 L fermentations. The results showed that the main hyphal length (ML) and branch length (BL) increased rapidly during the exponential growth phase of all fermentations (Figure 3.9). However, ML and BL were lower during microwell fermentations, especially, during fermentations carried out with higher fill volumes and lower shaking frequencies. This can be explained by the low growth rates observed during microwell fermentations carried out at low shaking frequencies and higher fill volumes due to lower oxygen transfer rates. This also explains the lower titers of erythromycin produced during microwell fermentations as compared to those obtained during 7 L scale.

The impact of fermentation pH on the kinetics of growth and erythromycin biosynthesis of *S. erythraea* CA340 at both the microwell and 7 L scales was investigated by implementing different strategies of pH control (Chapter 4). At the 7 L scale the implementation of base only or full pH control (NaOH and H_3PO_4 additions) significantly increased both the maximum growth rate and the biomass concentrations attained compared to fermentations without pH control. There was over a two-fold increase in erythromycin biosynthesis (Table 4.1) and the ratio of erythromycin A (EA) to erythromycin C (EC) increased from 2:1 to 6:1 (base only pH control) to 11:1 (full pH control). In order to measure the pH during microwell fermentations a specially designed microwell plate was built (Figure 2.2) that allowed the insertion of a miniature pH probe into each well. Using this, manual base only pH control was initially implemented in microwell fermentations, as discussed in Section 4.3.5, resulting in enhanced maximum specific growth rate and biomass concentration. Total erythromycin synthesis and the ratio of EA: EC were also significantly enhanced (Table 4.3). Due to the volume restrictions within

the microwell and the production of acidic metabolic products during the majority of the fermentation, only base was used to control the pH during microwell fermentations.

During shaking of viscous broths, the rotational fluid movement will increasingly tend to be out–of-phase, resulting in hampered mass transfer, altered metabolism and a reduction in the product titre (Peter *et al.*, 2004). The effect of three different types of media, SCM, OBM, and SBM on the kinetics of growth and erythromycin biosynthesis of *S. erythraea* CA340 and EM5 strains was next investigated during fermentations carried out in the 5 L and microwell scale (Chapter 5). During the 5 L fermentations, Sections 5.2.2-5.2.4, it was observed that growth of *S. erythraea* CA340 was quickest on the SCM and SBM (SCM 0.09 h^{-1}, SBM 0.12 h^{-1}), however, erythromycin production only reached a maximum of 200 mgL^{-1} compared to 400 mgL^{-1} obtained during fermentations carried out with OBM. The high product titres obtained during OBM fermentations was also associated with longer fermentation times (176 ±15 h). This trend of fast growth of *S. erythraea* CA340 on SCM and SBM accompanied by low product titres was also repeated during microwell fermentations (Table 5.3). Poor mixing was observed during microwell fermentations carried out with the OBM resulting in very low growth and production rates (Figure 5.7). Similar investigations on the effects of media in fermentation kinetics were also performed with the Pfizer *S. erythraea* EM5 strain, but quantitative results could not be disclosed due to reasons of commercial confidentiality. The outcome of this work led to the conclusion that SCM is the most suitable for use during microwell fermentations of *S. erythraea* CA340 due to short liquid phase mixing times (necessary for pH control) and sufficiently high

oxygen transfer rates (necessary for adequate cell growth and erythromycin biosynthesis).

The identified need to control key physio-chemical parameters such as pH during microwell fermentations finally led to the design and implementation of a system for pH control in parallel microwell fermentations (Chapter 6). This consisted of an integrated LabView PID controller, a Packard II liquid handling robot and a miniature pH probe (Figure 6.2). The pH was controlled by additions of NaOH solution throughout the course of S. *erythraea* CA340 microwell fermentation, where the pH was kept mostly constant at the set-point of pH 7 (Figure 6.5). The automated pH control system could also be used to facilitate fed-batch microwell fermentations of *S. erythraea* CA340. This was carried out by feeding a mixed solution of glucose, the main carbon source in the SCM, and NaOH concurrently into the wells to replenish the glucose content and control the pH of the fermentation at the same time. This fed-batch feeding strategy had no apparent impact on the growth rate of *S. erythraea* CA340, however, erythromycin A titre was increased by almost two fold (Figure 6.6).

7.2 Future Work

The outcome of this research has showed the potential benefits for implementing pH control during *S. erythraea* CA340 fermentation. It also highlighted the advantages for using automated microwell technology as a tool for monitoring and control during bioprocess operations. Suggested further areas for investigation include:

- Further mixing studies within the microwell are required to address issues associated with adapting the system to cope with high viscosities liquid-solid and liquid-liquid mixtures.
- The automatic pH control capability of the system can be improved to further incorporate parallel monitoring and control of other important process parameters, such as dissolved oxygen and optical density. Ideally in a commercially avaiable device.
- The demonstration of the generic benefits of implementing microwell pH control with other microorganisms with high specific growth rates e.g. *E. coli* and possibly mammalian cell systems where pH fluctuation is a challenge.
- The demonstration of the high throughput potential of pH controlled microwell fermentations with larger studies on strain selection or optimisation of fermentation process conditions using experimental design techniques.

8.0 References

Ahmed, Z.U., Shapiro S., Vining, LC. **1984**. Excretion of alpha-keto acids by strains of *Streptomyces venezuelae*. Can.J Microbiol 30, 1014-1021.

Allen D.G. and Robinson C.W. **1990**. Measurement of rheological properties of filamentous fermentation broths. Chem. Eng. Sci. **45**, No. 1, 37-48.

Altenbach-Rehm J., Drescher T., Weuster-Botz D. **1999**. Verfahren und Vorrichtung zur serienkultivierung von mikroorganismen, German Patent DE 197 09 603 C2.

Alvarez M.M, Zalc J.M, Shinbrot T, Arratia P.E and Muzzio F.J. **2002**. Mechanisms of mixing and creation of structure in laminar stirred tanks, A.I.Ch.E J, **48,** 2135:2148.

Ammanullah A., Baba A., McFarlance CM., Emery AN, Nienow AW., **1993.** The use of *Bacillus Subtilis* as an oxygen sensitive culture to simulate dissolved oxygen cycling in large scale fermenters. Trans IChemE Part C 71: 206-208.

Amanullah, A, McFarlane CM, Emery AN, Nienow AW, **2001**. Scale-Down model to simulate spatial pH variations in large-scale bioreactors, Biotech Bioeng 73, 390-399.

Anderson L, Yang S, Neubauer P, Enfors S-O. **1996**. Impact of plasmid presence and induction on cellular response in fed-batch cultures of *Esherichia coli.* J Biotecnnol, 46, 255-263.

Ariff, A.B, Sabih, B.A, Azudin, M.N, Kennedy, J.F, **1997**. Effect of mixing on enzymatic liquefaction of sago starch. Carbohydrate Polymers, 33, 101–108.

Atkinson B. and Mavituna F. **1991**. Biochemical Engineering and Biotechnology Handbook. 2nd edition Chapter 11, Macmillan, Basingstoke.

Badino A.C, Facciotti M.C.R, Schmidell W. **2001**. Volumetric oxygen transfer coefficient (k_La) in batch cultivations involving non-Newtonian broths. Bio Chem Eng J, 8, 111-119.

Bastin G, Dochain D: **1990**. On-line Estimation and Adaptive Control of Bioreactors. Amsterdam: Elsevier.

Bechtle, RM, 1974. Conversion of whey solids to an edible yeast cell mass. *US Pat.* 3818109.

Berg M, Undisz K, Thiericke R, immermannP Z, Moore T / Posten C. **2001**. Evaluation of liquid handling conditions in microplates.J Biomol Screen., 6, 47-56.

Björkman U. **1987**. Properties and principles of mycelial flow: experiments with a tube rheometer. Biotechnol. Bioeng. **29**, 114-129.

Bormann E.J, Herrmann R. 1968. On the secretion of pyruvate and ketoglutarate by *Streptomyces rimosus*. Arch.Mikrobiol. 63, 41-52.

Bouaifi M, Roustan M. 2001. Power consumption, mixing time and homogenisation energy in dual-impeller agitated gas-liquid reactors. Chem Eng Proces, 40, 87-95.

Brunati , Marinelli F, Bertolini C, Gandolfi R, Daffonchio D ,Molinari F. **2004**. Biotransformations of cinnamic and ferulic acid with actinomycetes. Enzy Microb Technol, 34, 1-82

Buchs J. **2001**. Introduction to advantages and problems of shaken cultures. Biochem Eng J, **7**, 91-99.

Buchs J, Maier U, Milbradt C, Zoels B. **2000**. Power consumption in shaking flasks on rotary shaking machines. II. Nondimensional description and flow regimes in unbaffled flasks at elevated liquid viscosity. Biotechnol Bioeng, 68, 594-601.

Buchs J, Lotter S, Milbradt C. **2001**. Out-of-phase operating conditions, a hitherto unknown phenomenon in shaking bioreactors. Biochem Eng J, 7, 135-142.

Bulgakova VG, Grushina VA, Orlova T I, Petrykina ZM, Polin AN, Mironov VA, Danilenko VN, **1993**. Metabolism of alpha-ketoacids in erythromycin biosynthesis in various strains of *Saccharopolyspora erythraea*, Antibot Chemoter 38, 14-19.

Bu'Lock, J.D. **1974**. Secondary metabolism of microorganisms. In Industrial Aspects of Microorganisms. Ed. by B. Spencer. Elsevier. 335-345.

Burbaum J, **1998**. Miniaturization technologies in HTS: how fast, how small, how soon? Drud Discov Today, 3, 299-352.

Bushell ME., Dunstan GL., Wilson GC, **1997**. Effect of small scale culture vessel type on hyphal fragment size and erythromycin production in *Saccharopolyspora erythraea*, Biotech Lett 19, 849-852.

Bushell, M E. **1988**. Growth, product formation and fermentation technology. In: Actinomycetes in Biotechnology, ed. M. Goodfellow, ST Williams, Mordarski. M, London: Academic Press, 185-217.

Cane, D. E. **1994**. Polyketide biosynthesis: molecular recognition or genetic programming Science 263, 338-340.

Carreras C, Frykam S, Ou S, Cadapan L, Zavala S, Woo E, Leaf T, Carney J, Burlingame M, Patel S, Ashley G, Licari P, **2002.** *Saccharopolyspora erythraea*-catalyzed bioconversion of 6-deoxyerythronolide B analogs for production of novel erythromycins, J Biotech 92, 217-228.

Carrington, R. **1986**. A review of antibiotic isolation techniques. In: *Bioactive Microbial Products* **3** 45-58. Ed by Stowell, J.D., Bailey, P.J. and Winstanley, D.J. Academic Press. London.

Cavanagh M.F, Ison A.P, Lilly, M.D, Carleysmith S.W, Edwards J. **1994**. The utilization of lipids during *Streptomycete* fermentations. IChemE Res. Institute of Chemical Engineering, Rugby, UK.

Chen MC, **1996**. Optimizing, the concentration of carbon, nitrogen and phosphorus in citric acid fermentation with response surface method, Food Technol 10, 13-27.

Clark GJ, Langley D, Bushell ME. **1995.** Oxygen limitation can induce microbial secondary metabolite formation: investigations with miniature electrodes in shaker and bioreactor culture. Microbiology 141, 663-669.

Corcoran J.W, A. Vygantas M, **1977**. Hydroxylation steps in erythromycin biogenesis, Fed Proc, Fed Am Soc Exp Biol 36, 663.

Corcoran JW, **1984**. In Macrolide Antibiotics: Chemistry, Biology, and Practice (Omura, S., Ed.), 231-259, Academic Press, Orlando, FL.

Cortes J, Velasco J, Foster G, Blackaby A P, Rudd B A, Wilkinson B. **2002**. Identification and cloning of a type III polyketide synthase required for diffusible pigment biosynthesis in *Saccharopolyspora erythraea*. Mol Microbiol., 44, 1213-1224.

Danielson P.B, Büchs J, Stöckmann C, Fogleman JC. **2004**. Maximizing cell densities in mini prep-scales cultures with H15 medium and improved oxygen transfer. Biochem Eng J, 17, 175-180.

Davies J.L, Baganz F, Ison AP, Lye GJ, **2000**. Studies on the interaction of fermentation and microfiltration operation: Erythromycin recovery from *Saccharopolyspora erythraea* fermentation broths, Biotech Bioeng 69, 429-439.

Davies J. **2001**, Process Synthesis for antibiotic recovery by microfiltration from *Saccharopolyspora erythraea* fermentations. PhD thesis. University College London.

Doig S.D, Baganz F, Lye G.J. **2004**. High throughput screening and process optimisation, In: Basic Biotechnology, Ratledge B, Kristiansen (Eds), 3rd ed., Cambridge University Press.

Doig SD, Pickering SCR, Lye GJ, Baganz F. **2005a**, Modelling surface aeration rates in shaken microtitre plates using dimensionless groups. Chem Eng Sci, 60, 2741-2750.

Doig SD, Diep A, Baganz F. **2005b**, characterisation of a novel miniaturised buble column bioreactor for high throughput cell cultivation. Biochem Eng J, 23, 97-105.

Doull JL, Vining L C **1990**. Global Physiological Controls. In: Genetics and Biochemistry of Antibiotic Production, ed. L. C. Vining, C. Stuttard, Boston: Butterworth-Heinemann, 9-63.

Drew S.W, Demain A.L. **1977**, Effect of primary metabolism on secondary metabolism. Ann Rev Mivrobiol. 31, 343-356.

Dunn I.J, Eninsle AJ, **1975**. Oxygen transfer coefficient by the dynamic method. J App Chem Biotech, 25, 707-720.

Dutez W, Ruedi R, Hermann K, O'Connor J, Buchs J, Witholt B, **2000**. Methods for intense aeration, growth, storage and replication of bacterial strains in microtiter plates. Appl. Environ. Microbiol 66, 2641-2646.

Dutez WA, Whitholt B. **2001**. Effectiveness of orbital shaking for the aeration of suspended bacterial cultures in square-deepwell micotitre plates. Biochem Eng J, 7, 113-115

Elibol M, **2002**. Product shifting by controlling medium pH in immobilised *Streptomyces coelicolor* A3(2) culture, Proc Biochem 37, 1381-1386.

Elmahdi I, Baganz F, Dixon K, Harrop T, Sugden D, Lye GJ, **2003**. pH control in microwell fermentations of *S. erythraea* CA340: influence on biomass growth kinetics and erythromycin biosynthesis. Biochem Eng J 16, 299-310.

Enfors S.O., Jahic M., Rozkov A., Xu B., Hecker M., Jurgen B., Kruger E., Schweder T., Hamer G., Beirne D. O', Noisommit-Rizzi N., Reuss M., Boone L., Hewitt C., McFarlane C., Nienow A., Kovacs T., Tragardh C., Fuchs L., Revstedt J., Friberg P.C., Hjertager B., Blomsten, Skogman G. H., Hjort S., Hoeks F. and Lin, H.-Y., **2001**. Physiological responses to mixing in large scale bioreactors, J Biotechnol., 85, 175-185.

Escalante L, Lopez H, del Carmen MR, Lara F, Sanchez S. **1982**. Transient repression of erythromycin formation in *Streptomyces erythraeus*. J of General Microbiol. 128 (Pt 9), 2011-2015.

Flores ME. **1996**. Nitrogen regulation of urease synthesis in Saccharopolyspora erthtraea ATCC 11365. FEMS Microbiol Lett 139, 57-62.

Flores M E., Sanchez S. **1985**. Nitrogen Regulation of Erythromycin Formation in *Streptomyces erythreus*. FEMS Microbiol Lett 26, 191-194.

Fisher SH. **1993**. Utilization of amino acids and other nitrogen-containing compounds. In: A.L. Sonenshein, J.A. Hoch and R. Losick, Editors, *Bacillus subtilis* and Other Gram-positive Bacteria, American Society for Microbiology, 221-228.

Girard P, Jordan M, Tsao M, Wurm FM. **2001**, Small scale bioreactor system for bioprocess development and optimisation. Biochem Eng J, 7, 117-119.

Goodfellow M., WilliamsS.T. and Mordarski M. **1983**. Introduction to and importance of actinomycetes. In: *The Biology of Actinomycetes*. 1-6.

Glazebrook MA, Vining, LC, 1992. Growth morphology of *Stretomyces oikyoshiensis* in submerged culture: influence of pH, inoculum and nutrients. Can J Microbiol, 38, 98-103.

Harms P, Kostov Y, Rao G, **2002**. Bioprocess monitoring, Current Openion Biotech 13, 124-127.

Hart T, **2001**. Future combinatorial strategies for chemistry and biology. Drug Discov Today 6, 937-939.

Henzler HJ, Schedel M. **1991**. Suitability of shaking flask for oxygen supply to microbial cultures. Bioproc Eng, 7, 123-131

Hermann R, Lehmann M, Buchs J, **2002**. Characterization of gas-liquid mass transfer phenomena in micotiter plates, Biotech Bioeng 81, 178-186.

Heydarian, MS., Mirjalili N. and Ison, AP. **1999**. Effect of shear on morphology and erythromycin production in *Saccharopolyspora erythraea* culture. *Bioprocess Eng.* 21, 31-39.

Heydarian, S.M. **1998a**. The influence of agitation on morphology, rheology and erythromycin production in *Saccharopolyspora erythraea* culture. PhD Thesis, University College London.

Heydarian, S.M., Ison, A.P. and Mirjalili, N. **1998b**. A rapid and simplified extraction method of erythromycin from fermentation broth with bond elut C18 cartridge for analysis by HPLC. Biotechnol. Tech. 12 155-158.

Heydarian, S.M., Lilly, M.D. and Ison, A.P. **1996**. The effect of culture conditions on the production of erythromycin by *Saccaropolyspora erythraea* in batch culture. Biotechnol. Lett. 18, 1181-1186.

Hilton M.D. 1999. Small scale liquid fermentations, in A.L. Demain J.E, Davies (Eds.), Manual of industrial microbiology, Washington, 49-60.

Hobbs, G., Obanye, A. I., Petty, J., Mason, J. C., Barratt, E., Gardner, D. C., Flett, F., Smith, C. P., Broda, P., Oliver, S. G. **1992**. An integrated approach to studying regulation of production of the antibiotic methylenomycin by *Streptomyces coelicolor* A3(2). J Bacteriol 174, 1487-1494.

Ives, PR, Bushell ME. **1997**. Manipulation of the physiology of clavulanic acid production in *Streptomyces clavuligerus*. Microbiology 143 (Pt 11), 3573-3579.

Jian Li Z., Shukla V., Wenger K.S., Fordyce A.P., Petersen A.G. and Marten M.R. **2002**. Effects of increased impeller power in a production-scale *aspergillus oryzae* fermentation, Biotechnol Prog., 18, 437-444.

John GT, Heinzle E, **2001**. Quantitative screening method for the hydrolases in microplates using pH indicators: Determination of kinetic parameters by dynamic pH monitoring, Biotech Bioeng 72, 620-627.

John GT, Kilmant I, Wittmann C, Heinzle E, **2003**. Integrated optical sensing of dissolved oxygen in microtiter plates: A novel tool for microbial cultivation, Biotech Bioeng 81, 829-836.

Junker B, Mann Z, Gailliot P, Byrne K and Wilson J. **1998**. Use of soybean oil and ammonium sulfate additions to optimise secondary metabolite production. Biotechnol. Bioeng. 60 580-588.

Karl S, **2001**. Progress in monitoring , modelling and control of bioprocess during the last 20 years, J Biotechnol 85, 149-173.

Karsheva M, Hristov J, Penchev I, and Lossev V. **1997**. Rheological behaviour of fermentation broths in antibiotic industry. App. Biochem. Biotech. 68 187-206.

Kato Y, Hraoka S, Tada, Y, Koh S.T, Lee Y.S.**1996**. Mixing time and power consumption for a liquid in a vertical cylindrical vessel, shaken in a horizontal circle. Trans IChemE, 74, 451-455.

Katz L. 1997. Manipulation of modular polyketide synthases. Chemical Reviews 97, 2557-2575.

Kebwage, CI, Roets E, Hoogmartens RJ, Vanderhaeghe H. 1987. Optimisation of the separation of erythromycin and related substraes by HPLC, J Chromatogr. 409, 91-100.

Kenny O, Doig SD, Ward, JM, Baganz F. **2005**. A novel method for the measurment of oxygen mass transfer in small scale vessels. Biochem Eng J, 25, 63-68.

Keun Jung Y, Hur W, **2000**. A new method of on-line measurment of buffer capacity and alkali consumption rate of a fermentation process, Biosci Bioeng 90, 580-582.

Kermis HR, Kostov Y, Harms P, Rao G. **2002**. Dual excitation ratiometric fluorescent pH sensor for non-invasive bioprocess monitoring: Development and applications. Biotechnol Prog, 18, 1045-1053.

Kojima I, Cheng YR, Mohan V, Demain A L. 1**995**. Carbon source nutrition of rapamycin biosynthesis in *Streptomyces hygroscopicus*. J Ind.Microbiol 14, 436-439.

Kostov Y, Harms P, Randers-Eichhorn L, Rao G, **2001**. Low cost microbioreactor for high throughput bioprocessing, Biotech Bioeng 72, 346-352.

Kumar S, Wittmann C, Heinzle E, **2004**. Minibioreactors, Biotechnol letters,10, 1-10.

Kurz RE (Ed.), 1996. Proceedings of the third european conference on optical chemical sensors and biosensors, Sensors and Actutators B38, 1-457.

Lamping SR, Zhang H, Allen B, Ayazi Shamlou P, **2003**. Design of a prototype miniature bioreactor for high throughput automated bioprocessing Chem Eng Sci J 58, 747-758.

Langheinrich C, Nienow AW, **1999**. Control of pH in large-scale, free suspension animal cell bioreactors: alkali addition and pH excursions, Biotech Bioeng 66, 171-179.

Leach M. **1997**. Marvellous microplates, Drug Disc Today, 2, 174-175.

Lee M.S, Kojima I, Demain A. L.**1997**. Effect of nitrogen source on biosynthesis of rapamycin by *Streptomyces hygroscopicus*. J Ind.Microbiol Biotechnol. 19, 83-86.

Leib TM, Pereira CJ, Villadsen, J. **2001**. Bioreactors: a chemical engineering perspective.Chem Eng Scie, 19, 5485-5497

Li G-Q, Qiu H-W, Zheng Z-M, Cai Z-L. and Yang, S-Z. **1995.** Effect of fluid rheological properties on mass transfer in a bioreactor. J. Chem. Tech. Biotechnol. 62 385-391.

Lilly M.D, Ison A. and Shamlou, P.A. **1992**. The influence of the physical environment in fermenters on antibiotic production by microorganisms. Harnessing-Biotechnol. 21st Century. 219-222.

Lubbe C, Wolfe S, Demain AL. **1985**. Repression and inhibition of cephalosporin synthetases in *Streptomyces clavuligerus* by inorganic phosphate. Archives of Microbiology 140, 317-320.

Luli G.W., Strohl WR. **1990.** Comparison of growth, acetate production, and acetate inhibition of *Escherichia coli* strains in batch and fed-batch fermentations. Appl.Environ.Microbiol 56, 1004-1011.

Lye GJ, Ayazi-Shamlou P, Baganz F, Dalby P, Woodley JM., **2003**. Accelerated design of bioconversion processes using automated microscale processing techniques, Trends Biotechnol 21, 29-37.

Madden T, Ward JM, Ison, A.P. **1996**. Organic acid excretion by *Streptomyces lividans* TK24 during growth on defined carbon and nitrogen sources. Microbiology 142 (Pt 11), 3181-3185.

Maier U, Büchs J. **2001**. Characterisation of the gas-liquid mass transfer in shaking bioreactors. Biochem Eng J, **7**, 99-107.

Manns R. **1999**. Microplate history, 2nd ed. May 1999.

Manners DJ, **1989**. Recent developments in our understanding of amylopectin structure. Carbohydr. Polym. 11, 87–112.

Martin, JF, Demain AL. **1978**. Fungal Development and Metabolite Formation. In: The Filamentous Fungi, Volume 3, ed. J. E. Smith, D. R. Berry, London: Edward Arnold, 424-450.

Martin JF, Demain AL, **1980**. Control of antibiotic biosynthesis, Microbiol Rev, 44, 230-251.

Martin SM, Bushell, ME. **1996**. Effect of hyphal morphology on bioreactor performance of antibiotic-producing *Saccharopolyspora erythraea* cultures. Microbiology 142, 1783-1788.

Melzoch K, De Mattos MJT, Neijssel OM. **1997**. Production of Actinorhodin by *Streptomyces coelicolor* A3(2) Grown in Chemostat Culture. Biotechnol.Bioeng. 54, 577-582.

Metz B, Kossen NWF, Van Suijdam LC, **1979**. The rheology of mould suspensions. Adv Biochem Eng 11, 104-156.

Miller GL, **1959**. Use of dinitrosalycylic acid reagent for determination of reducing sugar, Analytical Chem 31, 426-428.

Minas W, Brunker P, Kallio PT, Bailey JE, **1998**. Improved erythromycin production in a genetically engineered industrial strain of *Saccharopolyspora erythraea*, Biotech Prog 14, 561-566.

Minas W, Bailey JE, Duetz W, **2000**. Streptomycetes in micro-cultures: Growth, production of secondary metabolites and storage and retrival in the 96-well format, Antonie van Leeuvenhoek 78, 297-305.

Mirjalili N, Zormapaidis V, Leadlay PF, Ison AP, **1999**. The effect of rapeseed oil uptake on the production of erythromycin and triketide lactone by *Saccharopolyspora erythraea*, Biotech Prog 15, 911-918.

Nakayama GR, **2001**. Combinatorial chemistry. Curr Opin Chem Biol 5, 239-240.

Morari M, Zafiriou E: **1997**. Robust Process Control. UK: Pearson Education, 78-97.

Nealon AJ, Wilson KE, Pickering SCR, Clayton TM, O'Kennedy RD, Titchener-Hooker NJ, Lye GJ. **2005**. Use of operating windows in the assessment of integrated robotic systems for the measurement of bioprocess kinetics. Bitechnol Prog, 21, 283-291.

Nienow AW. **1998**. Hydrodynamics of stirred bioreactors. Appl Mech Rev., 51, 3-32.

Omura S, Tanaka H, **1984**. Production and antimicrobial activity of macrolides, in Macrolide Antibiotics: Chemistry, Biology, and Practice (Omura, S., Ed.), 3-36, Academic Press, Orlando, FL.

Packer HL, Thomas CR, **1990**. Morphological measurements on filamentous microorganisms by fully automatic image analysis. Biotechnol Bioeng 35, 729-742.

Pena, E, Galindo, Díaz M. **2002**. Effectiveness factor in biological external convection study in high viscosity systems, J Biotech., 95, 1-12.

Peter CP, Lotter S, Maier U, Buchs J. **2004**. Impact of out-of-phase conditions on screening results in shaking flask experiments. Biochem Eng J, 17, 205-215.

Pickup K.M, Nolan R.D and Bushell M.E. **1993**. A method for increasing the success rate of duplicating antibiotic activity in agar and liquid culture of *Streptomyces* isolates in new antibiotic screens. J. Ferm. Bioeng. 76 89-93.

Pirt **1964**. The maintenance of energy of bacterial in growing cultures. Proceeding of the Royal Society of London 165, 224-231.

Pollard M. **2001**. Process development automation: An evolutionary approach. Organic Proc Res and Develp., 273-282.

Potvin J, Peringer P. **1994a**. Ammonium Regulation in *Saccharopolyspora erythraea*. Part I: Growth and Antibiotic Production. Biotechnol Lett 16, 63-68.

Potvin J, Peringer P. **1994b**. Ammonium Regulation in *Saccharopolyspora erythraea*. Part II: Regulatory Effects Under Different Nutritional Conditions. Biotechnol Lett 16, 69-74.

Prosser JI, Tough AJ. **1991**. Growth mechanisms and growth kinetics of filamentous microorganisms. Crit Rev Biotechnol. 10, 253-274.

Reeves AR, Cernota WH, Brikun IA, Wesley RK. 2004. Engineering precursors flow for increased erythromycin production in *Aeromicrobuim erythreum*. Metabolic Eng, 6, 300-312.

Roth M, Noack D. and Reinhardt G. **1982**. Properties of non-differentiating derivatives of *Streptomyces hygroscopicus*. J. Gen. Microbiology. 128 , 2687-2691.

Seno E.T, Hutchinson C.R, **1986** Antibiotic Producing Streptomyces, In: Queener S.W, Day L.E, (Eds.). The Bacteria: A treatise on structure and function, Academic Press, NY, 9, 252-279.

Shomura T, Yoshida J, Amani S, Kojima M, Inouye S. and Niida T. **1979**. Studies on *Actinomycetales* producing antibiotics only on agar culture. 1. Screening, taxonomy and morphology-productivity relationship of *Streptomyces halstedii* strain Sf-1993. Journal of Antibiotics. 32 427-435.

Smith CG, Bungay HR., Pittenger, RC. **1962**. Growth-Biosynthesis relationships in erythromycin fermentation. Appl.Microbiol 10, 293-296.

Stocks SM, Thomas, CR. **2001**. Strength of mid-logarithmic and stationary phase *Saccharopolyspora erythraea* hyphae during a batch fermentation in defined nitrate-limited medium. Biotechnol.Bioeng., 73, 370-378.

Stoeckli M, Farmer TB, Caprioli RM. 1999. Automated mass spectroscopy imaging with a matrix-assisted laser desorption ionisation time of flight instrument. J Am Chem Soc, 10, 67-71

Tang IC, Okos MR, Yang ST, **1989**. Effects of pH and acetic acid on homoacetic fermentation of lactate by Clostridium formicoaceticum, Biotech Bioeng 34, 1063-1074.

Tibor A, and, Buchs J. Device for sterile online measurement of the oxygen transfer rate in shaking flasks.

Treskatis S-K, Orgeldinger V, Wolf H, Gilles ED, **1996**. Morphological characterisation of filamentous micorganisms in submerged cultures by on-line digital image analysis and pattern recognition. Biotechnol Bioeng 53, 191-201.

Ushio M. **2004**. A Metabolic Engineering Approach to Examine Polyketide Production by *Saccharopolyspora erythraea*. PhD Thesis. University College London.

Van't Riet K. **1979**. Review of measuring methods and results in non-viscous gas-liquid mass transfer in stirred vessels. Ind Eng Chem Process Des Des., 18, 357-364.

Van Suijdam JC, Kossen NWF, Joha AC. **1978**. Model for oxygen transfer in shake flask. *Biotechnol Bioeng* 20: 1695-1709.

Vazquez G, Alvarez E, Cancela A, Navaza JM. **1995**. Density, viscosity, and surface tension of aqueous solutions of sodium sulfite and sodium sulfite + sucrose from 25 to 40°C. J Chem Eng Data 40, 1101-1105

Veglio F, Beolchini F, Ubaldini S. **1998**. Empirical models for oxygen mass transfer: a comparison between shake flask and lab-scale fermentor and application to manganiferous or bioleaching. *Proc Biochem* 33, 367-376

Vinici V and Byng G. 1998. Strain improvement by the non-recombinant methods. In Demain AL, Davies JE (eds) Manual of industrial microbiology and biotechnology. Am Soc Micobiol, 103-113.

Voigt J, Hecht V, Schügerl K. 1980. Absorption of oxygen in counter-current multistage bubble columns. II. Aqueous solutions with high viscosity. Chem. Eng. Sci., 35, 1317–1323.

Voigt H, Schnitthelm F, Lange T, Kullick T, Ferretti R. **1997**. Diamond-like carbon gate Ph-isfet. Sensors and Actutators B44, 441-445.

Vrabel P, Rob GJM, Lans V, Luyben AM, Boon L, Nienow AW. **2000**. Mixing in large-scale vessels stirred with multiple radial and axial up –pumping impellers: modelling and measurement. Chem Eng Sci., 55, 5881-5896.

Vrabel, G.J.R. van der Lans, F.N. van der Schot, K.Ch.A.M. Luyven, B. Xu and S. Enfors. **2001**. CMA integration of fluid dynamics and microbial kinetics in modeling of large-scale fermentations. Chem Eng J, 84, 463-474.

Warren S.J, Keshevarz-Moore E, Shamlou P.A, and Lilly M.D. **1995**. Rheologies and morphologies of three actinomycetes in submerged culture. Biotech. Bioeng. 45 80-85.

Weiss S, John GT, Klimant I, Heinzle E, **2002**. Modelling of mixing in 96-well microplates observed with fluorescence indicators, Biotechnol Prog 18, 821-830.

Weiss R, Luiten R, Skranc W, Schwab H, Wubbolts M, and Glieder A. **2004** Reliable high-throughput screening with *Pichia pastoris* by limiting yeast cell death phenomena. FEMS Yeast Res., 5, 179-189.

Westgate PJ, Curtis WR, Emery PM, Hasegawa PF, **1991**. Approximation of continuous growth of *Cephalotaxus harringtinia* plant cell cultures using fed-batch operation, Biotechnol Bioeng. 38, 241-246.

Weuster-Botz D, Altenbach-Rehm J, Arnold M, **2001**. Parallel substrate feeding and pH control in shaking flasks, Biochem Eng J 7, 163-170.

Wilson, GC. Bushell, ME. **1995**. The Induction of Antibiotic Synthesis in *Saccharopolyspora erythraea* and *Streptomyces hygroscopicus* by growth rate decrease is accompanied by a down-regulation of protein synthesis rate. FEMS Microbiol Lett 129, 89-96.

Wittmann C, Hyung MK, John G, Heinzle E. **2003**. Characterization and application of an optical sensor for quantification of dissolved oxygen in shake flasks.Biotechnol lett., 25, 377-380.

Wolcke J, Ullman D, **2001**. Miniturazied HTS technologies – uHTS. Drug Discov Today, 6, 637-646.

Wong JS, Rein AJ, Wilks D, Wilks P. **1984**. Infrared spectroscopy of aqueous antibiotic solutions. Appl Spectrosc, 38, 32-35.

Yen-Chun Liu, Feng-Sheng Wang, Wen-Chien Lee, **2001**. Online monitoring and controlling system for fermentation processes. J Biochem Eng, 7, 17-25.

Zhang H, Williams-dalson W, Keshavarz-moore E, Shamlou, Parviz. **2005**. Computational-fluid-dynamics (CFD) analysis of mixing and gas–liquid mass transfer in shake flasks. Biotechnol Appl Biochem, 41, 1-8.

Zimmermann HF, Gernot TJ, Trauthwein H. **2003**. Rapid evaluation of oxygen and water permeation through microplate sealing tapes. Biotechnol progress, 19, 1061-1063.

Appendix A

Reducing Sugar (DNS) Assay Calibration Curve

Figure 1 shows a typical example of a calibration curve for the DNS reducing sugar assay. The assay mixture is calibrated against known concentrations of glucose, from which the glucose concentration of fermentation broth can then be determined.

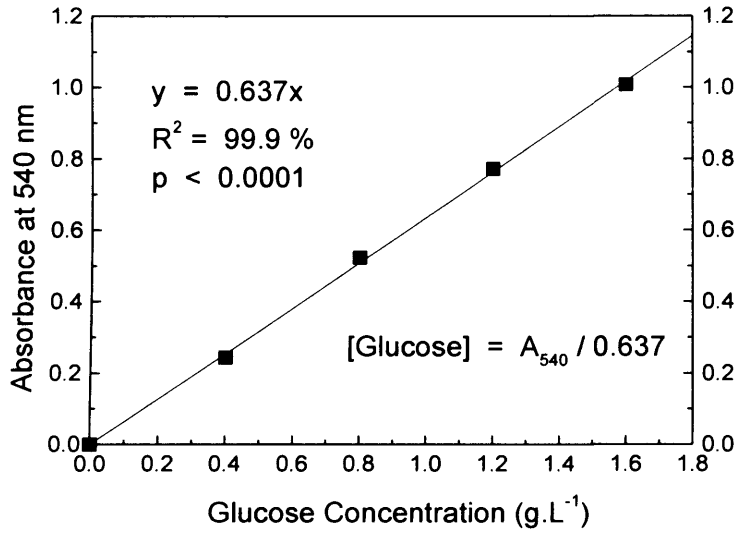

Typical calibration curve for the DNS reducing sugar assay, as described in Section 2.8.2.

Erythromycin Transmission Assay

Figure 2 shows an example of a calibration curve for the erythromycin assay. The assay mixture is calibrated against known concentrations of erythromycin, from which the erythromycin concentration of the broth can then be determined.

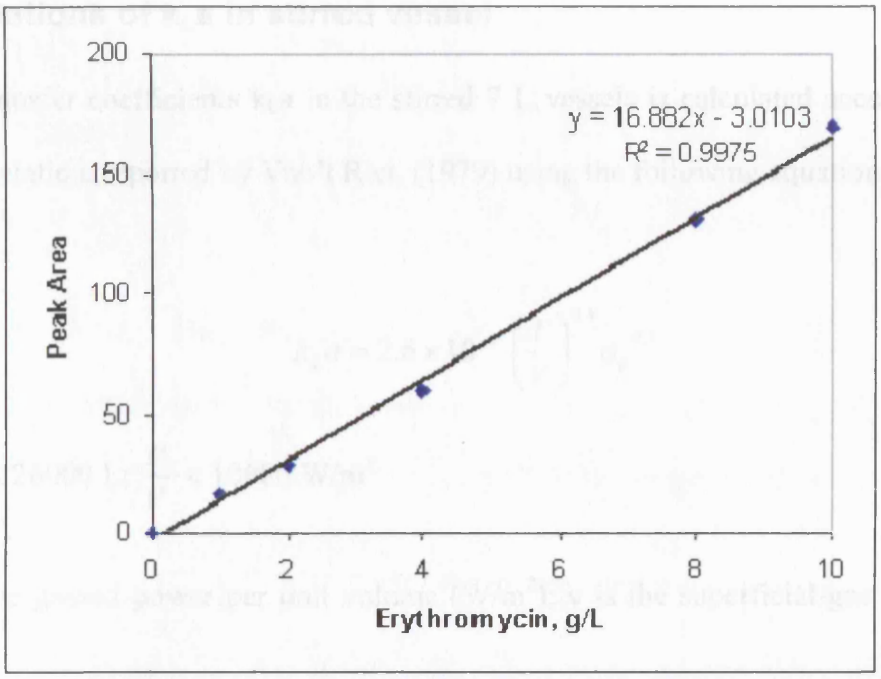

Typical calibration curve for the erythromycin concentration assay, as described in Section 2.8.5.

Image Analysis

The level of error for morphological measurements of *S. erythraea* CA340 mycelia was determined for 40 samples repeated in duplicate and the average standard deviation is summarized in Table 1.1.

Mean errors for morphological measurements.

Measurment	Mean Error (±)
Main Length (ML)	6.8
Branch Length (BL)	11.2

Calculations of k_La in stirred vessel

Mass transfer coefficients k_La in the stirred 7 L vessels is calculated according to the correlation, reported by Van't Riet, (1979) using the following equation

$$k_L a = 2.6 \times 10^{-2} \left(\frac{P}{V}\right)^{0.4} \upsilon_g{}^{0.5}$$

for; $V \leq 26000$ L; $\frac{P}{V} < 10000$ W/m^2

$\frac{P}{V}$ is the gassed power per unit volume (W/m^2); v is the superficial gas velocity (ms^{-3}) and:

$P = P_0 \rho N^3 D^5$

Where,

P_0 is the impeller power number

ρ is the density of water (kgm^{-3})

N is the impeller speed (rps)

D is the impeller diameter (m)

Appendix B: Scale-Down and Automation in Bioprocess Development

Introduction

Biopharmaceutical drug development process can take up to 10 years from discovery to final market launch. During this time there is a standard pathway through which all products are developed into unique, efficacious drugs. Bioprocess development falls into three main distinct areas:

- Route Scouting
- Process optimization
- Process definition/validation.

Route scouting

A large number of small-volume (1-10 mL) experiments are examined looking at different process operations, reagents and conditions. Sometimes only a "yes/no or better/worse type of answer is required. Often design of experiments (DoE) and statistical methods are used to indicate potential best conditions. This represents the starting point for further, more detailed examination. Route scouting occurs earlier on the project and has the most severe time constraints. A feasible-cost effective route must be rapidly identified to make initial samples for trial purposes.

Process Optimization

At this stage, fewer experiments in the scale of (10-100 mL) are carried out at bench-scale to optimize the best candidates from the route scouting stage. Better monitoring of operating parameters is required and more sophisticated types of control may be used. Again DoE and statistical methods may be used.

Process definition and validation

These are usually carried out using bioreactors at the scale of 1 L or larger scale, controlled and data logged in great detail in equipment with characteristics as close as possible to those of the proposed manufacturing plant.

The use of microwell technology within bioprocess development represents a potential solution to the bottleneck of process development within the drug discovery cycle. Additionally, the use of large scale operations mimics have been identified as the main procedure for bioprocess development. This method can be implemented at various stages within the cycle depending on the ultimate aim during process development. Automated microscale processing techniques are rapidly becoming a means to increase the speed of bioprocess development and reduce the costs involved.

Automated systems are often perceived overwhelming when observed in action, but their apparent complexity is a relatively straight forward process. With a good understanding of what the system is doing, it becomes clear that the basic operations are actually quite simple. The automated system's power relies in its ability to repeat these simple procedures rapidly, reliably and tirelessly. Automated systems are widely available commercially and their application covers a broad range of operations.

Aims and Objectives

The primary aim of this report is to investigate the repercussions of applying automated microwell technology as a tool for bioprocess development. Possible application of the automated pH control system, described in this thesis, in industry is assessed and the impact of economics and regulatory affairs are evaluated.

Applications of automated pH controlled microwell system

The automated pH controlled microwell system described in this thesis can have many potential applications within the bioprocess industry. These include:

- As a tool for measuring the pH during high throughput screening of potential candidates, where the metabolic state of the organisms in question is important.
- Application during fermentation process development as a mimic for larger scale operations for investigating important engineering and environmental parameters.
- As a quality assurance (QC) or a process analytical technology (PAT) tool. The system capability to monitor and control the pH can be developed to include dissolved oxygen and optical density monitoring. This will make it a potential tool for random checks of these parameters as well as a contamination detection tool.

Cost assessment

Classically a typical development scientist will run on average perhaps one experiment per day, at a current cost of £ 400 – 500, excluding consumables and labor costs. This is almost £ 1 per minute. Much of that time is spent setting up and then watching the experimental parameters and making notes, etc (Pfizer Ltd Kent staff, personal communication). If automation is to be used, productivity would increase by either running multiple parallel reactions or extending the working day, or both. This will significantly increase experimental throughput and simultaneously allow the scientist more time to plan, analyze and utilize scientific knowledge.

Anther factor to take into account is the rate of error for operating manual experimentation. Manual methods for carrying out complicated experiments can range between 10 – 30 %, while those reported with using fully automated methods are between 1 - 5 %.

Consumables can be the most expensive part of any biochemical process. These costs scale with the number of experiments or processes performed and therefore can be quite variable. In addition, the costs involved in disposing of these consumables are often overlooked. Chemical and biochemical hazard disposal can be very expensive and some reagents are more expensive to dispose of than to purchase. One of the main advantages of using automation is to reduce the cost of consumables. This reduction is further enhanced, by reducing the size of the process, if microscale operations with integrated robotic systems are used.

An initial capital investment on automated equipments purchasing is required, and the cost of equipment can range from £2,000 – 6,000,000 (including an annual 10 % service contract) depending on system capabilities and whether it is pre-integrated or custom made.

Regulatory Issues

As the regulatory targets that must be met during drug development increases every year and is consentingly brought forward into the early process development stages, microwell technologies must comply with these directives in order to become a useful bioprocess development tool.

If the automated pH control system is to be used as a QC tool during process development it is important to include all validation documents related to the equipment in the original validation master plan (VMP). Providing that the equipment is designed and commissioned according to the industry standards, it is

vital to include documents related to equipment operational procedures and safety checklists and documentations.

This system will perform pH measurement and liquid handling operations repetitively and with little user intervention. Validation should be designed by the developer to ensure the following:

- Accuracy: How close is the measured value of the pH to the true value?
- Precision: How close are several data values to each other under the same test conditions?
- Intermediate precision: how reliable is the measurement data obtained in different test environments.
- Repeatability: how close are multiple measurements of a sample by the system under the same conditions?
- Reproducibility: What is the precision level compared to other methods tested.
- Limits: What are the detection limitations of the system, and what are the quantified limits of the sample to be measured?

The liquid handling capabilities of the system can be tested by using industry standard methods of gravimetric and colourimetric methods to obtain an accurate representation of the performance of the equipment:

- Gravimetric method: gives the absolute volume dispensed within a plate. This is calculated by weighing a dry plate, dispensing water into it and then re-weighing.

- Colourimetric method: uses tartrazine to determine the volume dispensed per well by reading an absorbance, at 405 nm, on a plate reader. It shows the individual performance of each dispensing tip and the precision (CV) across the plate. This method requires a comparison with a standard curve set up by hand, meaning the accuracy of dispenses is only comparative to the curve and not absolute.